Turun yliopisto
University of Turku

UPCONVERTING DIAGNOSTICS:

Multiplex assays utilizing upconversion luminescence technology

Minna Ylihärsilä

TURUN YLIOPISTON JULKAISUJA – ANNALES UNIVERSITATIS TURKUENSIS
Sarja - ser. D osa - tom. 1117 | Medica - Odontologica | Turku 2014

University of Turku

Faculty of Medicine

Department of Virology

Institute of Biomedicine

Department of Biochemistry / Biotechnology

National Doctoral Programme of Advanced Diagnostic Technologies and Applications, DIA-NET, and Turku Doctoral Programme of Molecular Medicine, TuDMM

Supervised by

Docent Matti Waris, Ph.D.
Institute of Biomedicine / Department of Virology
University of Turku
Turku, Finland

Professor Tero Soukka, Ph.D.
Department of Biochemistry / Biotechnology
University of Turku
Turku, Finland

Reviewed by

Professor Matti Karp, Ph.D.
Department of Chemistry and Bioengineering
Tampere University of Technology
Tampere, Finland

Docent Hannimari Kallio-Kokko, Ph.D.
Haartman Institute / Department of Virology
University of Helsinki
Helsinki, Finland

Opponent

Docent Eeva Auvinen, Ph.D.
Haartman Institute / Department of Virology
University of Helsinki
Helsinki, Finland

The originality of this thesis has been checked in accordance with the University of Turku quality assurance system using the Turnitin OriginalityCheck service.

ISBN 978-951-29-5751-4 (PRINT)
ISBN 978-951-29-5752-1 (PDF)
ISNN 0355-9483
Painosalama Oy - Turku, Finland 2014

To my family

ABSTRACT

Minna Ylihärsilä
Upconverting diagnostics: Multiplex assays utilizing upconversion luminescence technology
Department of Virology, University of Turku, Turku, Finland
Annales Universitatis Turkuensis
Turku 2014

Conventional diagnostics tests and technologies typically allow only a single analysis and result per test. The aim of this study was to propose robust and multiplex array-in-well test platforms based on oligonucleotide and protein arrays combining the advantages of simple instrumentation and upconverting phosphor (UCP) reporter technology. The UCPs are luminescent lanthanide-doped crystals that have a unique capability to convert infrared radiation into visible light. No autofluorescence is produced from the sample under infrared excitation enabling the development of highly sensitive assays.

In this study, an oligonucleotide array-in-well hybridization assay was developed for the detection and genotyping of human adenoviruses. The study provided a verification of the advantages and potential of the UCP-based reporter technology in multiplex assays as well as anti-Stokes photoluminescence detection with a new anti-Stokes photoluminescence imager. The developed assay was technically improved and used to detect and genotype adenovirus types from clinical specimens. Based on the results of the epidemiological study, an outbreak of adenovirus type B03 was observed in the autumn of 2010.

A quantitative array-in-well immunoassay was developed for three target analytes (prostate specific antigen, thyroid stimulating hormone, and luteinizing hormone). In this study, quantitative results were obtained for each analyte and the analytical sensitivities in buffer were in clinically relevant range. Another protein-based array-in-well assay was developed for multiplex serodiagnostics. The developed assay was able to detect parvovirus B19 IgG and adenovirus IgG antibodies simultaneously from serum samples according to reference assays. The study demonstrated that the UCP-technology is a robust detection method for diverse multiplex imaging-based array-in-well assays.

Keywords: array-in-well, upconverting phosphor (UCP), imaging, adenovirus genotyping, epidemiology, parvovirus B19, immunoassay, serology

TIIVISTELMÄ

Minna Ylihärsilä
Käänteentekevää diagnostiikkaa: Luminesenssin käänteisviritysteknologian hyödyntäminen monianalyyttimäärityksissä
Virusoppi, Turun yliopisto, Turku, Suomi
Annales Universitatis Turkuensis
Turku 2014

Perinteiset diagnostiset testit mahdollistavat vain yhden analyysin ja tuloksen määritystä kohden. Väitöskirjatyöni tavoitteena oli kehittää uudenlaisia järjestelmä kuopassa tyyppisiä mallintavia monianalyyttimäärityksiä, joissa yhdestä näytteestä yhdessä reaktiokaivossa voidaan mitata samanaikaisesti useita analyyttejä ja niiden pitoisuuksia. Kehitetyt monianalyyttimääritykset perustuvat sekä nukleiinihappojen että proteiinien mittaukseen hyödyntäen leimoina valoa tuottavia epäorgaanisia lantanidi-ioneja sisältäviä loisteainepartikkeleita (UCP). Näillä partikkeleilla on ainutlaatuinen kyky virittyä matalaenergisen infrapunavalon vaikutuksesta ja emittoida korkeaenergisen näkyvän valon aallonpituuksilla, mikä mahdollistaa autofluoresenssista vapaan mittauksen ja näin ollen herkkien määrityksien kehityksen.

Väitöskirjatyössäni kehitin adenoviruksille DNA-tyypitysmäärityksen, joka perustui yksinauhaisen PCR-tuotteen ja adenovirus-tyyppispesifisten koettimien väliseen hybridisaatioreaktioon mikrotiitterilevyn kaivon pohjalla. Tulokset osoittivat, että UCP-leimateknologia ja uusi anti-Stokes luminesenssin kuvantamiseen kehitetty laite soveltuvat monianalyttimääritysten kvantitatiiviseen mittaukseen. Teknisesti parannettua adenovirusten DNA-tyypitysmenetelmää hyödynnettiin kliinisesti merkittävien adenovirustyyppien havaitsemisessa ja genotyypityksessä. Adenovirusinfektioiden epidemiologinen seuranta osoitti, että adenovirus tyyppi B03 aiheutti epidemian syksyllä 2010. Väitöskirjatyössäni kehitin myös kvantitatiivisen mallintavan monianalyytti-immunomäärityksen kolmelle antigeenille. Määrityksessä kaikille analyyteille saatiin kvantitatiivinen tulos, ja analyyttiset herkkyydet olivat kliinisesti merkittävällä alueella. Lisäksi väitöskirjatyössäni kehitin serologisen monianalyyttimäärityksen, jonka avulla mitattiin seerumista IgG-luokan adenovirus- ja parvovirus B19-vasta-aineita samanaikaisesti. Serologinen monianalyyttimääritys validoitiin näytepaneelilla ja tulokset korreloivat hyvin adenovirus IgG ja parvovirus B19 IgG referenssi-entsyymi-immunomäärityksien kanssa. Väitöskirjatyössäni osoitin, että UCP-teknologia soveltuu sekä oligonukleotidi- että proteiini-pohjaisten monianalyyttimääritysten kvantitatiiviseen kuvantamiseen.

Avainsanat: monianalyyttimääritys, loisteainepartikkelit, kuvantaminen, adenovirus, genotyypitys, epidemiologia, parvovirus B19, immunomääritys, serologia

TABLE OF CONTENTS

ABBREVIATIONS

ΔG	delta G
Ab	antibody
Ag	antigen
Anti-hIgG	anti-human immunoglobulin G
AP	alkaline phosphatase
bpp	bits per pixel
BSA	bovine serum albumin
CCD	charge-coupled device
CMV	cytomegalovirus
DCC	dicyclohexylcarbodiimide
DCS	disuccimidyl carbonate
DMS	dimethyl suberimidate
DNA	deoxyribonucleic acid
DSO	disuccinimidyl oxalate
EDC	1-ethyl-3-(3-dimethylaminopropyl) carbodiimide
EIA	enzyme immunoassay
ELF	enzyme-labeled fluorescence
ELISA	enzyme-linked immunosorbent assay
ETU	energy transfer upconversion
GST	glutathione S-transferese
hAdV	human adenovirus
HBV	hepatitis B virus
HCV	hepatitis C virus
HDV	hepatitis D virus
HEV	hepatitis E virus
HGV	hepatitis G virus
hIgG	human immunoglobulin G
His-tag	histidine tag
HIV	human immunodeficiency virus
HRP	horseradish peroxidase
HSA	human serum albumin
Ig	immunoglobulin
LH	luteinizing hormone
Ln	lanthanide
LOD	limit of detection
NHS	N-hydoxysuccinimide
NP	nasopharyngeal aspirate or swab and other respiratory specimens
NS	nasopharyngeal specimens
nt	nucleotide
PCR	polymerase chain reaction
PDITC	phenylendiisothiocyanate

PEG	polyethylene-glycol
PIII	plasma immersion ion implantation
PMT	photomultiplier tube
PSA	prostate-specific antigen
QD	quantum dot
qPCR	quantitative real-time PCR
RaM	rabbit anti-mouse
RNA	ribonucleic acid
RPA	reverse phase array
RSV	respiratory syncytial virus
RV	rubella virus
RVP	respiratory viral panel
SAM	sentrix array matrix
SARS	severe acute respiratory syndrome
SA-UCP	streptavidin conjugated UCP
SD	standard deviation
SERS	surface-enhanced raman scattering
SNR	signal-to-noise ratio
SPR	surface plasmon resonance
SPRi	surface plasmon resonance imaging
sulfo-NHS	N-hydroxysulfosuccinimide sodium salt
tiff	tagged image file format
TMB	3,3’,5,5’-Tetramethylbenzidine
TSH	thyroid-stimulating hormone
UCNP	upconverting nanoparticle
UCP	upconverting phosphor
UV	ultraviolet
VLP	virus-like particle

LIST OF ORIGINAL PUBLICATIONS

The thesis is based on the following original publications, referred to in the text by Roman numerals (**I-IV**).

I Minna Ylihärsilä, Timo Valta, Maija Karp, Liisa Hattara, Emilia Harju, Jorma Hölsä, Petri Saviranta, Matti Waris, and Tero Soukka. (2011). Oligonucleotide array-in-well platform for detection and genotyping human adenoviruses by utilizing upconverting phosphor label technology. *Analytical Chemistry* 83: 1456–1461.

II Minna Ylihärsilä, Emilia Harju, Riikka Arppe, Liisa Hattara, Jorma Hölsä, Petri Saviranta, Tero Soukka, and Matti Waris. (2013). Genotyping of clinically relevant human adenoviruses by array-in-well hybridization assay. *Clinical Microbiology and Infection* 6: 551–557.

III Henna Päkkilä, Minna Ylihärsilä, Satu Lahtinen, Liisa Hattara, Niina Salminen, Riikka Arppe, Mika Lastusaari, Petri Saviranta, and Tero Soukka. (2012). Quantitative multianalyte microarray immunoassay utilizing upconverting phosphor technology. *Analytical Chemistry* 84: 8628–8634.

IV Minna Ylihärsilä, Siina Alaranta, Susanne Lahdenperä, Satu Lahtinen, Benedict Arku, Klaus Hedman, Tero Soukka, and Matti Waris. (2014). Array-in-well serodiagnostic assay utilizing upconverting phosphor label technology. *Manuscript, submitted*.

In addition, some unpublished data is presented.

The original publications have been reproduced with the permission of the copyright holders.

1 INTRODUCTION

Multiplex assay technology (e.g., high-density microarrays, low-density arrays and multiplex PCR) has allowed a shift from traditional one-parameter-at-a-time analyses of biomolecules (e.g., DNA and proteins) to more high-throughput multiplex platforms where large number of analytes or analyte concentrations can be identified from one sample simultaneously (Yu *et al.*, 2010). Ekins and coworkers have demonstrated that an analysis of a small amount of target in a small area is more sensitive than an analysis of the same amount of target in a larger area (Ekins and Chu, 1992; Ekins *et al.*, 1990; Ekins, 1989). In principle, the array technology offers higher sensitivity due to improved signal-to-noise ratios as well as decreased reaction times due to shorter diffusion distances compared to conventional immunoassays. The main benefits of multiplexing are a smaller sample consumption and an increased information gain from one sample. Multiplex assays can be used broadly, for example, in clinical diagnostics, food safety testing, and environmental monitoring. In addition, the approval of DNA-microarray technology by US Food and Drug Administration has opened the door to new applications in the field of clinical diagnostics. The multiplex assay needs to fulfill many criteria before the assay is validated into a clinical diagnostic test (Lababidi, 2008; Težak *et al.*, 2006). The test should be specific, user-friendly and rapid to perform, robust, accurate, reproducible and preferably low-cost. The development of new detection technologies and instruments is also needed to facilitate the use of multiplex assays for clinical diagnostics. Multiplex assay technologies could be useful tools also in low-resource settings where rapid turnaround time, low-cost multiplex testing and point-of-care testing are needed.

DNA-array applications are commonly used, e.g., in the analyses of gene expression patterns and single nucleotide polymorphism, drug discovery, toxicology, disease characterization, and various diagnostic applications (Coppée, 2008; Hacia *et al.*, 1999; Heller, 2002; Schena *et al.*, 1995). DNA-array consists of a collection of microscopic spots with DNA fragments or oligonucleotides orderly arranged onto the surface of a solid support. The array is based on a hybridization reaction between the target nucleic acid strands and specific probe molecules attached to solid support (McLoughlin, 2011). In multiplex assays, the binding between the probe and its target can be detected using different label or label-free detection techniques. Imaging instrumentation has three components: a radiation source (e.g., laser diode) to illuminate the sample, a spectrally selective element (e.g., optics), and a detector (e.g., camera) to collect the images. Fluorescence-based technology is still a commonly used detection method in array applications (Dufva, 2009). However, new sensitive and specific detection technologies are needed for imaging-based arrays.

The success of highly multiplex assays on genomics has also increased the interest in the simultaneous measurement of many proteins in patient samples in one assay. The gold standard for single-protein measurement in a solution is an immunoassay and the most widely used format is the enzyme-linked immunosorbent assay (ELISA). The

immunoassays are based on either one or two antigen-specific immunoglobulins, used to capture the target antigen in the sample. A wide range of labeling and signal-enhancement strategies have been developed to allow the detection of antigen-antibody binding. Protein arrays are high-throughput and miniaturized versions of these traditional immunoassays enabling the parallel detection of biomarkers in clinical samples in a single assay.

The serological protein-based multiplex assays can be widely used in clinical research and diagnostics. They can be utilized for disease classification, monitoring disease progression, understanding disease mechanism, immunoglobulin class switching, and monitoring disease activity by analyzing the antibody titer. These assays can also be suitable for early diagnosis, differential diagnosis, disease staging or determining disease prognosis (Kingsmore, 2006). The arrays have become well-established research tools in basic and applied research.

2 REVIEW OF THE LITERATURE

2.1 Arrays as a tool for multiplex diagnostics

2.1.1 Array principle

The array-based assays are miniaturized versions of traditional solid-phase DNA/RNA dot blot assays and ELISA immunoassays, enabling a parallel analysis of target biomolecules. Arrays can be distinguished on the basis of the probe molecule (e.g., DNA or protein array), solid support (planar or suspension array), fabrication strategy (printed or *in situ* synthesized), and detection method (label or label-free). Many different probes can be attached as discrete spots to a solid support, and these probes interact with the intended target molecules in sample and produce either qualitative or quantitative data (Yu *et al*., 2010). In both DNA and protein assays the probe or capture molecule should have a high specificity (non-specific cross-reactions should be avoided) and an affinity for the target molecule (Dufva, 2009). Depending on the assay type different probes, including PCR products, genomic DNA, cDNAs, chemically synthetized oligonucleotides, proteins, antibodies, DNA/RNA aptamers, small molecules or carbohydrates, can be immobilized to solid support (Relógio *et al.*, 2002). The hybridization reactions take place simultaneously in parallel across the entire array. After hybridization reaction the captured biomolecules are detected by using various labeled reporter ligands or directly labeled target molecules. If fluorescence-based detection techniques are used for array detection, the fluorescent intensity at any particular probe location indicates the relative concentration of the target in the sample.

2.1.2 Array design

A multiplex assay platform can be defined as a planar or suspension, based on the choice of support (Ellington *et al.*, 2010). In two-dimensional planar array biomolecules are printed in rows and columns by an arraying device at known locations onto the same support, whereas in suspension-based arrays the biomolecules are coupled to the beads, which are randomly arranged to their final locations (Figure 1). Planar arrays are more commonly used than suspension arrays. Planar array allows a wide range of probe densities to be used, and the array is read using an array scanner. DNA-arrays can be divided into low- and high-density arrays (Lévêque *et al.*, 2013). The low-density arrays contain only a few probes for diagnostic applications, whereas the high-density arrays contain one million probes for high-throughput genome and transcriptomes studies (Dufva, 2009). The high-density planar arrays can have up to 10^6 spots in an area of 1–2 cm^2 (Heller, 2002). In a suspension the beads array have different codes for different targets, which are analyzed using a flow cytometry instrument. The multiplex capacity of a bead-based array is < 100 probes / assay (Luminex system, TX, USA).

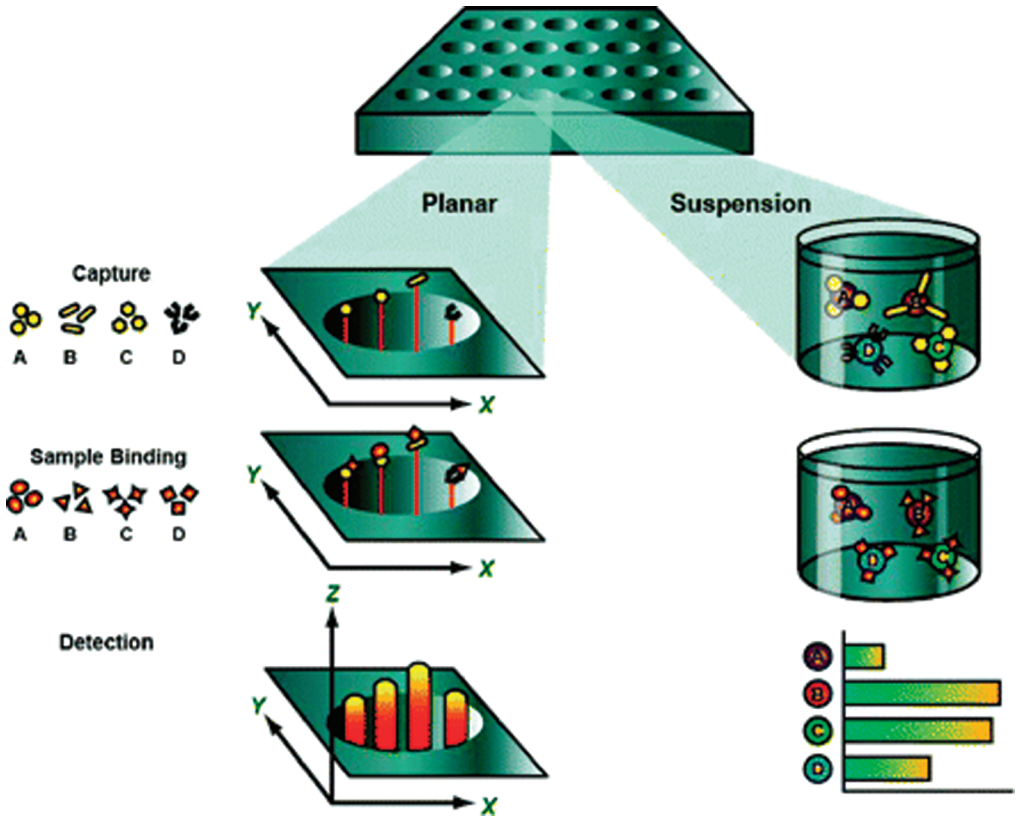

Figure 1. Planar and suspension array formats. In planar array, capture ligand biomolecules are immobilized on solid surface. In suspension array, capture biomolecules are attached on color-coded or size-coded microspheres. (Ellington *et al*., 2010)

Solid-phase arrays

The solid-phase array is fabricated by spotting multiple copies of the probe molecule onto a solid support, usually a glass slide, nylon membrane, or plastic surface, e.g., a microtiter well plate (Kusnezow and Hoheisel, 2003). Digital versatile disks, made of polycarbonate, have also been used as a solid support (Morais *et al.*, 2009). The spotting is carried out by array printers. In high-density arrays, different oligonucleotides can be synthetized *in situ* on the surface of the array by using photolithography (Affymetrix, CA, USA).

Also bead-based solid-phase array formats are available for high-density DNA and RNA analysis. Two BeadArray platforms, Sentrix Array Matrix (SAM) and Sentrix BeadChip (Illumina, San Diego, CA), are based on self-assembled color-coded silica beads (3-µm in diameter). In SAM platform the beads are immobilized on solid fiber-

optic bundles and in Sentrix BeadChip the beads are assembled on the planar silica slide having a uniform spacing of ~5.7 microns in both cases. In SAM, each bundle is an individual array consisting of 50,000 5-µm fiber-optic strands, each of which is chemically etched to create a microwell for a single bead. Each bead is covered with hundreds of thousands of copies of a specific oligonucleotide acting as the capture sequence. The bead location is mapped by a decoding process, where fluorescently labeled complementary oligonucleotides are used. (Fan *et al.*, 2006)

Suspension arrays

Suspension arrays or microsphere-based assays are based on polymer beads serving as the solid support for a multiplex flow cytometric assay. The beads are hybridized with fluorescently labeled target biomolecule and flow cytometry is used for detection. Multiplexing is based on different bead sizes and their related forward light-scattering characteristics determined by flow cytometry. Also the beads can contain unique fluorescence properties. In this case, the beads are uniform in size and filled with different levels of one or two fluorescent dyes. In the case of two dyes, red (658 nm emission) and infrared (712 nm emission) fluorochromes are used at various concentrations to produce beads with unique spectral characteristics. The commercially available Luminex xMAP technology of 100 fluorescently dyed (with two dyes) polystyrene microspheres, 5.6 µm in diameter, can detect up to 100 targets per assay (Luminex system). (Dunbar, 2006)

Microsphere-based immunoassays are suitable for multiplex detection of infectious diseases. These assays have been used for influenza virus antigen detection and characterization (Yan *et al.*, 2005), for identification of viruses causing gastroenteritis (Liu *et al.*, 2012), and for the identification of 12 common respiratory viruses (respiratory syncytial virus (RSV) A and B; influenza virus A and B; parainfluenza virus 1, 2, 3, and 4; human metapneumovirus; rhinoviruses; enteroviruses; and severe acute respiratory syndrome (SARS) coronavirus) (Sefers *et al.*, 2011). Suspension array based commercial kits, including the xTAG RVP test (Luminex), ResPlex II (Qiagen, Venlo, the Netherlands), and MultiCode-PLx (EraGen Biosciences, WI, USA), are also available for the detection and typing of respiratory viruses. These multiplex panels are able to detect influenza A and B viruses, RSV, human metapneumovirus, rhinovirus, and adenovirus. The xTAG RVP test additionally subtypes seasonal influenza H1 and H3 viruses. The ResPlex II also detects coronaviruses (229E, OC43, NL63 and HKU1), coxsackievirus, echovirus, bocavirus and differentiates adenoviruses (B, E). The MultiCode-PLx assay additionally detects coronaviruses (229E, OC43, and NL63); differentiates parainfluenza 4a and, 4b; and is also able to differentiate adenoviruses (B, C, and E). These commercial tests offer clinical laboratories new tools for the detection of respiratory viruses (Balada-Llasat *et al.*, 2011).

2.2 Multiplexing in clinical virology

Usually, the clinical signs or symptoms are not specific enough to diagnose the causative agent of the disease, and thus diagnostic tests are needed to help with that in order to guide the appropriate treatment of patient and proper use of antiviral agents, when available (Ginocchio, 2011). Clinical laboratories have conventionally used different diagnostic methods for either to show the presence of virus in patient samples, or to detect host responses (e.g., production of specific antibodies) caused by the viral infection. These methods include virus culture with neutralization assays, serological methods (e.g., hemagglutination inhibition tests, complement fixation tests, immunofluorescence assays and enzyme immunoassays), antigen detection assays, and nucleic acid detection methods, and are widely used for the typing, and characterization of viruses and viral infections (Mahony, 2008; Storch, 2000). However, the traditional methods are often time-consuming, labor-intensive (especially virus culture) and allow often only a single analysis and result per test (singleplex assays) (Krishna and Cunnion, 2012). Shortened detection times and increased assay sensitivity with less sample volumes needed are beneficial advances in the field of clinical virology, and multiplexing offers a mean to achieve this.

Especially sensitive nucleic acid detection methods such as PCR, sequencing and DNA-arrays offer rapid, sensitive and high-throughput methods for detection and genotyping of important pathogens. Novel PCR methods have helped to characterize quickly also new and emerging viruses such as human metapneumovirus (van den Hoogen *et al.*, 2001), human bocavirus (Allander *et al.*, 2005), two new polyomaviruses WU (Gaynor *et al.*, 2007) and KI (Allander *et al.*, 2007) as well as new respiratory viruses e.g., SARS coronavirus and swine-origin H1N1-influenza A virus causing serious infections in humans (Fraser *et al.*, 2009; Peiris *et al.*, 2003).

To be of use for diagnostic purposes multiplex assays should have at least the same performance (specificity and sensitivity) as corresponding singleplex assays. When this criterion is fulfilled the multiplex assays offer rapid and accurate qualitative or quantitative detection methods for many different pathogens simultaneously from one specimen (Mehlmann *et al.*, 2007; Raymond *et al.*, 2009). The multiplex assays can be used in diagnostics to recognize the causative agent of an illness, for molecular typing of the agents, as well as for epidemiological and vaccine studies in providing information on seasonality and geographical distribution, and identifying potential risk groups. The specific and rapid diagnosis also gives beneficial information to public health authorities who aim to follow which viruses are circulating in the community to adjust public health policy accordingly. For basic research purposes, multiplex assays can be utilized also to study e.g., the interactions between the virus and the host cell (Clewley, 2004; Mahony, 2008). Overall, multiplex assays can improve laboratories ability to diagnose wide range viral infections and simultaneously identify e.g., viruses that cause infections with similar symptoms (Poehling *et al.*, 2006).

2.2.1 Solid-phase DNA-arrays

DNA-array technology was first introduced in the middle of the 1990s (Schena *et al*., 1995). These arrays allow replicate analyses in a single assay, where replicate spots of the same probe are printed. Setting up a DNA-array is a multistep process based on identified target gene sequences, for which the probes for the detection are designed. The first step is to design PCR primers for amplification of the intended viral genome targets. The challenge for optimal primer design is that the PCR should amplify a wide range of viral genomes within the target virus groups (Clewley, 2004). To facilitate the detection of the amplified PCR-products the label can be included in the end of target strand by using fluorescently or otherwise labeled primers, or by using fluorescently labeled nucleotides for amplification (Relógio *et al*., 2002). After the amplification reaction, the PCR-product is applied to an array and hybridized to complementary sequence probes, usually 25-70 nucleotide (nt) long, representing targeted viruses. The array is washed to remove unbound DNA, and fluorescence intensities for each spot are detected and analyzed by using scanning or imaging techniques (McLoughlin, 2011).

There are many potential uses for DNA-arrays in clinical virology. The low-density oligonucleotide-based arrays are suitable platforms for the detection and typing of clinically significant levels of viruses in patient samples in both research laboratory and in clinical laboratory. The array-based assays are suitable for the detection of respiratory diseases because they can allow the simultaneous detection of viral and bacterial co-infections (Cannon *et al.*, 2010). There are many different oligonucleotide-based array applications for the detection and typing of RNA and DNA viruses, including arrays for influenza A and B viruses (Townsend *et al.*, 2006), influenza A virus (Dawson *et al.*, 2006; Ryabinin *et al.*, 2011), influenza B virus (Dankbar *et al.*, 2007), human papilloma virus (Oh *et al.*, 2004; Ritari *et al.*, 2012; Sandri *et al.*, 2009), adenovirus (López-Campos *et al.*, 2007), enterovirus (Susi *et al.*, 2009), and norovirus (Mattison *et al.*, 2011). The high-density oligonucleotide-based microarray (Lodes *et al.*, 2007) and resequencing microarray (Berthet *et al.*, 2013; Lin *et al.*, 2006a) have also been used for pathogen detection.

2.2.2 Multiplex PCR

In multiplex PCR more than one target sequence can be amplified by including more than one pair of primers in the reaction. Multiplex PCR can save time and work and be cost-effective. Multiplex PCR is a combination of several generic or more specific primers targeting different sequence regions in one amplification reaction capable of amplifying a wide range of viral genomes. (Elnifro *et al.*, 2000) The primer design is a crucial factor affecting PCR amplification efficacy. It is begun by aligning multiple genome sequences from as many strains of the virus as possible. A challenge of multiplex PCR is that all the primer pairs should enable similar amplification efficiencies for their specific target (Elnifro *et al*., 2000; Kim *et al.*, 2009; Lam *et al.*, 2007; Sotlar *et al.*, 2004).

Real-time quantitative PCR is nowadays the most often used method for nucleic acid detection. This method is based on the on-line quantitation of a fluorescent reporter during the PCR reaction. The signal increases in direct proportion to the amount of PCR product amplified in the reaction. Often used reporter in these assays is the fluorescent dye SYBR Green, which binds unspecifically to all double-stranded DNA (including primer-dimers and other possible non-specific reaction products). A more specific multiplex real-time PCR quantitation can be obtained by using fluorescent probes (e.g., TaqMan and molecular beacons) in the assay. These probes contain a fluorescent dye and a quenching dye on the opposite ends of the probe sequence. Compared to SYBR Green, these probes are sequence-specific and the detection of the signal is based on fluorescence resonance energy transfer quantitation. (Parida, 2008) Multiplex PCR utilizing fluorescently labeled probes for each target together with melting temperature analysis has been used e.g., for the detection of gastroenteritis panel, including norovirus group I and II, rotavirus, hepatitis A virus, and coxsackievirus (Kang *et al.*, 2013).

A nested PCR, which is also still an often used method, increases the sensitivity and specificity of the multiplex PCR through two independent PCR-reactions (the second using as a template the product from the first reaction) with two different primer sets (Avellón *et al.*, 2001; Coiras *et al.*, 2004; Renois *et al.*, 2010). Although, the nested PCR is usually very effective in generating products, but the drawback is that it is complicated to perform, it is time-consuming, and it increases the possibility of false-positive results due to carry-over contamination.

An asymmetric multiplex PCR is another new method, which is used to amplify the single-stranded target strand along with the double-stranded DNA. This approach can be used when single-stranded target DNA is needed (e.g., in array-based assay or sequencing). The PCR reaction is carried out using an excess of the primer labeled for the targeted strand. After the PCR reaction, the single-stranded labeled target is hybridized with the virus-specific oligonucleotide probes immobilized on array surfaces (Park *et al.*, 2010; Wang *et al.*, 2013b).

The multiplex PCR techniques have been used to screen and identify viral pathogens in many clinical settings (Mahony, 2008). This technique is used to e.g., study virus infection associations with disease. The multiplex assay can be designed to detect a group of different viruses causing similar signs of disease, or viruses that are transmitted by similar pathways. Several test panels have been developed for respiratory pathogens, including influenza A virus (H1N1, H3N2, and H5N1); influenza B virus; parainfluenza virus types 1, 2, 3, 4a, and 4b; respiratory syncytial virus A and B; human rhinoviruses; human enteroviruses; human coronaviruses OC43, 229E and SARS; human metapneumoviruses; adenoviruses (A to F); and *Mycoplasma pneumonia*, *Chlamydophila pneumonia*, and *Legionella pneumophila*, (Lam *et al*., 2007). Also for human herpes viruses a panel, including herpes simplex virus type 1 and 2; varicella-zoster virus; Epstein-Barr virus; CMV; human herpes

virus 6A/B, and human herpes virus 7, has been developed (Tanaka *et al.*, 2009). For central nervous system infections, a multiplex PCR was combined with an array technique for the detection and typing of viruses, including herpes simplex virus type 1 and 2; varicella-zoster virus; cytomegalovirus; Epstein-Barr virus; human herpesvirus type 6, 7, and 8; and the human enteroviruses (Leveque *et al.*, 2011). For human retroviruses, a multiplex PCR utilizing differently colored molecular beacons have been used for the detection of human immunodeficiency virus (HIV) types 1 and 2; and human T-lymphotrophic virus types 1 and 2 (Vet *et al.*, 1999). In addition, a method based on multiplex PCR has been developed for the simultaneous detection of viruses causing exanthema (measles, parvovirus B19, and rubella virus (RV) (del Mar Mosquera *et al.*, 2002).

2.2.3 Solid-phase protein-arrays

The earliest protein-array application for protein expression studies was described in the late 1990s (Lueking *et al.*, 1999). Protein-arrays are fast, high-throughput methods that can be divided into three groups: functional, reverse phase, and analytical arrays. Functional arrays are used to study protein-protein interactions (e.g., protein-protein, enzyme-substrate, ligand-receptor, protein-DNA), protein function, and enzymatic activities (MacBeath and Schreiber, 2000; Sun *et al.*, 2013; Yu *et al.*, 2010). These arrays are prepared by immobilizing on a solid surface, a selection of capture proteins (e.g., antibodies, antigens, lysates, peptides, or aptamers), which then bind the target analyte in the sample (Hall *et al.*, 2007). In reverse phase arrays (RPA), the sample (e.g., cultured cells, tissue lysates, blood samples, or other) is printed onto an array surface, which is then probed with antibodies against the protein of interest. RPAs are used to detect altered proteins from patient samples (e.g., phosphorylated proteins), which may be indicative of diseases. In diagnostic applications RPA can also be used to help to profile a particular signaling pathway that may be dysfunctional in the cell aiding to recognize and treat the disease of interest (Liotta *et al.*, 2003; Mueller *et al.*, 2010). Analytical arrays can be used to recognize and quantify target proteins in a specimen, and to profile disease-related proteins.

Protein arrays can also be classified as antigen- or antibody-based arrays, the latter of which represent a powerful approach for the large-scale characterization of candidate antigens in specimens. This approach is based on miniaturized parallelized sandwich immunoassays.

Antigen- and antibody-based arrays

The antigen-based arrays are used for the multiplex detection of specific antibody responses to various infectious agents. The first viral protein-arrays were developed to screen and monitor the presence of IgG-antibodies against multiple SARS-coronavirus proteins in sera from SARS-patients (Qiu *et al.*, 2005; Zhu *et al.*, 2006). Also a multiplex proof-of principle serodiagnostic assay has been developed to type and screen blood donors for the presence of antibodies against important blood-borne

pathogens such as hepatitis C and HIV (Burgess *et al.*, 2008). This assay was based on two different scannings: after obtaining the erythrocyte-specific signal (i.e., blood typing), the labeled secondary antibody was added to the array and scanned for the viral antibody-specific signal.

Multiplex influenza antigen-based arrays have been used for profiling serum IgG antibody responses (Koopmans *et al.*, 2012) and characterizing vaccine immunogenicity in individuals of varying ages (Price *et al.*, 2013). Multiplex serological immunoassays have also been used for the monitoring of the specific antibody responses against HIV-1, syphilis and hepatitis C virus (HCV) (Lochhead *et al.*, 2011) and for the detection of antibodies against Epstein–Barr virus, cytomegalovirus (CMV), Toxoplasma gondii, and HCV (Feron *et al.*, 2013). Sivakumar *et al*., 2013 have developed an array for the simultaneous detection of virus-specific antibodies of measles, rubella (RV), mumps, Varicella-Zoster, and Epstein-Barr viruses (Sivakumar *et al.*, 2013). A multiplex assay for five hepatitis virus (HBV, HCV, HDV, HEV and HGV) has been developed for the detection of both viral antigens and antibodies. The assay can simultaneously detect two viral antigens (HBsAg, HBeAg) and seven viral antibodies (HBsAb, HBcAb, HBeAb, HCVAb, HDVAb, HEVAb, HGVAb) from serum samples (Xu *et al.*, 2007). Serological arrays can also be developed for simultaneous detection of different antibody classes. Liu *et al.,* 2013 have demonstrated the simultaneous detection of IgG and IgM antibodies against herpes simplex virus type 1 and 2, CMV and RV in serum and cerebrospinal fluids (Liu *et al.*, 2013). The studies described above demonstrate that the protein-arrays can be used for the large-scale identification of virus-specific antibodies in sera.

Protein-based array challenges

Proteins have wide molecular variability and concentration range in different samples. In multiplex assays, the challenge is to detect low and high abundance proteins simultaneously in a complex biological sample material (Haab *et al.*, 2001). Another challenge is to avoid cross-reactivity. Especially, when antibody-based arrays are developed, the immobilized antibodies used to capture the target proteins should be highly specific to the targeted analytes, otherwise cross-reactivity between the used antibody and other non-target proteins in the specimen may occur. Furthermore, quantifying antibody concentrations in multiplex serological assays could broaden the applicability and acceptance of protein-arrays as routine biomedical research tools. Because antibody concentrations and affinities vary in serum, it would be useful to know whether the calculated amount of the bound antibody is proportional to the antibody concentration in solution. With singleplex traditional ELISA, a standard curve can be used to quantify the concentration of target antibodies. However, in the multiplex assays no common standard is used for the detection of antibodies binding to different targets on an array. Along with appropriate calibration curves, improvements in the sensitivity and linearity of the dynamic range are also needed to aid to detect low-abundance antibodies in clinical serum samples. Yet an array

nonlinear calibration method has been developed for quantifying antibody binding to the surface of protein-array. The method is based on a known amount of IgG standards printed to an array to form a nonlinear standard curve. Based on the standard curve, the amount of IgG antibodies bound to the surface of the protein spot can be calculated. This method has been shown to improve the linear dynamic range and reduce assay variation compared to a linear standard curve method. (Mezzasoma *et al.*, 2002; Yu *et al.*, 2013)

2.3 Immobilization of biomolecules onto solid surfaces

In this section, two-dimensional oligonucleotide and protein immobilization methods are discussed. The immobilization strategy is very important because it may influence the background signal, stability of the bond between the probes and the solid support, probe density, hybridization efficiency, spot morphology (shape and homogeneity of the spot), spot density and spot reproducibility. (Dufva, 2005, 2009) A uniform surface is also of importance in array fabrication. A heterogeneous surface will cause variations in the amount of the attached biomolecule. Biomolecules can be attached to non-porous and porous two-dimensional surfaces such as glass slide or plate (Afanassiev *et al.*, 2000; Wiese *et al.*, 2001), silicon chips (Cretich *et al.*, 2011), polystyrene microtiter plates (Gehring *et al.*, 2008; Petryayeva *et al.*, 2013; Viitala *et al.*, 2013), polycarbonate slides (Kosobrodova *et al.*, 2014), or nitrocellulose coated slides (Mujawar *et al.*, 2013). When choosing the array substrate a few criteria should be considered. The substrate should be easily modified for biomolecule attachment, and it should have a homogenous biomolecule attachment surface, high binding capacity towards the biomolecule as well as low intrinsic fluorescence (low background noise) when using fluorescence-based detection.

The spotted arrays in miniaturized size are produced either by contact printing (contact pin printing and microstamping) or by non-contact printing (photochemistry-based methods, laser writing, electrospray deposition, and inkjet technologies). The main difference between these two technologies is that contact printing involves direct contact between the substrate surface and a pin. The main advantages of non-contact printing methods are avoided direct surface contact, reduced contamination, and higher throughput because several arrays can be simultaneously produced (Barbulovic-Nad *et al.*, 2006; Gutmann *et al.*, 2004). The non-contact piezoelectric inkjet printer aspirates the sample into a borosilicate glass capillary surrounded by a piezoelectric element that fits around the glass capillary like a collar. The sample is dispensed by the application of a voltage to the piezoelectric collar, producing a droplet typically less than 1 nL in volume (Delehanty and Ligler, 2003). The disadvantages of non-contact printing are pin clogging by air bubbles or particulates, splashing and satellite droplets causing contamination and irregular spot sizes (Espina *et al.*, 2003).

The printing buffer should also be optimal for all the spotted biomolecules in the array. Usually protective substances such as glycerol (MacBeath and Schreiber, 2000),

trehalose (Kusnezow *et al.*, 2003), or polyethylene-glycol (PEG) (Lee and Kim, 2002) are added in the printing buffer to prevent the dehydration of the spotting solution and to improve the stability of the protein. The printing buffer composition also affects the spot morphology and the spot signal intensities (Delehanty and Ligler, 2003). Achieving good spot quality is very important, as uniform spot morphology and size will produce reliable results and also aid in array data analysis. After the biomolecule immobilization, the surrounding areas need to be blocked before the array surface can be used. Depending on the immobilization strategy (non-covalent or covalent), other proteins or chemical methods can be used for blocking the remaining binding sites and also quenching the unreacted functional groups on the on the surface.

2.3.1 Attachment of oligonucleotides to solid support

Spotted probe arrays utilize synthetic oligonucleotides attached to the solid surface in precise locations. When designing the probes, their length should be considered: while the typical probe length is 25-80 bp, different probe lengths (25-30 nt and 60 nt long) have been tested to demonstrate the effect of oligonucleotide length on hybridization signal (Relógio *et al*., 2002). The 30 nt long probes had a sensitivity 3-fold lower compared to 60 nt long oligonucleotide probes, but the shorter probes were more specific, and therefore more applicable to the array assay than longer probes. The decreased specificity of long probes is due to their higher melting temperatures, while they have greater mismatch tolerance (especially in the center region of the sequence) during the hybridization reaction than shorter ones. The probe-target melting temperature, which is dependent on the probe length and base composition, is used to measure the stability of a nucleic acid duplex. However, melting temperature makes no statement about the binding affinity at the actual hybridization temperature, and therefore thermodynamic models of probe-target hybridization are increasingly used to predict of an array probe behavior. A probe length, oligonucleotide sequence information (e.g., GC content), hybridization temperature, surface density of the probe, and chemical environment (e.g., the presence of Na^+ ions) all effect on probe-target hybridization strength (Peterson *et al.*, 2001; Relógio et al., 2002).

The addition of spacers (linkers) coupled to short oligonucleotides or the application of a higher probe concentration during printing can improve hybridization signal strength. The linker can be a poly-dT spacer (Guo *et al.*, 1994), an oligodeoxyribonucleotide with a hairpin stem-loop anchor structure containing five phosphorothioates in the loop comprising six adenosines (Zhao *et al.*, 2001), or a poly carbon atom (e.g., C_{36}, $C_{18,}$ $C_{12,}$ C_8), coupled to the probe during the oligonucleotide synthesis (Afanassiev *et al*., 2000). The linker must be hydrophilic, chemically stable under the hybridization conditions used, and sufficiently long to minimize steric interference. The linker should also have no non-specific binding to the solid surface. The surface density of the oligonucleotides is also an important factor affecting the hybridization signal of the probe-target hybrid (Lee *et al.*, 2013). A low surface coverage will yield a low hybridization efficiency, whereas too closely packed probes

cannot participate in the hybridization reaction because of the steric hindrance or electrostatic interactions (Shchepinov *et al.*, 1997; Vainrub and Pettitt, 2003). The oligonucleotides need to be tightly bound to the solid surface, and accessible for hybridization, and the attachment chemistry needs to be reproducible (Zhou and Thompson, 2004).

A probe can be immobilized on the solid surface with different techniques, e.g., non-covalent adsorption, covalent immobilization, and streptavidin-biotin interaction. When using adsorption, the oligonucleotides are attached to the solid surface through ionic interaction. The surface is modified to contain primary amine groups (NH_3^+) covalently attached to the surface. The amines carry a positive charge at neutral pH, permitting the attachment of oligonucleotides through the formation of ionic bonds with the negatively charged phosphate backbone (Lemeshko *et al.*, 2001). However, the electrostatic interaction will easily break under high salt and/or high temperature conditions.

Covalent immobilization

The covalent immobilization technique is the most common method used for attaching oligonucleotides to a solid surface. Here, the oligonucleotide contains functional groups used for covalent attachment to the solid surface (Table 1). The oligonucleotides are preferably 5' or 3' end modified to contain a functional group, which can be used for probe attachment to a reactive group on the solid surface. The modified surface linkages need to be chemically stabile, sufficiently hydrophilic, and resistant to nonspecific binding to the surface. To fulfill these criteria, the two-dimensional surface is typically activated with silanes carrying terminal functional groups (e.g., amine, epoxide, thiol, or aldehyde) to produce a uniform layer for biomolecule attachment (Guo *et al*., 1994; Zammatteo *et al.*, 2000). In printed amine-modified DNA-array, succinic anhydride reaction, bovine serum albumin adsorption (BSA), or BSA-N-hydroxysuccinimide have been used to block unreacted functional groups having low affinity for the DNA (MacBeath and Schreiber, 2000; Schena *et al*., 1995; Taylor *et al.*, 2003).

Table 1. Strategies for attaching oligonucleotides to solid surfaces.

Oligonucleotide modification	Surface group	References
unmodified (negatively charged phosphate groups)	amino or epoxy silane, poly-L-lysine, poly carbodiimide	(Belosludtsev *et al.*, 2001; Kimura *et al.*, 2004; Lemeshko *et al*., 2001; Majtán *et al.*, 2004)
amines (-NH_2)	aldehyde, epoxy, isothiocyanate, succinimidyl esters (NHS-ester), imidoester	(Guo *et al*., 1994; Majtán *et al*., 2004; Sethi *et al.*, 2009)
succinylated	aminophenyl or aminopropyl silane	(Joos *et al.*, 1997)
thiols (-SH)	mercaptosilanized, amino silane, epoxy, gold activated surface	(Chrisey *et al.*, 1996; Csáki *et al.*, 2001; Rogers *et al.*, 1999; Sethi *et al*., 2009)
hydrazide	aldehyde, succinimidyl esters (NHS-ester)	(Raddatz *et al.*, 2002)
biotin	streptavidin	(Sabanayagam *et al.*, 2000)
phosphates (PO_3)	epoxy silane	(Mahajan *et al.*, 2006)

Attaching amino-modified oligonucleotides

There are several strategies for attaching 5'amino-modified oligonucleotides to the solid surface (Figure 2). Aldehyde and epoxy functional groups on a solid support are commonly used for the covalent coupling of amino-modified oligonucleotides. Carbodiimide, such as 1-ethyl-3-[3-dimethylaminopropyl]carbodiimide hydrochloride (EDC) or dicyclohexylcarbodiimide (DCC), can be used to activate carboxylic acid groups on the solid surface for conjugation to primary amine modified oligonucleotides. The carboxylic acid groups on the solid surface react with carbodiimide to form an O-acylisourea intermediate. The primary amine group on the 5'end of the oligonucleotide reacts with the original carboxyl group forming an amide bond and releasing an isourea by-product. To improve the coupling reaction, N-hydoxysuccinimide (NHS) is commonly included in the reaction. Adding NHS to the coupling reaction forms an NHS ester intermediate, which is more stable than O-acylisourea. Another option to form a stable covalent attachment between amino-modified oligonucleotide and solid support is to use phenylendiisothiocyanate (PDITC), disuccimidylcarbonate (DCS), disuccinimidyloxalte (DSO) and dimethylsuberimidate (DMS) crosslinking. These crosslinking agents convert solid

surface amino groups to isothiocyanates, N-hydroxysuccimimidy-esters (NHS-esters) or imidoesters, respectively (Beier and Hoheisel, 1999).

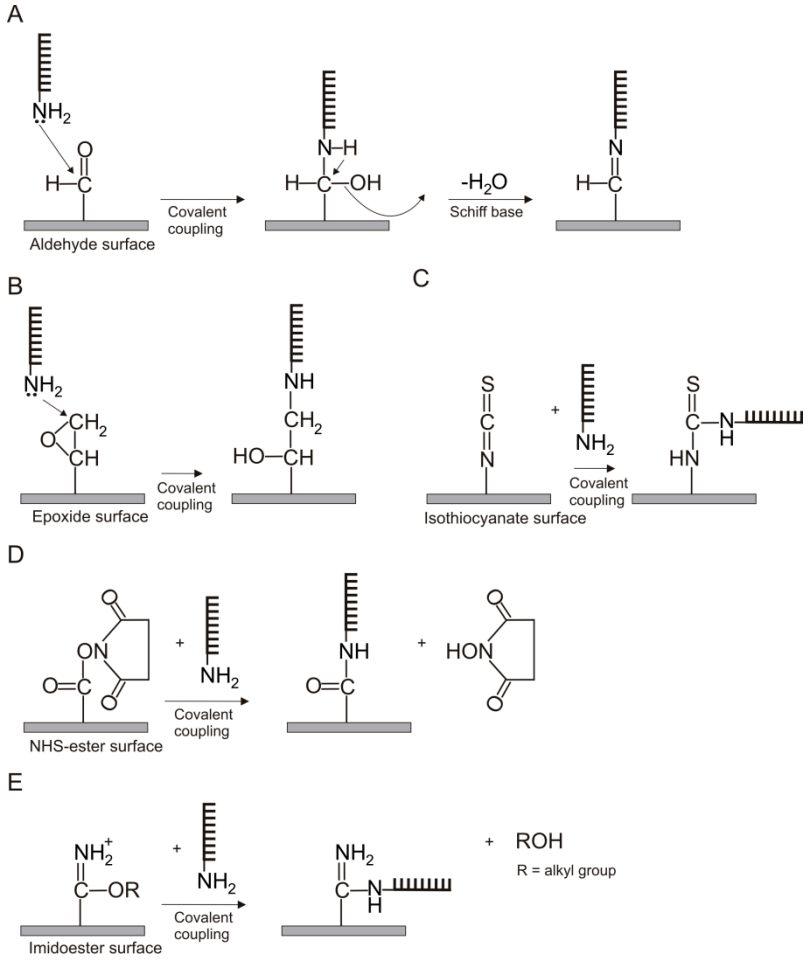

Figure 2. Attachment strategies for amino-modified oligonucleotides. (A) An aldehyde-surface forms a covalent linkage with the amino-modified oligonucleotide through dehydration (Schiff base formation) yielding a stable secondary amine. (B) Immobilization to an epoxy-surface, where the primary amine-group on the oligonucleotide mediates a nucleophilic attack and a covalent coupling to the surface. (C) Isothiocyanate on the surface forms thiourea upon reaction with the amino-modified oligonucleotide (D) An NHS-ester reacts with a nucleophilic group (NH_2) of the oligonucleotide creating a strong amide bond (E) An imidoester surface can be used to form a stable amide bond between the amino-modified oligonucleotide and a solid surface.

2.3.2 Immobilization methods for protein attachment

The protein immobilization strategy is a key step in creating a successful protein-array (Rusmini *et al.*, 2007). The immobilization of proteins to solid surface is more challenging than fabricating DNA-arrays, because protein structures are complex and they can easily lose their biochemical function due to denaturation (MacBeath and Schreiber, 2000; Ramachandran *et al.*, 2008; Templin *et al.*, 2003). It is important to achieve low non-specific binding of analytes and other components within the biological sample. Another challenge is finding an immobilization method suitable for all the attached proteins while maintaining their biological function (Kusnezow and Hoheisel, 2003; Kusnezow *et al*., 2003). Antibodies with high affinity and specificity should be used for antibody-based array fabrication (Templin *et al.*, 2002). In antigen-based assays, the antigen size variation makes array fabrication challenging; the antigen size may influence the surface interaction between antigen and solid support. The antigen may also cause steric obstacles or it may be susceptible to conformational changes upon immobilization.

Randomly orientated non-covalent immobilization

Proteins can be adsorbed to surfaces through electrostatic or hydrophobic (van der Waals) interactions, conformational changes, polar interactions and Lewis acid-base forces (Gray, 2004; Hlady and Buijs, 1996). Compared to DNA arrays, this makes protein arrays more susceptible to non-specific adsorption to hydrophobic surfaces, whereas, compared to proteins, it is much easier to suppress DNA's spontaneous adsorption to a surface because of its negative charge (Jonkheijm *et al.*, 2008). The non-covalent interaction through adsorption depends on the protein and surface used for the immobilization (Figure 3A). A problem in adsorption is insufficient accessibility of active sites. If the protein is absorbed on the solid surface in a disoriented way its conformation may change. The protein should preserve its biological function and the functional sites accessible to target molecules (Zhu and Snyder, 2003). This problem can be solved by using hydrogel arrays (Figure 3B). These arrays are composed of three-dimensional hydrophilic polymeric networks containing water, which helps the protein to preserve its native structure. However, the disadvantage of hydrogel arrays is that unbound protein is difficult to remove from the gel (Nakanishi *et al.*, 2008).

Randomly orientated covalent immobilization

Proteins can also be covalently attached to a modified two-dimensional solid surface (Figure 3D). Usually, the surface used for immobilization lacks suitable functional groups necessary for protein immobilization. The surface needs to be modified or coated before proteins can be attached. For example, in ELISA applications a widely used microtiter plate material is polystyrene, which can be chemically modified (1) by a plasma oxidation treatment with organosilanes to generate thiol-groups on a poly(dimethylsiloxane) surface, (2) by a 1,6-hexanediamine treatment to generate an amine surface on a poly(methyl methacrylate) surface, or (3) by the sulfonation of a

polycarbonate surface to generate sulfate groups for protein immobilization. (Jonkheijm *et al*., 2008) Plasma immersion ion implantation (PIII) is another surface modification technique used for polymers, that has been utilized in antibody array applications. The PIII treated nitrocellulose slides enable antibody immobilization without using linker chemistry (Kosobrodova *et al*., 2014).

The lysine side-chain amine groups in proteins together with free amino terminus are mostly used for covalent immobilization (Rusmini *et al*., 2007). The NHS-ester is the reagent most commonly used to form a stabile amide bond between protein amine groups and a solid surface. Another common method is to use an aldehyde surface, which reacts with primary amines on the proteins to form a labile Schiff's base linkage (MacBeath and Schreiber, 2000). The labile linkage can be stabilized by reduction creating a stable secondary amine linkage (Rusmini *et al*., 2007). Isothiocyanate- and epoxide- surfaces can also be utilized for the covalent immobilization of proteins through the amine groups in lysine residues. A protein molecule usually displays many lysines on its surface, and in addition to the terminal amino group, it can be covalently bound in variable orientations. Protein carboxylic acid groups (aspartic and glutamic acids form a major fraction of protein surface groups) can also be used for covalent immobilization onto an aminated surface utilizing a chemical coupling reagent (e.g., carbodiimide activation) (Fernandez-Lafuente *et al.*, 1993). In covalent immobilization, the immobilization efficiency depends on pH value, concentration, ionic strength, and reaction time (Jonkheijm *et al*., 2008).

Orientated immobilization of proteins

Oriented immobilization of the proteins will improve the surface homogeneity and the accessibility of the protein active sites for enhanced array detection. Different biologically active fusion proteins and fusion tags, e.g., cutinase (a serine-esterase), glutathione S-transferese (GST), Asp-Tyr-Lys-Asp-Asp-Asp-Asp-Lys (FLAG) peptide, and hexahistidine tag (His_6-tag) can be used for the oriented attachment of proteins to solid surfaces (Cha *et al.*, 2004; Hodneland *et al.*, 2002; Nakanishi *et al*., 2008) (Figure 3C, 3E-G). The enzyme cutinase binds to a glycol-terminated monolayer surface presenting phosphonate ligase. Hodneland *et al*., 2002, demonstrated that the protein calmodulin fused to cutinase can be used for site-specific protein immobilization. GST-tagged proteins can be immobilized onto a glutathione functionalized surface (Nakanishi *et al*., 2008). The octapeptide affinity tag FLAG has been used for subtilisin immobilization on a surface coated with protein A-conjugated anti-FLAG antibody (Wang *et al.*, 2001). Kwon *et al*., 2006, have developed a traceless fusion tag system based on split-intein-mediated protein immobilization (Kwon *et al.*, 2006). This traceless protein immobilization method is based on the interaction of N-intein attached to the protein and C-intein fragments attached to the surface. After the two fragments interact, they form an active intein domain, which binds the protein onto a solid surface. A polyhistidine-tag, or His-tag, typically consists of a string of 5–6 histidine amino acid residues. The His-tag approach combines protein purification and immobilization steps needed for inert

coating. Another benefit of His-tag approach is that the protein structure or function is not usually interfered with. However, the binding of His-tag to a nickel-coated surface is not strong (binding affinity ~ 1 μM) and this may cause the immobilized proteins to dissociate from the surface (Nakanishi *et al*., 2008; Rusmini *et al*., 2007). In addition, Kwon *et al*., 2006 have developed a traceless fusion tag system based on the split-intein-mediated protein immobilization (Kwon *et al*., 2006). This traceless protein immobilization method is based on the interaction of N-intein attached to the protein and C-intein fragment attached to the surface. After the two fragments interact, they form an active intein domain, which binds the protein onto a solid surface.

A bioaffinity approach using the high binding affinity ($K = 10^{15}\ M^{-1}$) between biotin and streptavidin is also commonly utilized in protein immobilization (Figure 3E). Streptavidin has four identical subunits, each binding one biotin molecule. The primary amine groups of the target protein are coupled with a biotin reagent. The basic biotinylation reagent is composed of the bicyclic biotin ring at one end of the structure and a reactive functional group at the other end for the biomolecule attachment. These biotinylation reagents are commercially available with linkers of different lengths. The site-specific antibody biotinylation increases the analyte-binding capacity of the streptavidin-coated surface compared to the randomly biotinylated antibodies (Peluso *et al.*, 2003). Unpaired heavy-chain cysteine of a recombinant antibody has been used for site-specific antibody biotinylation (Ylikotila *et al.*, 2005).

Antibodies can be randomly oriented on the surface, as mentioned above, but it is possible to achieve a more controlled orientation by using protein A or protein G (Figure 3F). They bind specifically to the heavy-chain constant (Fc) region of the antibody, and the antibody binding sites located on the Fab variable region remains accessible for the target antigen (Aybay, 2003). Protein A was found in the cell wall of *Staphylococcus aureus* and protein G on the surface of streptococcal cell. Both proteins interacted mainly with the Fc part of IgGs. However, the protein G is able to bind both the Fab and Fc portions of IgG, and protein A is able to bind the Fab fragment of human IgM (Aybay, 2003). Protein G offers a broader binding capacity towards different immunoglobulin species (including goat, sheep, and all murine isotypes) and IgG subclasses than protein A (Nomellini *et al.*, 2007). DNA-directed protein immobilization is another site-specific protein attachment bioaffinity strategy. In this approach, proteins are coupled with single-stranded DNA moieties through direct covalent attachment, bifunctional linkers, streptavidin-biotin interaction, or expressed protein ligation (Washburn *et al.*, 2011).

Oriented covalent protein immobilization can be achieved if only one thiol (-SH) group in the cysteine amino acid side chain is used for the attachment. The cysteine residues should be exposed in a solvent-accessible region of the protein so that the structural elements are not involved in the immobilization process. The thiol group selectively reacts with α-haloacetyl- and maleimide-modified surfaces forming a stable thioether bond (Rusmini *et al*., 2007). Free thiol groups are present at selected

locations on antibodies, but they can also be generated by chemically reducing the disulfide bridges. Cysteine can also be utilized as a functional surface. C-termini thioester conjugated proteins can be attached to a N-terminal cysteine residue surface. Copper-catalyzed 1,2,3-triazole also called "click" chemistry can be used for site-specific protein immobilization (Lin *et al.*, 2006b). This chemical method is based on alkyne- or azide-functionalized proteins which are spotted onto an azide- or alkyne-functionalized surface, respectively. Another cycloaddition reaction used for covalent protein immobilization is heat initiated Diels-Alder reaction (Sun *et al.*, 2006). The reaction usually takes place between an electronically matched dienophile and a conjugate diene to form an unsaturated six-membered cyclohexene ring structure.

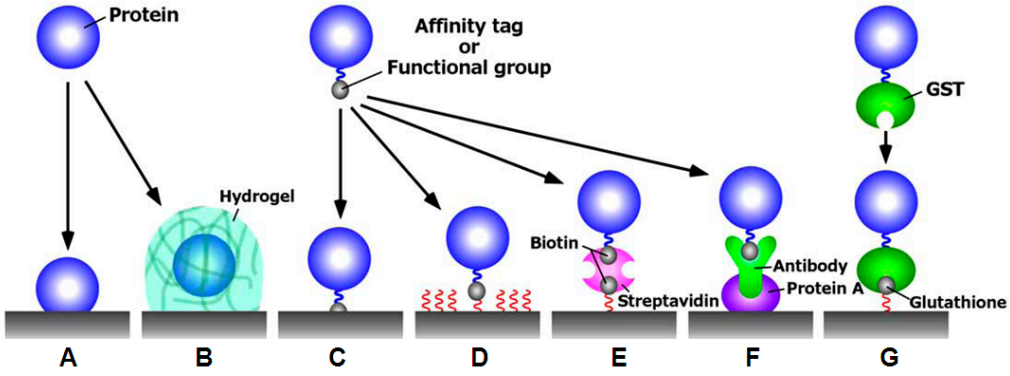

Figure 3. Protein immobilization methods. (A) Physical adsorption, (B) Hydrogel immobilization method, (C) His-tag immobilization to the Ni-coated surface, (D) Immobilization to chemically modified surface, (E) Streptavidin-mediated, (F) FLAG-tag-mediated and (G) Glutathione/GST-mediated immobilization (modified from Nakanishi *et al*., 2008).

2.4 Optical detection methods for solid-phase array

2.4.1 Fluorescent labels

Conventional optical detection methods (e.g., fluorescence, chemiluminescence, colorimetry, and surface plasmon resonance) offer sensitive and specific detection of biomolecules in sample material (Heller, 2002; Sassolas *et al.*, 2008). The traditional way of read-out the hybridization of a surface-bound target on a two-dimensional array, especially DNA arrays, is fluorescence-based detection (Nagl *et al.*, 2005). Fluorescence is a three-step process where a fluorophore or fluorescent dye absorbs a photon of light, moves to an excited state and eventually returns to ground state. In the

third stage of the process where the photon returns to the ground state it loses the energy by emission at a different wavelength than the incident light (Espina *et al.*, 2004). Fluorescence is the most attractive array detection technique due to its excellent sensitivity and specificity as well as the low cost and flexibility of the method.

Organic dyes

The most commonly used labels in bioaffinity assays are organic fluorophores. These labels are simple to use, and they are easily conjugated to different biomolecules. In addition, they have high stability, solubility and biocompatibility in aqueous buffer solutions (Nagl *et al*., 2005). The most commonly used fluorescent labels for array read-out are cyanine 3 (Cy3) and cyanine 5 (Cy5) dyes, which are usually used in one-color or two-color detection (Patterson *et al.*, 2006; Shalon *et al.*, 1996). In a one-color approach the hybridized sample is labeled with a single fluorophore (e.g., Cy3 or Cy5), whereas in a two-color approach, two samples (e.g., experimental and control) are labeled with different fluorophores (Cy3 and Cy5) and hybridized together in a single array (Patterson *et al*., 2006). Cy3 has green fluorescence (~550 nm excitation, and ~570 nm emission) and Cy5 has red fluorescence (~649 nm nm excitation and ~650/670 nm emission). Other typical organic fluorescent dyes used for array detection are derivatives of Alexa Fluor, fluorescein, rhodamine, and BODIPY (Espina *et al*., 2004; MacBeath and Schreiber, 2000).

Organic labels have many drawbacks limiting their use in bioaffinity assays. These dyes are sensitive to photobleaching, which means that the luminescence is irreversibly turned off (Schäferling and Nagl, 2006). Organic dyes are rarely bright enough to permit quantitative specific signal detection over the background fluorescence and these conventional labels have a short life-time. This is a clear disadvantage in bioaffinity assays. Moreover, their fluorescence spectra are not symmetrical and each fluorophore is characterized by its specific optimal wavelength of excitation, which limits their multiplexing capabilities (Nagl *et al*., 2005; Resch-Genger *et al.*, 2008).

Nanoparticles

Highly luminescent nanoparticles can be utilized in multiplex imaging. The nanoparticles are composed of a core-shell structure with a silica, polymers, semiconductors, metals or inorganic crystals shell and doped with luminescent materials. The silica nanoparticles embedded with Alexa Fluor 647 have been shown to increase the DNA-array detection sensitivity (Liu *et al.*, 2011). The main advantage of using nanoparticles instead of single dye molecules is that the shell structure can encapsulate many dye molecules by protecting the dopants from environmental influences in the surrounding aqueous matrix (Nagl *et al*., 2005). The shell structure also protects the fluorescent dye molecules from photobleaching, which in turn enhances the fluorescence. The functional groups on the shell also enable chemical coupling to biomolecules and can be of further use as labels in bioanalytical assays.

Quantum dots (QDs) are highly fluorescent colloidal semiconductor nanocrystals (Dabbousi *et al.*, 1997), that are 20–100 times brighter than organic fluorescent dyes (Rousserie *et al.*, 2010). Their fluorescence emission wavelengths can be adjusted by varying their size (Dabbousi *et al*., 1997). QDs of different diameters (colours) can be excited with the same excitation wavelength using a single blue or UV light source. QDs provide unique possibilities for multiplexing without an overlap of signals from different labels, enabling the quantitative detection of low fluorophore-specific signal over background fluorescence (Eastman *et al.*, 2006). Their advantages also include excitation in a broad range, narrow (20–30 nm) non-overlapping emission peaks, photostability, high quantum yield of luminescence, and good chemical stability (Resch-Genger *et al*., 2008). However, QD size (2.5–100 nm depending on the coating thickness) and stability are dependent on the core/shell components (Hardman, 2006). The drawbacks of these labels are single crystal emission blinking and a lower quantum yield compared to the organic dyes (Bagwe *et al.*, 2004). A further drawback is also that the QD core is composed of toxic heavy metals (e.g., cadmium) making these labels unsuitable for *in vivo* applications (Hardman, 2006). Fluorescent organic dyes and QDs are normally excited by ultraviolet or visible light, which may induce autofluorescence, resulting in low signal-to-noise ratio and limited sensitivity. Because of these drawbacks, another novel label technology with crystals known as upconverting phosphors have been developed.

2.4.2 Upconverting phosphors

Upconverting phophors (UCPs) are inorganic crystals composed of a host lattice doped with trivalent rare earth lanthanide ions (Ln^{3+}). These Ln^{3+} ions can exhibit sharp luminescence emissions via electronic transitions (Auzel, 2004). They have also remarkable luminescence properties, such as narrow bandwidth, long-time emission, and anti-Stokes emission. Conventional fluorescent labels are downconverting, which means that they convert higher-energy (shorter wavelength) light to lower-energy (longer wavelength) emitted light. However, UCPs have a capability to sequentially absorb two or more photons when they are excited with low-energy near-infrared radiation and they emit photons of higher energy at the visible wavelengths (Figure 4). Thus, the UCP emission is anti-Stokes shifted. Most of the Ln^{3+} ions can undergo an upconversion process, but only a few Ln^{3+} ions (e.g., Er^{3+} and Tm^{3+}) produce efficient upconversion. The activator dopant ions, commonly Er^{3+}, Tm^{3+} and Ho^{3+}, are absorbing and emitting the photons. Usually, UCP crystals are doped with two ions, an activator ion and a sensitizer ion (usually Yb^{3+}), to enhance the upconversion efficiency (Haase and Schäfer, 2011). The sensitizer ions absorb the excitation energy and transfer it to the activator ions, which produce the emission (Figure 5A). The principle of upconversion is illustrated in Figure 5B.

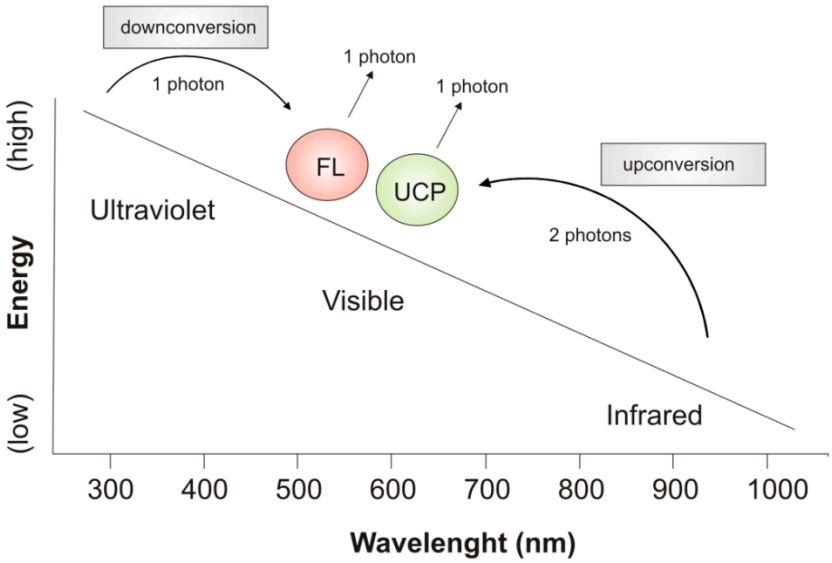

Figure 4. Basic principle of downconversion and upconversion photoluminescence processes. Fluorescent label (FL) absorbs a single high-energy photon and emits a lower energy photon. In contrast, upconverting phosphor (UCP) sequentially absorbs two (or more) low energy photons and emits one higher energy photon at visible wavelengths.

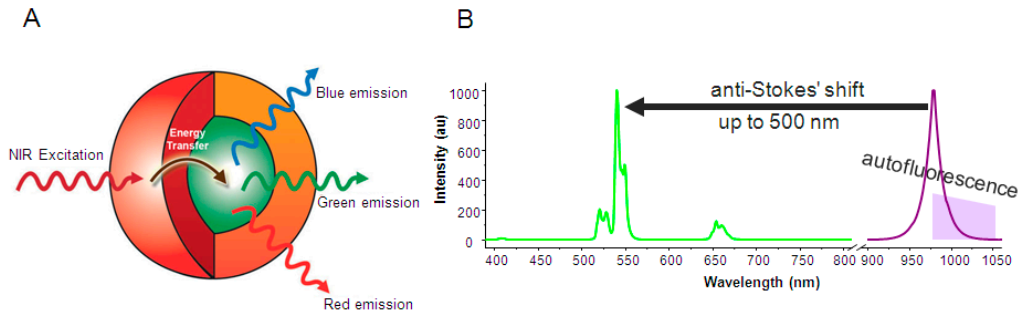

Figure 5. (A) Illustration of nanoparticle architecture showing the absorption of NIR light by the shell (red) and subsequent energy transfer to the Er^{3+} / Yb^{3+} co-doped core (green), which leads to emission in the blue, green, and red wavelength regions. (Vetrone *et al.*, 2009) (B) The anti-Stokes photoluminescence, i.e., upconversion process of the UCPs. UCPs are excited with low-energy near-infrared radiation and emit photons of higher energy at visible wavelengths in the absence of autofluorescence (modified from Soukka *et al*., 2005).

Halides (e.g., $NaYF_4$), oxides (e.g., Y_2O_3) and oxysulfides (e.g., Y_2O_2S) have been used as host materials. The most common and efficient near-infrared to visible upconverter host is $NaYF_4$ halide. Compared to other halides (e.g., chlorides and bromides) $NaYF_4$ fluoride is a more suitable host material due to its high refractive index, high chemical stability, high transparency arising from low-energy phonons, and minimized energy loss by non-radiative relaxation. Chlorides and bromides are also sensitive to moisture and are, therefore, unsuitable for labeling biomolecules. These advantages further lead to a low probability of nonradiative decay and increased luminescence quantum yield. In addition to the host material also the crystal structure influences the efficiency of the upconversion emission (Heer *et al.*, 2004; Wang *et al.*, 2011). The challenge is to synthetize UCPs with controlled particle shape while maintaining uniformity in size and surface functionality. These challenges have limited the use of UCPs in bioanalytical studies.

Upconversion mechanism

Converting long-wavelength infrared radiation into short-wavelength light is called an anti-Stokes emission process. Simultaneous two-photon absorption is a well-established method for generating anti-Stokes emissions from a host of luminescent materials, such as semiconducting nanoparticles (Larson *et al.*, 2003). Alternatively, second-harmonic generation can be used to produce an anti-Stokes emission (Franken *et al.*, 1961). However, these two methods require expensive pulsed lasers with high-density excitation (10^6–10^9 W cm^{-2}). Another anti-Stokes emission process called upconversion process involves real long-lived metastable states with lifetimes on the microsecond scale, and in this case inexpensive continuous-wave lasers can be used to excite the upconverting materials. Upconversion, typically energy transfer upconversion (ETU), is an efficient way to produce an anti-Stokes emission. ETU is realized through energy transfer between two neighboring ions in close proximity. In this process, a sensitizer ion absorbs a photon and is excited to the intermediate level (located in the NIR). The sensitizer ion non-radiatively transfers the energy to the activator ion, which excites to the intermediate level while the sensitizer ion relaxes back to the ground stage. A second energy transfer promotes the activator ion to the emitting level (located in the visible wavelengths). Two other basic upconversion mechanisms are excited state absorption, and photon avalanche (Wang and Liu, 2009). $NaYF_4$ doped with Yb^{3+} and Er^{3+} produces green, red and blue upconversion luminescence. A change in the temperature, the particle morphology and size, the average distance between the neighboring dopant ions, and dopant ion concentration all have dramatic effects on the UCP efficiency and the luminescent properties. The most obvious effect is a change in the color of the emitted light. (Suyver *et al.*, 2005; Vetrone *et al.*, 2004)

Surface modification

Synthetized UCPs have no functional surface groups that could be used for the attachment of a biomolecule (e.g., proteins, DNA, or biological macromolecules). A surface modification step is needed to turn the UCPs from hydrophobic into water-

dispersed and introduce functional groups on the particle surface for subsequent biomolecule conjugation. Surface modification by a silica shell is the most common, and practical approach, which creates functional groups (e.g., amino or carboxylic acid groups) on the UCP surface. The silica shell has some attractive properties as it is chemically inert, optically transparent, and resistant to swelling or porocity changes in the event of a pH variations. The functional groups introduced on the silica shell can be used for linking biomolecules covalently to UCPs; the biomolecule must also bear a functional group to form the covalent bond. After the UCP biomolecule conjugation reaction the unbound biomolecules and unreacted chemicals can be separated from the bioconjugated UCPs by using a high gradient magnetic separation system based on the intrinsic paramagnetic properties of the lanthanide ions. This process is especially suitable for the purification of nanosized upconverting particles (UCNPs). (Arppe *et al.*, 2013)

UCP reporters in bioanalytical assays

Previous work with UCPs has demonstrated the high sensitivity potential of this reporter technology in multiple applications (Corstjens *et al.*, 2005; Kuningas *et al.*, 2005b; Rantanen *et al.*, 2009; Soukka *et al.*, 2008; Zijlmans *et al.*, 1999). UCP technology has been used in *in vitro* nucleic acid assays and immunoassays for the assay detection. It is also a suitable photoluminescence imaging technique for *in vitro* and *in vivo* applications because the NIR excitation is safe for biological tissue and enables deep tissue penetration. UCPs have already been used in *in vivo* luminescence imaging (Mi *et al.*, 2011; Wang *et al.*, 2013a). They have many advantages that make them attractive labels for imaging based assays. A main advantage is that the background is eliminated at visible wavelengths under infrared radiation. The autofluorescence originating from the assay material (e.g., plastic microtiter plate) or biological sample and scattered infrared excitation light can be avoided by using an infrared flux to excite the UCPs and collecting the emission at the visible wavelengths. This enables a simple fluorescence read-out and fluorescence scanning or imaging from solid-phase, similar to conventional fluorescence, but it also adds the advantage of total background reduction enabling sensitive assays (Soukka *et al.*, 2005; van de Rijke *et al.*, 2001).

2.4.3 Instrumentation

For the detection of surface-bound targets many different array readers can be used. The fluorescence array readers are based on the fluorescence intensity measurement. These instruments are composed of an excitation light source, optical filters and a detector. There are basically two different approaches for array detection: scanning the array surface point by point or the illumination of the entire array surface simultaneously (imaging). Both of these techniques are discussed in more detailed below.

Scanning

Scanners are opto-electro-mechanical devices for array read-out. The instruments are equipped with one to three laser light sources, a detector, and electricity along with moving mechanical parts (Bally *et al.*, 2006; Schäferling and Nagl, 2006). With a focused laser beam of a few microns in diameter, line-by-line scanning of the array surface is performed deflected in the x and y directions, and moving the array or lenses relative to the laser beam (Lyng *et al.*, 2004). Based on the moving mechanical parts, the scanners can be classified as lens moving array scanners, where the lenses in the scanner move while the array is scanned, or as moving array scanners (Figure 6), in which the array platform moves while scanning is in process. The latter approach causes less scanning errors than the former one. For the sample illumination, different light sources (e.g., laser or white light) can be used along with the optical filters enabling the selection of the proper excitation wavelength for the fluorescent dyes. The mirrors, filters, and lenses enable the separation of dye emitted light from unwanted light. The array is scanned pixel by pixel and the emission is collected by a photo multiplier tube (PMT) or charge-coupled device (CCD) camera. The detector amplifies the signal from each photon, and the amplified photons are converted into a digital value that represents the signal intensity at each pixel position creating an image (Pickett, 2003). In the confocal array scanner, a focused laser beam is used for the projection of excitation light and only a focused light is collected through a pinhole (Perraut *et al.*, 2002). When using confocal detection optics, the fluorescent background signal originating from the bulk solution can be reduced because these photons have a low probability of reaching the detector through the pinhole (Bally *et al*., 2006).

The most common scanner is the two-color array scanner utilizing PMT detection. The scanner uses two independent lasers, and depending on the laser, one or two independent PMTs for signal detection. The lasers are used to excite the red and green fluorescent molecules either simultaneously or in subsequent scans. The separate bands of the emitted red and green photons are passed through optical filters to PMT for detection. The two images of the entire array, one for each dye, are constructed after transforming the photons into a digital value. Typically a 16-bit tagged image file format (tiff) image corresponding to the intensity and location of each color of fluorescent molecule is created. Bits per pixel (bpp) determine how many colors or shades of gray each pixel can represent (e.g., a 1 bpp image uses 1-bit for each pixel, so the pixel can be either on or off: $2^1 = 2$ colors; 16 bpp: $2^{16} = 65{,}536$ colors). (Schäferling and Nagl, 2006)

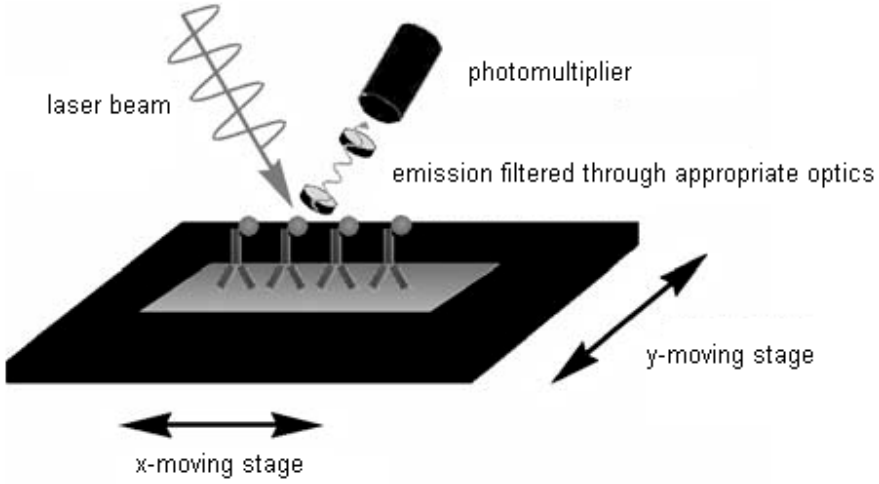

Figure 6. The main components of a moving array scanner (Schäferling and Nagl, 2006).

Hyperspectral scanning

In standard array scanners, the wavelength selectivity is obtained by positioning band-pass filters in front of a detector. However, hyperspectral scanners can be used for multicolor array detection. They record the entire visible emission spectrum within the imaged array area. This allows the discrimination of multiple, spectrally overlapping fluorescent labels with minimal use of optical filters. Hyperspectral scanning uses two lasers for the excitation of dyes in the visible and near-infrared spectral regions. In addition, two-sided oblique line illumination is used. This is generated with a Powell lens combined with proper optics and CCD detector. The scanned data is assembled into a three dimensional hyperspectral data cube containing the full emission spectrum for each x-y location on the sample. Hyperspcetral scanning coupled with multivariate analysis enables the elimination of unwanted artifacts and produce contaminant-free images. (Erfurth *et al.*, 2008; Sinclair *et al.*, 2004; Timlin *et al.*, 2005)

Imaging

Imaging is another technique used for array detection. Compared to scanning, imaging an array saves time and eliminates alignment problems. The CCD arrays can be used for 2-D imaging to improve time-resolution and perform real-time imaging (Mogi *et al.*, 2011). The CCD photodetector is constructed from silicon, which is organized as a regular array of thousands or millions of light-sensitive regions called pixels. The photodiodes are used for photon detection by capturing and storing image information in the form of a localized electrical charge that varies with incident light intensity.

CCD's are not as accurate as PMT's but they have multiple pixels that allow the imaging of the entire array at once (Schäferling and Nagl, 2006). The imaging significantly reduces the time needed for array detection compared to array scanning.

Array detector performance

The reader instruments should have high sensitivity, resolution, signal-to-noise ratio, and wide dynamic range in order to produce reliable digital images. The pixel saturation rate and signal-to-noise ratio (SNR) are two important characteristics used to evaluate the array detector performance, i.e., signal quality and reliability. The pixel saturation is caused by the physical limitation of the array detector. This happens when the detected number of photons exceeds the maximum number that the detector can process (Yang *et al.*, 2011). If the saturation is reached, the measured spot intensity is underestimated. The pixel saturation can be avoided by adjusting the detector voltage appropriately. In case of low-intensity spots higher detector settings can be used to improve the SNR. The SNR quantifies how well a system can separate the specific spot signal from the background noise. The detectors, such as PMT and CCD, have many sources of noise. The major sources of noise associated with the CCD camera are dark noise, read-out noise, and shot noise (Salama *et al.*, 2004). The read-out noise originates from the conversion of the electrons in each pixel to a voltage on the detector output node. Shot noise present on the image itself is due to the random arrival or fluctuation of photons on the detector, which produces noise electrons. Dark signal is inherent from electrons generated by thermal excitation instead of by photoexcitation and it increases with long exposure times. To reduce dark signal and to achieve better SNRs CCD's are cooled before the detection (Golden and Ligler, 2002).

2.4.4 Other selected detection methods and their applications

Surface-enhanced Raman scattering

Surface-enhanced Raman scattering (SERS) is enhanced Raman scattering of molecules adsorbed on a surface. The Raman signal provides information about the unique vibrational modes of molecules. A Raman dye can be either fluorescent or nonfluorescent, and a dye molecule can be chemically modified to have a different Raman spectrum (Cao *et al.*, 2002; Kneipp *et al.*, 1999). The Raman labels have many advantages. Firstly, photobleaching is absent in Raman scattering. Secondly, SERS peaks are narrow (below 0.5 nm), so spectral overlap is minimized, and thus a large number of coding can be created by a combination of chemicals (Chen *et al.*, 2008). The Raman signal from the sample can be significantly enhanced via adsorption on a metallic nanostructured surface. The signal amplification results from an increased electromagnetic field experienced by the molecules in close proximity to the metal surface (Driskell *et al.*, 2010). The characteristic Raman spectrum can act as a vibrational fingerprint to directly identify molecules in proximity to the metal substrate. The Raman reporters coupled to gold nanoparticles (Hong and Li, 2013;

Kim *et al.*, 2012; Li *et al.*, 2008) or silver nanoparticles (Jun *et al.*, 2007) are used to enhance the Raman scattering of molecules adsorbed on metallic surface. The SERS nanoparticle labels are suitable for low-density multiplex testing (Cao *et al.*, 2003). The functionalized multicolor single-walled carbon nanotube Raman tags can also be used for multiplex assays (Chen *et al*., 2008). The SERS method has been used in multiplex rotavirus diagnostics. Driskell *et al*., 2010, developed a rapid and sensitive assay for the detection and typing of rotaviruses. The assay was able to discriminate the rotavirus-positive samples from the rotavirus-negative samples by the spectral shape. In addition, the SERS spectra are similar for each positive strain but based on the relative intensities of each band the strain and genotype could be determined (Driskell *et al*., 2010). Another example of multiplex SERS detection is a silver nanorod array for the rapid detection of influenza viruses, adenoviruses, and respiratory syncytial viruses (Shanmukh *et al.*, 2006).

Chemiluminescence

The ELISA microwell immunoassays are applicable for the development of chemiluminescence-based insoluble array assays (Avseenko *et al.*, 2002). In the chemiluminescence process the emitted light is produced by a chemical reaction. Alkaline phosphatase (AP) and horseradish peroxidase (HRP) are commonly used enzymes in chemiluminescence detection systems. Mendoza *et al*., 1999, used the AP enzyme to catalyze the enzyme-labeled fluorescence (ELF) substrate, which produced a fluorescent precipitate. The emission from a precipitated spot was detected by scanning the array with a CCD imager equipped with a UV light source (Mendoza *et al.*, 1999). Wiese *et al*., 2001, have developed a quantitative multiplex ELISA for the simultaneous measurement of PSA, α_1-antichymotrypsin-bound PSA, and interleukin-6 (Wiese *et al*., 2001). An antigen-based allergen array utilizing tyramide signal amplification was developed. This method used Alexa546-labeled tyramide coupled to a biotinylated anti-hIgE and a streptavidin-coated HRP system as the reporter for allergen-specific IgE's on array. The tyramide amplification system was sensitive enough to detect amounts below 1 fg of allergen-bound IgE in human serum (compared to 24 fg without tyramide amplification) (Bacarese-Hamilton *et al.*, 2002).

Colorimetry

Enzymes used for chemiluminescence detection can also be used in colorimetric detection to form a colored precipitate. The colorimetric detection method is not as sensitive as the fluorescence or chemiluminescence systems, but it can be utilized in a low-density array detection method. A DNA-array based on enhanced colorimetric detection has been developed e.g., for the detection of Staphylococci species, the enhancement was obtained by using the silver precipitation onto nanogold particles. In this colorimetric multiplex approach, the detection limit was comparable with that of the conventional fluorescent label based array detection (Alexandre *et al.*, 2001). In addition, Le Goff *et al*., 2011, have used immobilized glucose oxidase on a porous membrane for the local *in situ* production of the hydrogen peroxide necessary for

3,3',5,5'-Tetramethylbenzidine (TMB) oxidation by HRP. This enhanced colorimetric detection yielded blue precipitated positive spots (Le Goff *et al.*, 2011). Moulton *et al*., 2011 have utilized a signal amplified ampliPHOX colorimetric detection method for influenza DNA-array. Here, the biotinylated targets are captured on the array and labeled with a streptavidin coupled photoinitiator (ampliTAG). In the next step, light activates the ampliTAG, which generates signal amplification through the polymerization of an organic monomer (ampliPHY) only in regions with ampliTAG targets. After polymerization transparent solid polymer spots are formed, and the spots are finally stained red (Moulton *et al.*, 2011).

Label-free detection

Label-free detection requires sophisticated instrumentation and it is usually not as sensitive as label-based detection (Ray *et al*., 2010). Two selected label-free methods, i.e., surface plasmon resonance imaging and imaging ellipsiometry are discussed. Surface plasmon resonance imaging (SPRi) technology is a label-free real-time method for visualizing the array with a laser diode and capturing the whole array image by a CCD camera. The SPRi measures the reflectivity of the incident light at a fixed angle and the reflectivity is correlated with the changes on the array surface (Yu *et al.*, 2006). The SPRi have been used for the rapid and specific multiplex detection of bacterial pathogens (Bouguelia *et al.*, 2013). Immobilized proteins on a gold-covered glass prism surface provide SPRi information from each active spot simultaneously. With the real-time visualization of the entire biochip surface, SPRi can monitor the reflection intensity of hundreds of molecular interactions continuously and simultaneously. This creates a multi-array format of molecular probes formed as circular or square spots. The array quality can be monitored by viewing the surface image of the measurement area. The regions of interest are selected, for example, according to spot shape, size and quality. Direct image control of the surface also helps to identify and reduce the ubiquitous problem of non-specific binding by defining spots without receptors and spots on gold, to be used as negative control surfaces. However, the drawbacks of SPRi are low sensitivity and non-specific adsorption, which cause high background reflection intensity. Higher sensitivity is achieved when SPRi is used with a combination of fluorescent label. Gold nanoparticles can also be used for signal enhancement in SPRi (Scarano *et al.*, 2010).

Imaging ellipsiometry is another label-free detection method that can be utilized for array detection. Imaging ellipsiometry measures change in the polarization state of the incident light, which depends on the thickness of thin films and the optical properties of surface layers. In this detection method, the surface of an array can be scanned by a laser beam with an x/y-resolution of approximately 1 μm. The polarization analyzer is combined with a CCD camera and ellipsometric contrast images can be generated, visualizing the thickness of a surface coating in relation to the blank area around the spots. (Ray *et al.*, 2010; Schäferling and Nagl, 2006) Imaging ellipsiometry is preferentially used for array development, quality control purposes, and the

characterization of monolayer properties. In one application, this method has been used for the detection of hepatitis B virus markers in an array format (Qi *et al.*, 2009).

2.5 Viruses and proteins used in the studies

2.5.1 Human adenoviruses

Human adenoviruses (hAdVs) belong to the genus *Mastadenovirus* of the family *Adenoviridae*. In humans, there are over 60 different adenovirus (hAdV) genotypes, which are classified into seven sub-groups or species designated A to G (Robinson *et al.*, 2013). An adenovirus particle is composed of an icosahedral, non-enveloped, medium sized (70–90 nm diameter) nucleocapsid. Inside the capsid, there is a linear double-stranded DNA genome (~ 35 kb). The outer side of the capsid is composed of two major proteins: hexons (n = 240) as trimeric subunits and pentons (n = 12). Pentons are composed of two distinct structural units: a pentameric penton base associated with a trimeric fiber (Figure 7). The fiber facilitates the virus attachment to host cell receptors. Along with the different DNA homology and genome stability (e.g., GC content), the fiber length varies between the hAdV genotypes (Ádám *et al.*, 1986). The type-specific determinants are present in the hexon and penton proteins (Wigand *et al.*, 1982). Based on sequence analysis, hexon protein sequence can be divided into four conserved (C1 to C4) and three variable regions (V1 to V3) (Figure 8). The conserved regions (765 amino acids) are constant in length, and the protein sequences differ by less than 15%. Many approaches for the detection and typing of hAdVs are specifically based on the hexon variable or conserved sequences (Biere and Schweiger, 2010; Cao *et al.*, 2011; Ebner *et al.*, 2005; Ebner *et al.*, 2006; Lu and Erdman, 2006). Due to the very efficient nuclear entry mechanism of the adenovirus and its low pathogenicity for humans, adenovirus vectors have become widely used as gene transfer and vaccine vectors for the treatment or prevention of malignant diseases (Shiver *et al.*, 2002; Sullivan *et al.*, 2000; Vogels *et al.*, 2003).

Epidemiology

Adenoviruses cause epidemic (many cases in a given area in a short period of time), endemic (constantly present in a population), and sporadic (occasional cases) infections worldwide. Adenovirus infections usually occur during late winter, spring, and early summer, but infections may occur throughout the year (Chen *et al.*, 2013; Jin *et al.*, 2013). Most adenovirus infections occur early in life, and by the age of 10 years, most children have been infected with at least one type (Jin *et al*., 2013; Pacini *et al.*, 1987). Adenovirus infections are also frequent among adults. The epidemiological characteristics of hAdV infection vary by viral genotype. Different hAdV types cause a wide range of acute and chronic diseases and, depending on the geneotype of the virus, adenovirus can cause acute respiratory syndrome, conjunctivitis, keratoconjunctivitis, gastroenteritis, and haemorrhagic cystitis. Not all of the known hAdV types cause illness, and approximately half of the types are only rarely encountered and may or may not act as pathogens in a recognizable disease.

Acute respiratory diseases are mainly caused by species B, C, and E (C01, C02, E04, C05, C06 B03, B07, B11, and B14) (Guo *et al.*, 2012; Lai *et al.*, 2013; Zou *et al.*, 2012). Types D08, D19, and D37 in sub-group D are known to cause epidemic keratoconjunctivitis characterized by inflammation of the conjunctiva and cornea (Kaneko *et al.*, 2009). Gastroenteritis has been mainly associated with sub-group F types F40 and F41 (Li *et al.*, 2004; Uhnoo *et al.*, 1984). The presence of hAdV type D36 antibodies in the serum has been associated with pediatric obesity and severe obesity in adults but direct evidence of obesity induced by the virus comes only from animal experiments (Almgren *et al.*, 2012). Diseases caused by hAdV types are usually mild, but severe infections are not uncommon. Children, and in some circumstances also healthy adults, may develop pneumonia or even acute respiratory distress syndrome, and in immunocompromised patients (e.g., patients with one of the immunodeficiency diseases, patients being treated with cytotoxic and immunosuppressive drugs, or blood and bone marrow transplant recipients) hAdV infection can cause life-threatening disease (Chen *et al*., 2013; Chuang *et al.*, 2003; Hierholzer, 1992; Kuo *et al.*, 1990; La Rosa *et al.*, 2001).

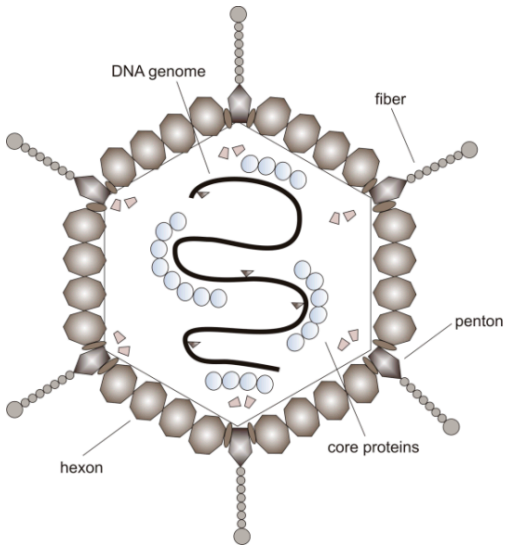

Figure 7. Adenovirus particle. Adenoviruses are non-enveloped, double-stranded DNA viruses with icosahedral capsid. Viral capsid is mainly composed of hexon proteins and pentons. Fiber facilitates the virus attachment to host cell receptors.

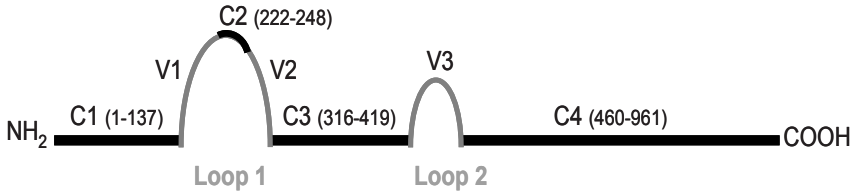

Figure 8. Schematic illustration of the hexon protein sequence structure. Conserved region can be divided into four regions C1 to C4 (amino acid positions). The amino acid positions are based on the reference serotype C02. Variable regions (V1 to V3) are located in the loops 1 and 2. The V1 to V3 regions are on the outer surface of the virus particle and represent potential epitopes for recognition by neutralizing antibodies (modified from Ebner *et al*., 2005).

Adenovirus types B03, E04, and B07 are more virulent and are more likely to spread than other hAdVs and they commonly cause outbreaks (Barraza *et al.*, 1999; Kim *et al.*, 2003; Lebeck *et al.*, 2009; Mizuta *et al.*, 2006). These types are most commonly associated with acute respiratory infections. In addition, the hAdV types B04 and B03 have been reported to cause outbreaks of febrile disease with conjunctivitis by spreading in small lakes or swimming pools without adequate chlorination (Artieda *et al.*, 2009; D'Angelo *et al.*, 1979; Xie *et al.*, 2012).

Since 2007, previously rarely reported hAdV type B14 has been associated with several outbreaks of acute respiratory illness among U.S. military recruits and the general public (Louie *et al.*, 2008; Tate *et al.*, 2009). The hAdV type B14 was first reported in Oregon in 2005 as the dominant hAdV type (Lewis *et al.*, 2009). This type has also emerged in Europe and China causing severe and also fatal infections (Carr *et al.*, 2011; Huang *et al.*, 2013; O'Flanagan *et al.*, 2011; Parcell *et al.*, 2014) The development of new rapid diagnostic tools for the identification and improved surveillance of these emerging genotypes and new variants causing severe diseases is important and may assist in the development of targeted antiviral agents or type-specific vaccines. The benefits of vaccination against hAdV infections have been demonstrated by the experience in the US military where, from 1970, basic trainees were vaccinated against hAdV genotypes E04 and B07. In the mid-1990s, the adenovirus vaccine manufacturer stopped the vaccine production, and in 1999, the supplies were exhausted, after which especially the genotype E04-associated febrile respiratory illness returned to basic training installations. Recently, the adenovirus tablet vaccine was restored to use at all U.S. military recruits. Disease and adenovirus genotype E04 isolation rates have fallen dramatically since vaccinations resumed in October 2011 and they continue to remain very low (Hoke and Snyder, 2013).

2.5.2 Human parvovirus B19

Human parvovirus B19 (B19V), belonging to the family *Parvoviridae* and genus *Erythrovirus*, was first identified in 1974 (Cossart *et al.*, 1975; Siegl *et al.*, 1985). B19V is a small, icosahedral, non-enveloped (18–25 nm diameter) virus. Inside the protein shell, i.e., the capsid, is a single stranded linear DNA genome. The virus capsid is formed of 60 subunits of two capsid proteins, VP1 (4% of the capsid, molecular mass 84 kDa) and VP2 (96%, 58 kDa). These two structural proteins have identical amino acid sequences, but VP1 has an extra, unique sequence region at the N-terminus. (Kaufmann *et al.*, 2004; Ozawa and Young, 1987) The B19V is replicating in erythrocyte precursors (Heegaard and Brown, 2002). In patients with hemolytic disorders, the B19V may cause an aplastic crisis, which transiently halts the production of red blood cells in the bone marrow. In immunocompromised patients, a persistent B19V infection will cause pure red cell aplasia and chronic anemia. The B19V is causing infections worldwide. In children, B19V causes erythema infectiosum (i.e., rash), whereas in adults, the infection is often asymptomatic, but may also be associated with arthralgia, which produces polyarthritis resembling rheumatoid arthritis. Polyarthritis is defined as inflammation (i.e., swelling, tenderness, and warmth) of five or more small joints. In pregnant women, the primary B19V infection may cause foetal damage, such as fetal death *in utero*, fetal hydrops, or development of congenital anemia especially before 20 weeks gestation (Giorgio *et al.*, 2010; Heegaard and Brown, 2002).

Virus-like particles

B19 virus-like particles (B19-VLPs) made of VP2 proteins are self-assembling non-infective bionanoparticles that are identical to natural virions, but contain no DNA (Pattenden *et al.*, 2005; Sánchez-Rodríguez *et al.*, 2012). On their surface, these particles expose multiple conformational epitopes that are recognized by IgG antibodies produced in acute phase of infection as well as during convalescent phase. By contrast, chemically denatured VP2 particles exhibiting linear epitopes are recognized exclusively by acute-phase IgG antibodies (Söderlund *et al.*, 1995b). Self-assembled VLPs (VP2) can be produced *in vitro*. Typically, recombinant VP2 protein is expressed in a baculovirus expression system and production is carried out in eukaryotic expression systems (e.g., *Spodoptera frugiperda* cells). (Kaikkonen *et al.*, 1999) pH, temperature and ionic strength are critical parameters that determine the VLPs' stability. Homogeneous VLPs assemble at neutral pH, while the small intermediates are formed at acidic and basic pHs, with low ionic strength. The *in vitro* self-assembled VLPs are highly stable at 37°C, and a significant fraction of these particles remain assembled after 30 min at 80°C (Sánchez-Rodríguez *et al*., 2012).

Prevalence and diagnosis of B19V infection

The diagnosis of B19V infection is primarily based on the detection of B19V specific IgM and IgG antibodies in serum by an immunoassay. The IgM antibodies appear within 2 to 3 days after onset of symptoms (rash) and may persist up to 4 months

(Heegaard and Brown, 2002). B19V IgG appears a few days after IgM and usually the immunity lasts for a lifetime (Heegaard and Brown, 2002). Acute or recent infection is usually diagnosed by measuring serum IgM antibody levels, IgG seroconversion, or rising titres of IgG (Enders *et al.*, 2006; Sabella and Goldfarb, 1999). Two ELISA assays based on IgG epitope-type specificity (Söderlund *et al*., 1995b) and IgG avidity measurement (Söderlund *et al.*, 1995a) have also been developed to discriminate primary B19V infection from secondary infections. It has been demonstrated that IgG antibodies are synthesized against an immunodominant heptapeptide (Lys-Tyr-Val-Thr-Gly-Ile-Asn) epitope in the VP2 molecule, exclusively, in the acute phase of B19V infection (Kaikkonen *et al*., 1999). Besides the peptide, chemically denatured VLPs also exhibiting linear epitopes are recognized exclusively by acute-phase IgG antibodies (Kaikkonen *et al.*, 2001; Söderlund *et al*., 1995b).

The prevalence of IgG antibodies directed against B19V increases with age. In infants under one year of age, the maternally derived anti-B19V IgG antibody levels fade with time. The anti-B19V IgG prevalence varies from 2–15% in small children between the ages of 1-5 years, 15–60% in older children and in young adults between the ages of 6-19 years, 30–60% in adults, and > 85% in the geriatric population. (Anderson *et al.*, 1986; Cohen and Buckley, 1988; Tsujimura *et al.*, 1995). As B19V infection may cause complications during pregnancy, especially at the beginning when the fetus has not developed an immune system, the screening of B19V specific IgG and IgM antibodies in pregnant women is important.

2.5.3 Selected analytes for multiplex immunoassay

Prostate-specific antigen (PSA), thyroid-stimulating hormone (TSH), and luteinizing hormone (LH) were selected as model analytes in the quantitative multianalyte immunoassay study performed for the purposes of this thesis. Even though the measurement of this panel of analytes in an array format is not clinically very relevant, these markers were chosen for a practical reason because of their availability. Furthermore, diagnostic tests have been developed for these analytes to measure specific antigen levels in serum or plasma.

Prostate specific antigen

Prostate specific antigen (PSA) is widely used as a serum biomarker to assist in the diagnosis of prostate cancer and to assess patient response to treatment and recurrence of cancer. PSA belongs to the protease family of kallikreins and is also known as human kallikrein 3. The PSA protein can exist in the blood by itself as free PSA, or bound to other substances (e.g., protease inhibitors) as complexed PSA (Lilja *et al.*, 1991). Total PSA is the sum of the free and the bound forms and it is measured with the standard PSA test or an antibody-based array test (Järås *et al.*, 2012; Mitrunen *et al.*, 1995). A test for the measurement of four different kallikrein forms in blood (total PSA, free PSA, and intact PSA and kallikrein-related peptidase 2) can reduce unnecessary biopsy during prostate cancer screening (Vickers *et al.*, 2010).

Thyroid-stimulating hormone

TSH is essential for the maintenance of normal thyroid function, and it is used in the diagnosis of thyroid gland disorders (e.g., primary and secondary hypo- and hyperthyroidism) (Kaplan, 1999). Congenital hypothyroidism may cause low birth weight and lead to mental retardation. Sensitive TSH assays are needed for screening of neonatal hypothyroidism. (Bernal *et al.*, 2003; Korada *et al.*, 2009; LePage *et al.*, 2004). Sensitive TSH assays are also suitable for monitoring thyroid hormone therapy and patient responses to treatment, evaluating thyroid dysfunction in nonthyroidal illnesses, and screening for thyroid dysfunction. A highly sensitive spot-based solid-phase immunoassay has been developed for the detection of very low levels of TSH (Ylikotila *et al*., 2005).

Luteinizing hormone

Luteinizing hormone (LH) is a glycoprotein that stimulates the gonads in both males and females. This hormone plays a central role in reproduction. LH levels are used to diagnose central precocious puberty and menopause, to pinpoint ovulation, and to diagnose pituitary disorders (Ahmed Ebbiary *et al.*, 1994; Hall *et al.*, 1998; Houk *et al.*, 2009; Young *et al.*, 2003). Increased LH concentrations are measured during renal failure, cirrhosis, hyperthyroidism, and severe starvation, while low levels may indicate infertility in both males and females. (Balen *et al.*, 1995; Karagiannis and Harsoulis, 2005; Smith *et al.*, 1975; Tsutsumi and Webster, 2009). A commercial quantitative multiplex fertility biomarker immunoassay on 96-well plates for the simultaneous measurement of LH, follicle stimulating hormone and progesterone using electrochemiluminescence detection has been developed (Meso Scale Discovery, MD, USA).

3 AIMS OF THE STUDY

The overall aim was to study the feasibility of upconverting phosphor label technology in multiplex assay platforms. For this purpose, DNA- and protein-based array-in-well model assays in 96-well microtiter plate format were developed for human adenovirus genotyping, multiplex antigen detection, and multiplex viral serodiagnostics. In all of the studies, luminescent upconverting phosphor label technology was used as the detection method. The upconverting phosphor fluorescence emission intensity was detected by a new imaging device suitable for anti-Stokes photoluminescence imaging and it was used in all of the studies for capturing the images from the wells.

The specific aims of the study were:

1. To develop an oligonucleotide-based array-in-well hybridization assay utilizing upconverting phosphor labels and a new anti-Stokes photoluminescence imager.

2. To evaluate the capability of using upconverting nanoparticle labels in a quantitative antibody-based multianalyte immunoassay.

3. To study human adenovirus epidemiology in Finland by an array-in-well assay method.

4. To create a multiplex serodiagnostic array-in-well assay utilizing upconverting phosphor label technology.

4 MATERIALS AND METHODS

The detailed descriptions of the materials and methods employed in this study can be found in the papers (**I-IV**). A brief summary with some additional information is presented here.

4.1 Reagents and samples

4.1.1 Upconverting phosphors (I-IV)

Synthesis

The crystalline $NaYF_4$:Yb^{3+} Er^{3+} materials used in Study **I** were prepared with the co-precipitation method as described previously (Hyppänen *et al.*, 2009) and the nanosized $NaYF_4$:Yb^{3+},Er^{3+} materials used in Studies **II-IV** with the oleic acid solvent method as described in Study **II** (Supplementary material). The particles were synthetized in the Laboratory of Materials Chemistry and Chemical Analysis, University of Turku.

Surface modification and biomolecule conjucation to UCPs

The inorganic $NaYF_4$:Yb^{3+},Er^{3+} materials have no functional groups on the particle surface. The surface is chemically modified which creates reactive functional groups useful for the covalent conjucation of biomolecules. The surface modifications and biomolecule conjugation are described in more detailed in Studies **I-IV**. Using monomeric tetraethyl orthosilicate (Acros organics, Geel, Belgium), N-(3-trimethoxysilyl)propyl)ethylene diamine (Sigma-Aldrich, St. Louis, USA), and 3-(trihydroxysilyl)-propyl methylphosphonate (Sigma-Aldrich), the particles were coated with a thin layer of silica containing functional amino-groups. After the silica-encapsulation the UCPs were conjugated to biomolecules. The amino-groups on the surface of the particles were converted into carboxylic acid groups with glutaric anhydride (Sigma-Aldrich), which in turn were activated with 1-ethyl-3-[3-dimethylaminopropyl]carbodiimide hydrochloride and N-hydroxysulfosuccinimide sodium salt (Fluka, Buchs, Switzerland). The streptavidin (**I-II**) or antibodies (**III-IV**) were covalently coupled to the particles through the amino-groups of the biomolecule and the carboxylic acid groups of the UCPs. Finally, the coupling reaction was stopped with an excess of amino-groups (50 mM glycine pH 11). The coated UCPs were stored at 4°C.

4.1.2 Oligonucleotide sequences (I-II)

The primer and probe sequences used in these studies can be found in Study **I** and in Study **II** supplements.

The primers for the detection of hAdVs by an asymmetric quantitative real-time PCR (qPCR) were designed to amplify 167 bp (**I**) and 270 bp (**II**) long products derived from the conserved hAdV hexon gene region. They were selected on the basis of their reported ability to detect all the hAdVs belonging to groups A-G (Avellón *et al*., 2001). The adenovirus type-specific and generic oligonucleotide probes were designed on the basis of the published hexon sequences (Ebner *et al*., 2005; López-Campos *et al*., 2007). The HPLC-purified primers and probes were obtained from http://www.Biomers.net (Ulm, Germany). The synthetized probes were 23-31 nt long. Each probe had three extra T or C nucleotides as spacers at their 5'-end and an amino-C6 modification at the 5' terminus. Oligonucleotide probes 1–11 were designed to detect and genotype the hAdV genotypes C01, C02, B03, E04, C05, C06, B07, B14, B21, and A31 (**I**). Additional oligonucleotide probes 12–16 were designed to detect and genotype hAdV genotypes D08, D19, D36, D37, and F40/F41 (**II**). Probes gADV1 and gADV2 or probe mixture g1-8 (**I** and **II**, respectively) were used for the generic detection of hAdVs.

The thermodynamic behavior of the designed probes (**I**) was evaluated by calculating the Gibbs free energy (ΔG) change of the probe-target hybrid. The predicted ΔG values of the probes were calculated with the DINAMelt web server at http://dinamelt.bioinfo.rpi.edu/ (Markham and Zuker, 2005). The calculations were performed using a two-state hybridization model and perfectly matching duplexes were assumed. The values used were: 60 °C temperature, 2 nM total strand concentration, and 0.61 M sodium concentration.

4.1.3 Adenovirus prototypes (I-II)

The prototypes of hAdV genotypes C01, C02, B03, E04, C05, C06, B07, B11, B14, A18, A31, D36, and D37 were originally obtained from the Centers for Disease Control and Prevention (CDC, Atlanta, GA). The prototypes D19 and B21 were kindly provided by HUSLAB, Helsinki. The prototypes C01, C02, B03, C05, and C06 were cultivated in the Hela cell culture (human cervix carcinoma cell-line Hela Ohio/Salisbury, Wiltshire, UK) and prototypes E04, B07, B11, B14, A31, D36, and D37 in the A549 cell culture (human lung carcinoma cell-line A549, American Type Culture Collection, ATCC, Rockville, Maryland, USA) for the isolation of viral DNA. The Hela and A549 cells were maintained in Eagle's minimal essential and Ham's F12 medium (both from Gibco, Invitrogen, Carlsbad, CA), respectively, at 37°C in 5% CO2.

4.1.4 Clinical specimens (I-IV)

In Study **I**, anonymously coded clinical nasopharyngeal specimens (n = 55) were used for the oligonucleotide array-in-well assay validation. The specimens were selected from the processed clinical specimens sent to the Department of Virology, University of Turku, for respiratory virus antigen detection between December 2008 and March

2010. They had been tested positive for hAdV hexon antigen using time-resolved fluoroimmunoassay (Waris *et al.*, 1988) and stored frozen at -20 °C.

In Study **II**, anonymously coded nasopharyngeal (*n* = 86), ocular swab (*n* = 119), stool (*n* = 16), other types of respiratory specimens (*n* = 3), others (*n* = 5) and unknown (*n* = 2) specimens were selected from the processed clinical specimens sent to the Department of Virology, University of Turku, for hAdV detection between April 2010 and April 2011. All specimens had been tested positive for the hAdV using time-resolved fluoroimmunoassay (16% of specimens) (Hierholzer *et al.*, 1987), singleplex PCR (Honkinen *et al.*, 2012), multiplex PCR detection (Seeplex; Seegene, Seoul, Korea) (20%), or virus culture (64%). The hAdV negative specimens (*n* = 30) specimens with influenza A or B virus (*n* = 5), parainfluenzavirus 1 or 3 (*n* = 2), coronavirus (*n* = 1), varicella zoster virus (*n* = 1), herpes simplex virus type 1 or 2 (*n* = 6), rhinovirus (*n* = 3), enterovirus (*n* = 1), or respiratory syncytial virus (*n* = 3) were also tested to evaluate the assay specificity.

In Study **III**, a blood sample was collected from a female volunteer and used in the assay with her informed consent. Plasma separated from the blood was stored at -20 °C before its use in a multianalyte assay. The plasma was spiked with the standard concentrations of PSA and the multianalyte array-in-well immunoassay was performed as described earlier. As a reference, the PSA level in the sample was measured by a published PSA assay (Väisänen *et al.*, 2006)

In Study **IV**, anonymously coded serum samples (*n* = 89) were originally collected for routine diagnostic purposes and obtained for this study from the Diagnostic Service Unit of the Department of Virology, University of Turku, Finland. All the serum samples had been tested positive or negative both for parvovirus IgG by commercial kit (Biotrin International Ltd., Dublin, Ireland) and for hAdV IgG using in-house enzyme immunoassay (EIA). The samples were stored frozen at -20 °C.

4.1.5 Proteins (III-IV)

In Study **III**, the printed antibodies were monoclonal anti-PSA antibody MabH117 (Piironen *et al.*, 2001; Piironen *et al.*, 1998; Rajakoski *et al.*, 1997), monoclonal recombinant anti-TSH antibody fragment Fab5404 (Ylikotila *et al*., 2005), monoclonal anti-LH MabM21241 (Fitzgerald Industries International, Acton, MA), and polyclonal rabbit anti-mouse immunoglobulins (RaM) (DakoCytomation, Glostrup, Denmark). The monoclonal antibodies anti-PSA MabH50 (Piironen *et al*., 2001; Piironen *et al*., 1998; Rajakoski *et al*., 1997), anti-TSH Mab5409 (Medix Biochemica, Kauniainen, Finland), and anti-LH Mab8D10 (Nilsson *et al.*, 2001) (Delfia LH kit, Wallac, Finland) were used for UCNP coating (**III**). Antigens used in Study **III** were PSA (Rajakoski *et al*., 1997), human TSH (Immuno Diagnostic, Hämeenlinna, Finland), and human LH (Sigma-Aldrich). In Study **IV**, the printed antigens and antibodies were hAdV type C02 hexon, hAdV type C05 hexon (both from the Department of Virology, University of Turku), B19-VLPs (Kaikkonen *et al*., 1999), polyclonal human IgG

(Sigma), and polyclonal anti-human IgG Fc fragment specific (Thermo Fisher Scientific, MA, USA). Human serum albumin (Sigma) was used as negative control.

4.1.6 Array-in-well plates (I-IV)

Studies **I-II**, were oligonucleotide-based array-in-well assays for the detection and typing of adenoviruses. The amino-modified probes were covalently attached to the bottom of transparent 96-well microtiter plates (Corning, Amsterdam, The Netherlands) (**I**) or white 96-well microtiter plates (Nunc, Thermo Fisher Scientific) (**II**). Study **III** was an antibody-based array-in-well assay for the detection of LH, TSH, and PSA antigens, as well as control RaM antibody. The biotinylated antibodies were attached to the bottom of streptavidin coated white 96-well microtiter plate (Kaivogen, Turku, Finland). The array-in-well plates used in Studies **I-III** were prepared at the VTT Medical Biotechnology Centre, Turku. In Study **IV**, the biotinylated B19-VLPs, adenovirus type C02 and C05 hexon antigens along with the control proteins were immobilized on the white streptavidin coated 96-well microtiter plates (Pierce, Thermo) using non-contact Nano-Plotter 2.1 array printing instrument (Gesim, Germany).

4.2 Instrumentation

4.2.1 Anti-Stokes photoluminescence imager (I-IV)

The array-in-well assays (**I-IV**) were measured with the microtiter plate reader (Hidex Oy, Turku, Finland) modified for the anti-Stokes photoluminescence imaging (Figure 9). The used radiation source was an infrared laser diode delivering an optical power of 0.5-8.0W at the wavelength of 976±2 nm. A round diffuser was added (**II-IV**) between the collimator and long-pass filter to spread the laser beam homogeneously over the whole area of the well. The laser beam passed through a 850 nm long-pass filter and was reflected to the array well using a hot (dielectric) mirror. The fluorescence signal coming from the sample well was collected with a 50 mm camera lens, and the scattered laser radiation was blocked by two short-pass filters. The green emission of UCPs was detected via a 650 nm short-pass filter, and the images were captured with a CCD camera with a 50 mm objective lens using the following parameters: 2x binning; 30 s (**I**), 1 s (**II, III**), or 2 s (**IV**) exposure per well; and 7 W laser power. For multianalyte immunoassay (**III**), also 0.2 and 5 s exposure times were used. For serological array-in-well assay 1 s exposure time per well was used. The images were saved as 16-bit sif-file format.

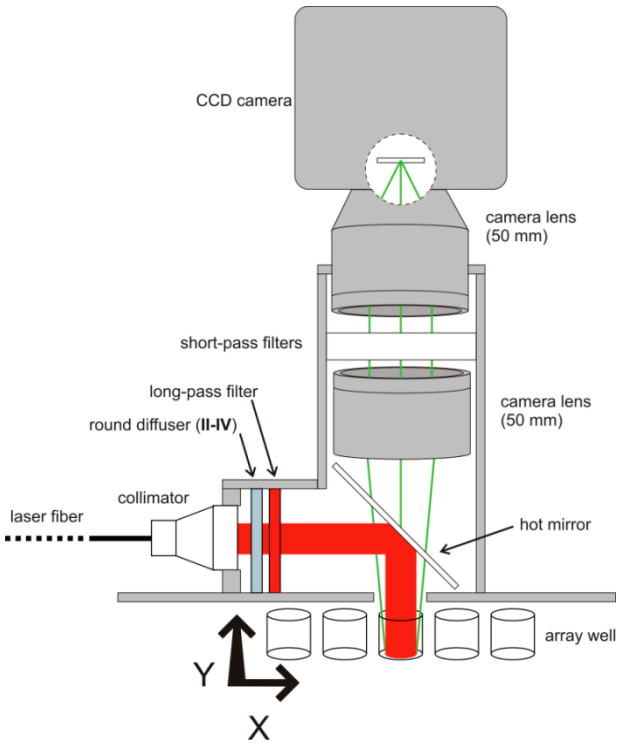

Figure 9. Anti-stokes photoluminescence imager (**I**).

4.2.2 Microtiter plate reader (III)

In quantitative multianalyte immunoassay (**III**), the modified microtiter plate reader (Hidex Oy, Turku, Finland) was utilized in the detection of the UCNP photoluminescence emission in the whole-well and array-in-well assays. The photoluminescence intensities were measured by scanning the well with a 7 × 7 or 3 x 3 raster using 0.8 or 1 mm distance between the measurement points for array-in-well and whole-well assays respectively, and a 2 s reading. The microtiter plate fluorometer used a 980 nm laser diode radiation source, and the UCPs green emission was measured with a 535/50 nm band-pass filter. The instrument is described in more detail in a paper by Soukka *et al*., 2005.

4.3 Array-in-well assay methods

In this section, brief descriptions of the multiplex assays carried out in the studies are described. The array-in-well assay specifications of the array-in-well assays (**I-IV**) are summarized in Table 2.

Table 2. Summary of the specifications used in the array-in-well assays.

Study	**I**	**II**	**III**	**IV**
Array type	DNA	DNA	Antibody	Antigen
Immobilization Chemistry	Covalent Amino-link	Covalent Amino-link	Affinity SA-biotin	Affinity SA-biotin
Printing type	Contact	Contact	Contact	Non-contact
Label conjugate	SA-UCP	SA-UCNP	Antibody-UCNP	Antibody-UCNP
Spot size (µm)	200	200	1000	~400
Spots / well	39	58	4	16
Sample	NS	Eye swab NP, others*	Buffer (plasma)	Serum
Assay result	Qualitative	Qualitative	Quantitative	Qualitative

*NS = nasopharyngeal specimens. NP = nasopharyngeal aspirate or swab and other respiratory specimens. Others include: urine, stool, tissue and colonoscopy specimens.

4.3.1 Asymmetric real-time quantitative PCR and sequencing (I-II)

PCR amplifications targeted to hAdV hexon gene region and melting curve analysis were performed by using Maxima SYBR Green qPCR Master Mix (Fermentas, St. Leon-Rot, Germany) and Rotor-Gene instrument (Corbett Research, Mortlake, Victoria,Australia). A real-time PCR reaction was performed in a mixture containing 0.1 µM of ADHEX2F forward primer (**I**) or 0.1 µM of each ADHEX2F1, ADHEX2F2 and ADHEX2F3 forward primers (**II**); and 0.45 µM (**I**) or 0.9 µM (**II**) of 5-end biotinylated ADHEX1R reverse primer. A 5 µL aliquot of DNA was added to a final volume of 25 µL.

The PCR reactions were performed under the following conditions: denaturation and enzyme activation at 95 °C for 15 min, 40 cycles of denaturation at 94 °C for 15 s, annealing at 53 °C (**I**) or 50 °C (**II**) for 60 s, extension at 72 °C for 45 s and final melting curve generation steps from 72 to 95 °C with 1ºC increments for every 5 seconds.

The 167 bp (**I**) and 270 bp (**II**) long PCR products were purified with QuickClean, PRC purification kit (GenScript, USA) before sequencing. The PCR products were sequenced in both directions using ADHEX2F and ADHEX1R in Study (**I**). In Study (**II**) ADHEX2F1, ADHEX2F2, or ADHEX2F3 was used as a sequencing primer. The amplicons were sequenced in the DNA Sequencing Service Laboratory of the Turku Centre for Biotechnology, Turku, Finland.

4.3.2 Array-in-well assays

Array-in-well assay principles (**I-IV**) are shown in Figure 10.

Adenovirus typing assay (I-II)

In both studies **I** and **II**, an oligonucleotide array-in-well assay was used for hAdV genotyping. The biotinylated PCR-products were diluted 10-fold in denaturation solution (25 mM NaOH, 5 mM EDTA) and incubated for 10 min at room temperature. A 25 µL sample of the denatured product was transferred to the array wells containing 25 µL of a neutralization solution (100 mM Tris pH 7.75, 850 mM NaCl, 0.1% (v/v) Tween 20). The plate was incubated at 60 °C for 1 h with shaking and washed. Streptavidin-coated UCPs (5 µg/mL in reaction) were added in assay buffer (50 mM Tris-HCl pH 7.8, 450 mM NaCl, 0.05% (w/v) NaN3, 0.5% (w/v) BSA, 0.01% (v/v) Tween-40, 0.05% (w/v) bovine gamma-globulin and 20 µM diethylenetriaminepentaacetate) and the assay was incubated for 30 min at room temperature with shaking. The wells were washed and the plate was dried. The assay was imaged with the anti-Stokes photoluminescence imager. See section 4.2.1 for instrument settings.

Quantitative array-in-well immunoassay (III)

In Study **III**, a quantitative multianalyte array-in-well immunoassay for three target analytes (LH, PSA, and TSH) was developed. The biotinylated capture antibodies and a positive control polyclonal RaM antibody were printed on the bottom of streptavidin-coated 96-well microtiter plates as 2 x 2 array format. The standard dilutions of the LH (0-60 U/L), PSA (0-60 ng/mL), and TSH (0-200 mU/L) were done in the assay buffer (50 mM Tris base pH 7.75, 150 mM NaCl, 0.05% (w/v) NaN3, 0.01% (v/v) Tween-40, 0.05% (w/v) bovine gammaglobulin, 20 µM diethylenetriaminepentaacetic acid, 0.5% (w/v) BSA, 20 µg/mL cherry red, and 0.2% (v/v) polyvinyl alcohol). A 10 µL of the standard dilution and 30 µL of the assay buffer containing antibody-coated UCNPs for TSH and PSA were added to the array well. The assay was incubated for 10 min at room temperature with shaking. After a

10-minute incubation, 10 µL of the antibody-coated UCNPs for LH were added and the array-in-well assay was incubated for 30 min at room temperature with shaking. The concentration of each UCNP was 20 µg/mL in the reaction. Anti-LH-UCNPs were added 10 min later than other UCNPs as, if added earlier, the anti-LH-UCNPs would have bound to the TSH-spots as well. The tracer antibody for LH had an affinity towards the alpha chain of the TSH molecule, which is identical in both LH and TSH molecules. After the incubation, the wells were washed and the plate was dried before imaging. See section 4.2.1 for anti-Stokes photoluminescence imager settings. The array-based multianalyte assay was also measured with a plate reader. See section 4.2.2 for instrument settings. To verify potential cross-reactions and interference caused by the presence of reporters for other analytes in the multianalyte assay, single-analyte assays for PSA, TSH, and LH were carried out in the array-in-wells in parallel with the multianalyte assay. Single-analyte assays were also measured with the microwell imager. See section 4.2.1 for instrument settings.

Serodiagnostic array-in-well assay (IV)

The biotinylated virus antigens (B19-VLP, hAdV type C02, and C05 hexons) and control proteins (hIgG, anti-hIgG, and HSA) were printed on the bottom of the streptavidin-coated 96-well microtiter plates. With the array-in-well assay, 89 serum samples were screened. Briefly, 50 µL of the 1/200 diluted serum sample in assay buffer containing 25 mM Tris-HCl, pH 7.75, 75 mM NaCl, 0.25% (w/v) gelatin, 0.005% (w/v) Tween-40, 10 µM diethylenetriaminepentaacetic acid, 0.0025% (w/v) NaN_3, 10% (v/v) inactivated fetal calf serum, 1% (w/v) Tween-20, and 0.0025% (v/v) cherry red in PBS; pH 7.2 was added in duplicate to the array well and incubated for 1 h at room temperature with shaking. After the incubation, the wells were washed. A 50 µL of anti-human IgG coated UCNPs (7.5 µg/mL concentration in the reaction) were added to the array wells and incubated for 1 h at room temperature with shaking. The wells were washed and the plate was dried before the assay was imaged with an anti-Stokes photoluminescence imager. See section 4.2.1 for instrument settings. To evaluate the inter-assay imprecisions, six control serum samples were included in each assay run, i.e., each plate. To control intra-assay imprecisions, six replicates of one random serum sample were also included on each plate. The multiplex array-in-well results were compared to the reference B19V IgG and C02 IgG EIAs.

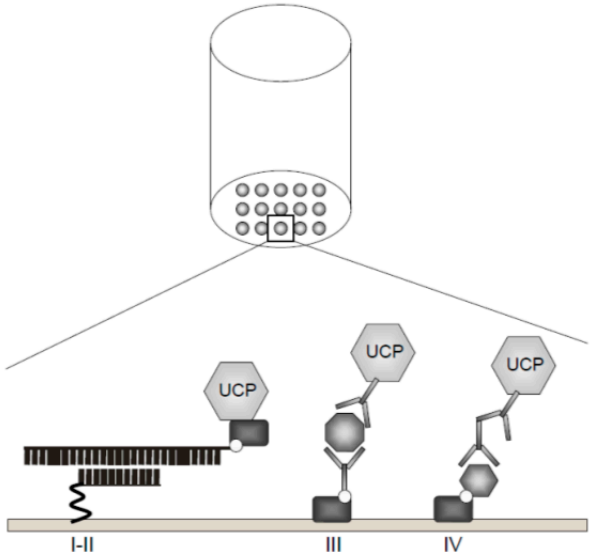

Figure 10. Array-in-well assay principles (**I-IV**). In Studies **I-II**, the covalently immobilized hAdV-specific amino-modified probes were hybridized with the biotinylated PCR-products. The SA-UCPs were used for the detection of probe-target hybridization. In Study **III**, biotinylated antibodies for three analytes (PSA, TSH, and LH) and control RaM antibody were printed on the bottom of streptavidin-coated microtiter wells. The analytes and RaM antibody control were detected with a mixture of antibody-coated UCNPs. In Study **IV**, the biotinylated antigens (B19-VLP, C02, and C05 hexons) and control proteins were printed on the bottom of the streptavidin-coated microtiter wells. Serum IgG antibodies' binding to antigens and positive controls were detected using secondary anti-hIgG coated UCNPs.

Data analysis (I-IV)

The image analysis (**I-IV)**, spot detection (**I-IV**), and quantification (**I, III, IV**), were performed with ImageJ software version 1.43n (http://rsbweb.nih.gov/ij/index.html). In Study **III**, the standard curves using linear fitting were performed with Origin v8.0773. The lower limits of detection (LOD) were calculated from the standard curves as the analyte concentrations corresponding to a signal of three standard deviations (SD) of the blanks. In the reference whole-plate assay (**III**), the photoluminescence intensities were measured at four measurement points in the 7 x 7 raster (array-in-well assay) and at nine measurement points in the 3 x 3 raster (reference whole-well assay). In Study **IV**, the cut-off values for B19V, C02, and C05 positivity were set at the average signal + 10x standard deviations (SD) of the corresponding spot in the reagent (no sample) background well.

5 RESULTS

5.1 UCPs and the imaging device (I-IV)

The $NaYF_4$:Yb^{3+} Er^{3+} material produced strong anti-Stokes photoluminescence in the 520-560 nm (green) and in the 650-700 nm (red) regions under NIR radiation (data not shown). The UCP-particles were functionalized with a silanization process and coated with streptavidin (**I-II**) or antibodies (**III-IV**). The coated particles were utilized as reporter molecules in the array-in-well assays. The transmission electron microscope (TEM) images showed that especially the nanosized particles were uniform in size making them applicable labels for imaging-based bioaffinity assays (Figure 11).

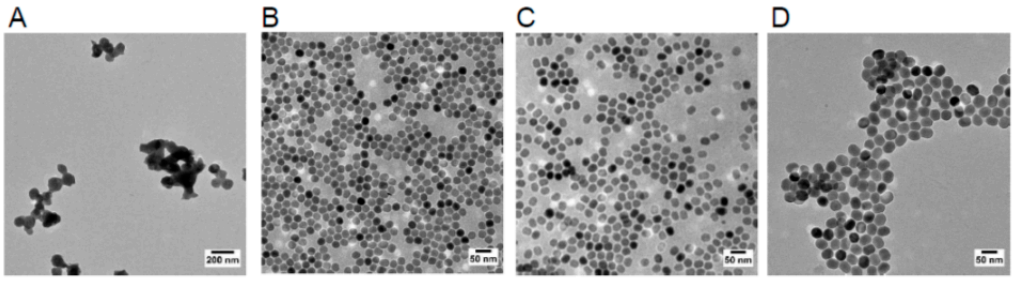

Figure 11. TEM images of the single-crystal upconverting materials before biomolecule conjugation (**I-IV**). (A) The $NaYF_4$:Yb^{3+},Er^{3+} particles (size 110 nm) synthesized with the co-precipitation method (**I**); (B, C, and D) The $NaYF_4$:Yb^{3+},Er^{3+} particles (~25-40 nm) synthesized in organic oils (**III**, **IV**, **II**, respectively).

The anti-Stokes photoluminescence imager for upconversion imaging was constructed for multiplex testing using inexpensive infrared laser diode (8 W) excitation light source with a combination of camera lenses, as well as long-pass and short-pass filters. The device used a 96-well microtiter PlateChameleon for moving the plate in X- and Y –dimensions and a cooled charge-coupled device (CCD) as a detector for capturing the two-dimensional images. The instrument was used for imaging the solid-phase array-in-well assays (**I-IV**). Transparent (**I**) and white (**II-IV**) 96-well microtiter plates were used as a solid support for the immobilized biomolecules in the array-in-well assays. The signal-to-background ratios were not improved with the white plate as the signal outside the spots originating from the non-specific binding of the label was also increased in the white wells (**unpublished**). The exposure times used in the multiplex assays with the white plates ranged from 1-2 s, while with the transparent plates it was 30 s; the exposure time was approximately 30 times shorter with white

plate compared to the transparent plate making the assay implementation more user-friendly.

In Study **III,** the limited dynamic range was, to some extent, compensated by measuring the array wells with different exposure times (Figure 12A). With the longer 5 s exposure time in the multianalyte assay format, lower LOD for TSH (0.38 mU/L) was obtained compared to the LOD obtained with 1 s exposure time (0.64 mU/L), but the drawback was that the CCD rapidly reached the saturation charge level. With a shorter 0.2 s exposure time, the smallest analyte concentrations did not deviate from the background level, but higher analyte concentrations could be measured without CCD saturation. By combining different measurement times, a standard curve covering a wider analyte concentration range can be obtained. In Study **IV**, the serum sample dilution series in a multiplex serodiagnostic assay was imaged with two different exposure times: 1 s and 2 s per well (Figure 12B). When using the 2 s exposure time, the hAdV signals reached the detector saturation level in the 1/1000 serum sample dilution. However, a wider dynamic range was achieved when 1 s exposure time per well was used; here, the hAdV signal saturation was reached at 1/200 serum sample dilution.

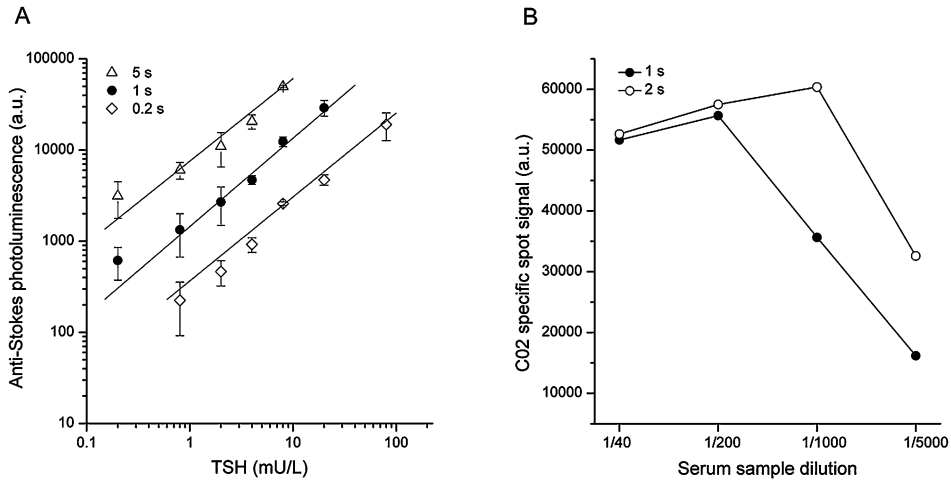

Figure 12. (A) Different exposure times (0.2 s, 1 s, and 5 s) in the multianalyte immunoassay using TSH as a model analyte (**III**). (B) Standard curves for hAdV type C02 hexon specific spot signals using the imager with 1 s and 2 s exposure times (**IV**). a.u., arbitrary unit.

5.2 Adenovirus genotyping assay (I-II)

5.2.1 Oligonucleotide probes

In Studies **I** and **II**, 23-31 nt long 5'-terminus amino-modified oligonucleotide probes were designed to be specific to the targeted hAdV types. Generic control probes that recognize all the different hAdV types belonging to different groups (A to F) were also designed. The thermodynamic behavior of the designed probes (**I**) was evaluated by calculating the ΔG change of the probe-target hybrid. The ΔG provides a thermodynamic measure of the affinity between a probe and a target, with lower negative ΔG values being indicative of higher binding affinities. The designed oligonucleotides (**I**) showed a clear correlation (R = 0.74) between the hybridization intensity and ΔG values of the oligonucleotides (a ΔG value of -14 kcal/mol or lower was required for the detection of hybridization, and a value lower than -16 kcal/mol was required for strongly positive signals).

5.2.2 Asymmetric real-time quantitative PCR

An asymmetric real-time quantitative PCR (qPCR) was used to produce more biotinylated single-stranded target DNA strand. The hAdV PCR was targeted to the hexon coding regions (position 238 to 404) (**I**) and (position 130 to 404) (**II**). In the study **I**, one primer pair was used for amplifying the hAdV DNA in the nasopharyngeal clinical samples and hAdV prototype stains. In Study **II**, it was necessary to expand the targeted PCR region in order to include more hAdV specific probes to the array. The assay (**II**) was widened to include the most common and clinically relevant hAdV types belonging to groups A to F. A mixture of three forward primers and one biotinylated reverse primer was used to amplify hAdV genome (**II**). The real-time qPCR (**II**) was able to amplify hAdV types belonging to different groups. The qPCR sensitivity was tested with hAdV C02 genotype. The C02 genotype was detected at concentrations of fewer than 10 copies per qPCR reaction (**I, II**). The PCR detected all the hAdV prototypes and clinical nasopharyngeal specimens (n = 55) included in Study (**I**). In Study **II**, the PCR detected 223 (97 %) of the 231 clinical specimens that had originally been tested hAdV positive. However, the PCR specificity was not limited to hAdVs, as the PCR also showed non-specific late amplifications (Ct > 30). Threshold values for hAdV prototypes and hAdV positive clinical samples and the melting temperatures are shown in Figure 13.

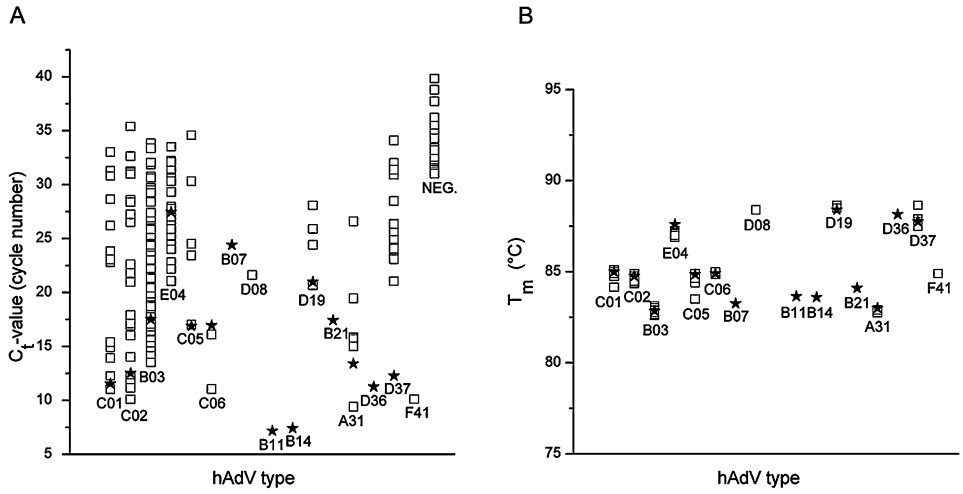

Figure 13. Asymmetric real-time qPCR data (**II**). (A) Threshold cycles for hAdV prototype strains, hAdV positive and negative clinical specimens (B) melting temperatures for hAdV positive clinical specimens and hAdV prototype strains (**unpublished**).

5.2.3 Oligonucleotide-based array-in-well assay (I-II)

In Study **I**, the multiplex oligonucleotide hybridization assay was developed for the detection and genotyping of the most common hAdV genotypes causing human infections. Eleven adenovirus genotype-specific 5'-terminus amino-modified probe spots were covalently printed in an array format on transparent microtiter wells. In each well, generic controls were also spotted. The oligonucleotide probes were hybridized with the single-stranded biotinylated PCR-products and the bound products were detected with streptavidin-coated UCPs.

An anti-Stokes photoluminescence imager with laser diode excitation and a CCD image sensor was built and utilized for the detection. Synthetized single-stranded 5'-biotinylated target oligonucleotides and qPCR amplified hAdV (C01, C02, B03, E04, C05, C06, B07, and B21) prototype strains were used for the optimization of the assay. The qPCR amplified hAdV positive clinical nasopharyngeal specimens (n = 55) were used for the array-in-well assay validation. The combination of probe signals gave a specific hybridization pattern for each targeted hAdV prototype and clinical nasopharyngeal specimens. The sequencing was used as a reference method, to confirm the array results. The sequencing results were comparable with the array-in-well results. Among the 55 clinical specimens, types C01 (18.2% of the samples), C02 (25.5%), B03 (21.8%), E04 (14.5%), C05 (7.3%), and C06 (12.7%) were found.

Improved oligonucleotide array-in-well assay

In Study **II**, the previously published assay (**I**) was expanded. Three new forward primers were designed for qPCR because more variation in the hexon sequence was needed for the probe design. Additional hAdV type specific probes (probes 12-16) and a mixture of generic probes were designed to genotype clinically relevant hAdV types belonging to groups A to F (C01, C02, B03, E04, C05, C06, B07, D08, B11/14/16/34/35, D19, B21, A31, D36, D37, and F40/41). The assay (**II**) was technically improved compared to the one used in Study **I**. Smaller (30 nm) nanosized upconverting nanoparticles (UCNPs) and white microtiter well plates (**II**) were used instead of larger > 100 nm UCPs and transparent plates (**I**).

5.2.4 Epidemiological study of hAdV genotypes (II)

The improved assay was used to detect clinically relevant hAdV types circulating in Finland between April 2010 and April 2011. A total of 231 hAdV positive respiratory, ocular swab, stool, and other types of specimens were included in the study. The specimens had originally been tested positive for hAdV with reference methods. After a real-time PCR amplification targeting the hAdV hexon gene, the array-in-well assay identified the presence of hAdV genotype B03 (n = 122; 58% of all specimens); E04 (29; 14%); C02 (21; 10%) and D37 (14; 7%); C01 (n = 12); C05 (n = 5); D19 (n = 4); C06 (n = 2); D08 (n = 1); A31 (n = 1); and F41 (n = 1). The targeted hAdV genotypes showed strong or partial hybridization to specific probe spots. No hybridization signal was obtained in hAdV negative specimens or specimens with other viruses, including rhinovirus, influenza A or B virus, parainfluenza virus 1 or 3, herpex simplex virus type 1 or 2, enterovirus, or respiratory syncytial virus. (n = 30). The non-targeted hAdV type A18 hybridized only to the control probe spots. The array-in-well hybridization assay gave a specific hybridization pattern for each of the targeted hAdV prototypes and clinical specimens (Figure 14). The sequencing was used as a reference method, to confirm the array results. One female patient had subsequent infections by the genotypes C02 and B03, six months apart. The hAdV genotypes C01, C02, C05, and C06 were mainly detected in children under four years of age. The genotype A31 was detected in one immunocompromised female patient only.

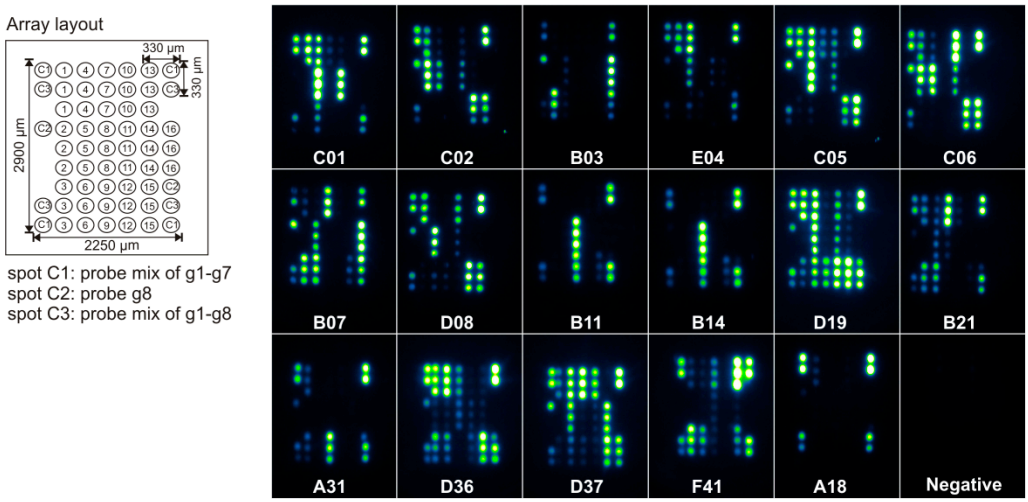

Figure 14. Array-in-well images for eleven different hAdV genotypes (C01, C02, B03, E04, C05, C06, D08, D19, A31, D37, and F41) among the sample panel, the prototype strains (B07, B11, B14, B21, and D36), non-targeted hAdV A18 genotype and hAdV negative specimen (**II**).

Ten co-infected specimens were detected among the sample panel. One boy had a co-infection of hAdV genotype C05 and coxackievirus 24 detected in stool. The other nine co-infections were detected in girls and boys (under the age of 14 years) in respiratory specimens: hAdV genotype C02 and rhinovirus; B03 and parainfluenza virus type 3; C01 and respiratory syncytial virus; C01 and influenza virus B; C01 and rhinovirus; C02 and influenza virus B; C01 and respiratory syncytial virus; C01 and metapneumovirus; and C02 and metapneumovirus. The age range of the patients was from <1 to 67 years (Figure 15) with a median age of 25 years. There were 100 (47%) males and 111 (53%) females in this study. Most hAdV infections were prevalent in adults: 125 (59%) patients were aged 18 or more and 73 (60%) were females. Fever, cold, cough, pharyngitis and conjunctivitis were the most commonly reported clinical manifestations among the patients. The hAdV genotype B03 was distributed throughout all age groups. The highly prevalent type B03 was mostly detected in ocular swabs (Figure 16).

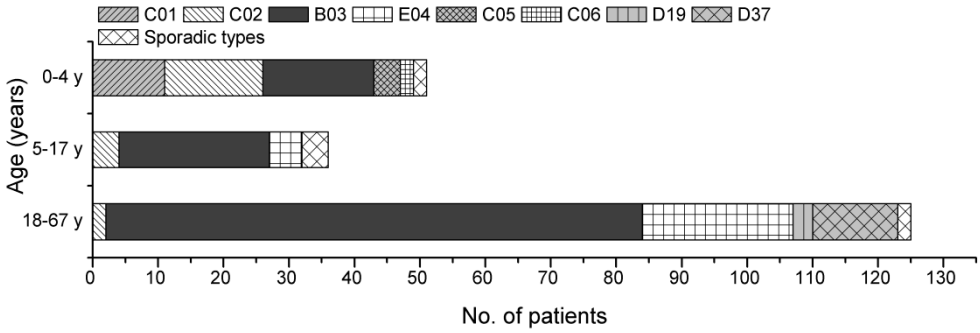

Figure 15. Age distribution of the patients (*n*= 51, 36, 125, in age group 0–4 years, 5–17 years and 18–67 years, respectively). Sporadic types in age group 0–4 years: E04 and F41; 5–17 years: C01, C05, D19 and D37; 18–67 years: D08 and A31 (**II**).

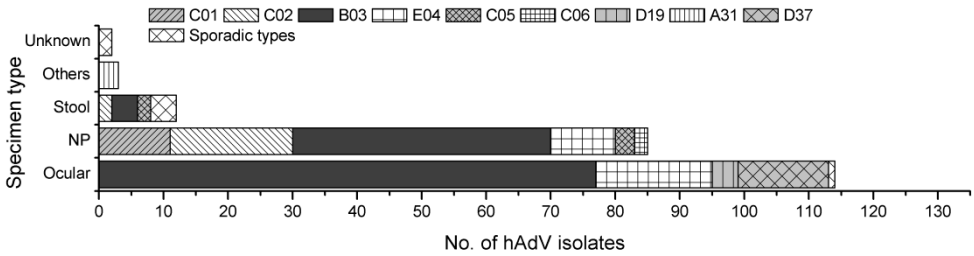

Figure 16. Different specimen types (*n* = 216): ocular (*n* = 114); NP = nasopharyngeal aspirate or swab, and other respiratory (*n* = 85); stool (*n* = 12); others (*n* = 3) including tissue, urine, and colonoscopy specimens; and unknown (*n* = 2) specimens. Sporadic types in ocular swab specimens: D08; in stool specimens: C01, E04, A31, and F41; in unknown specimens: C02 and B03 (**II**).

Four year epidemiological study

An epidemiological follow-up study of hAdV genotypes in Finland between January 2009 and December 2012 was established (**partly unpublished**, Figure 17). A total of 499 adenovirus positive respiratory, ocular swab, stool, and other types of specimens were included in the study. The specimens were first amplified with the asymmetric real-time qPCR based on the adenovirus hexon gene, and the PCR products were typed by the oligonucleotide array-in-well assay (**II**). The E04 (*n*=110, 22%), C02 (87, 17%), and C01 (46, 9%) genotypes were detected in all seasons (Figure 15). Overall, epidemic activity of type B03 (160, 32%) was observed in the autumn of 2010 (**II**), after that only sporadic cases were found. Genotypes D08, D19, and D37 (42, 8%), which are known to cause epidemic keratoconjunctivitis, were detected in ocular swab

specimens. Two new types were found among the sample panel: genotypes B35 and D56. Among randomly selected samples, these two types were sequenced to assure the typing result.

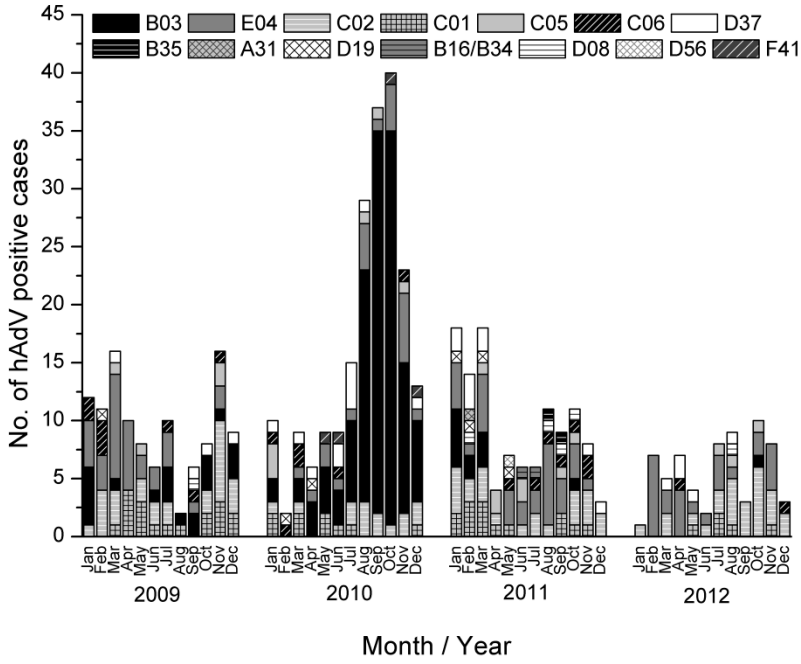

Figure 17. Seasonal distribution of hAdV genotypes during the four year study period. The specimens from April 2010 to April 2011 were detected and typed in Study **II** (**partly unpublished**).

5.3 Quantitative multianalyte immunoassay (III)

In Study **III**, a quantitative array-in-well immunoassay for three target analytes (LH, PSA and TSH) was developed. Biotinylated antibodies were printed in the 2 x 2 array format on streptavidin-coated microtiter wells. The captured analyte spots were detected with a mix of secondary antibody-coated UCNPs. The multianalyte assay performance was compared with a single analyte assay carried out in the array-in-wells and a reference whole-well assay for each target analyte.

In the multianalyte assay, there was no binding of non-target analyte on the specific spots indicating that no cross-reactivity was present. Cross-reactivity was tested in the single analyte array-in-wells in the presence of three different antibody-coated UCNPs

(anti-TSH, anti-PSA and anti-LH) in the same reaction well. The analytes bound only to the corresponding spots and no cross-reactions were detected. Using a mix of secondary antibody-coated UCNPs did not cause any significant cross-reactions or interferences in the multianalyte immunoassay (Figure 18).

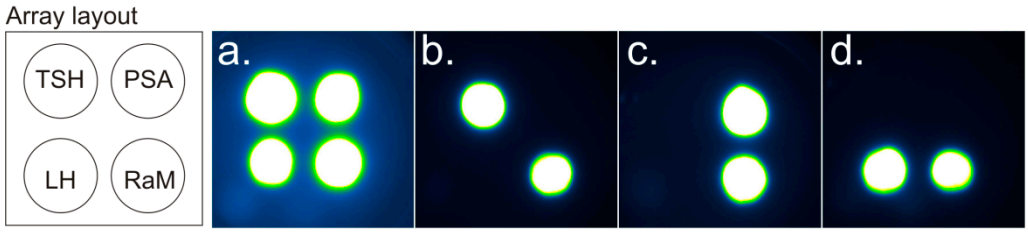

Figure 18. Fluorescent array-in-well images. (a) An array well containing all analytes TSH (200 mU/L), PSA (60 ng/mL), and LH (60 U/L). The array-in-well images of the single-analyte array-in-well immunoassay results for (b) TSH (200 mU/L), (c) PSA (60 ng/mL), and (d) LH (60 U/L) analytes (**III**).

A quantitative response was obtained with all three analytes in all assay formats (Figure 19). The LODs of the multianalyte assays were comparable both with the LODs in the single analyte assays performed in the array wells and with the reference assays measured with the plate reader (Table 3). In the reference assays, the LODs were lower when measured with the plate reader than when measured with the imager. However, the UCNP concentration was not optimized for the reference assay. The multianalyte array-in-well assay was also scanned with the plate reader. The scanning did not increase the linear range of the multianalyte assays, and it yielded lower LODs for PSA and LH (0.05 ng/mL and 0.20 U/L, respectively) compared with the imager scans. However, the LOD for TSH was higher when the multianalyte array-in-well assay was scanned with a plate reader than when it was imaged. This was due to the high nonspecific binding of the label to the area around the TSH spot. The dynamic ranges of the assays in the multianalyte format were approximately 2 orders of magnitude. A clinical sample material was tested in the single analyte assay. The standard curve obtained in lithium heparin plasma was similar to that in buffer although the signal levels were lower (Figure 20). The measured total PSA level in the female plasma sample was 0.06 ng/mL, which was below the detection limit of the array-in-well assay (Table 3).

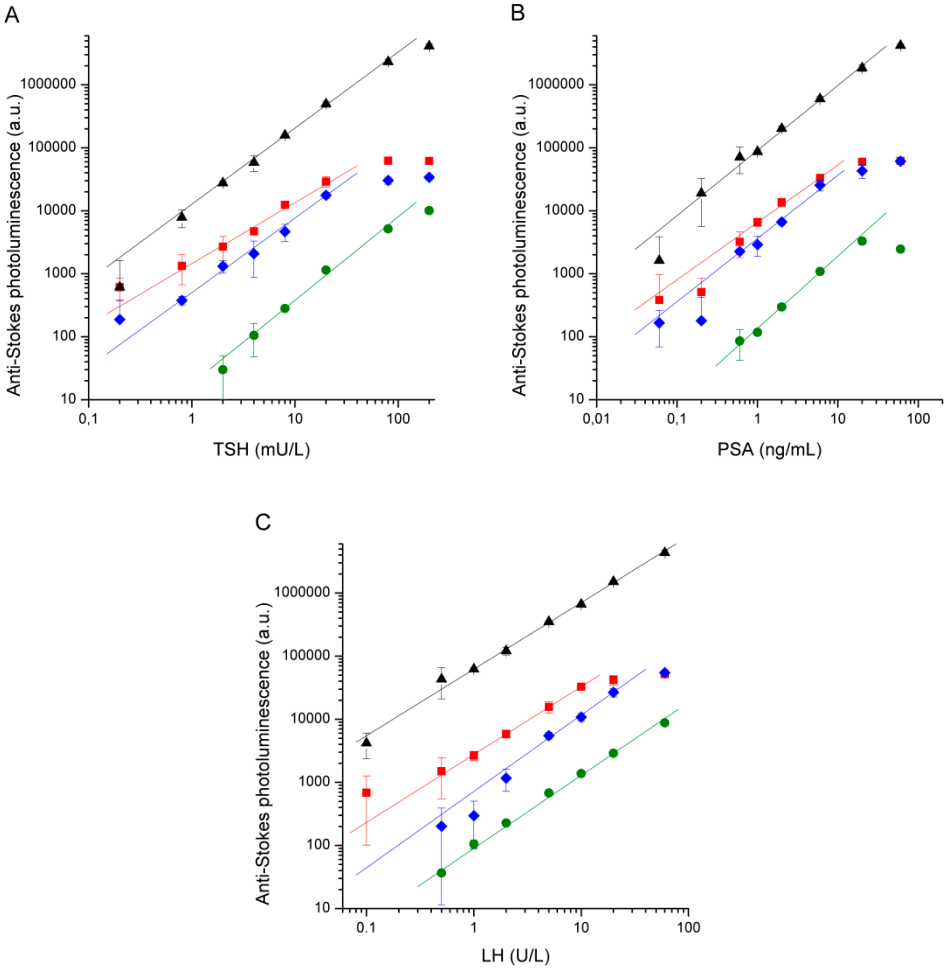

Figure 19. Calibration curves for (A) TSH, (B) PSA, and (C) LH in multiplex array-in-well assay (red squares), single analyte assay in array wells (blue diamonds), whole-well reference assay using plate reader (black triangles), and whole-well reference assay using imager (green circles) (**III**). a.u., arbitrary unit.

Table 3. LODs[a] for different assay formats (**III**).

Analyte		**TSH**	**PSA**	**LH**
Assay type	**Detection instrument**	**LOD** mU/L	**LOD** ng/mL	**LOD** U/L
multianalyte in array	imager	0.64	0.17	0.45
single-analyte in array	imager	0.53	0.15	0.36
reference whole well	imager	4.5	1.0	0.55
reference whole well	plate reader	0.31	0.23	0.031
multianalyte in array	plate reader	1.7	0.05	0.20

[a]Limit of detection.

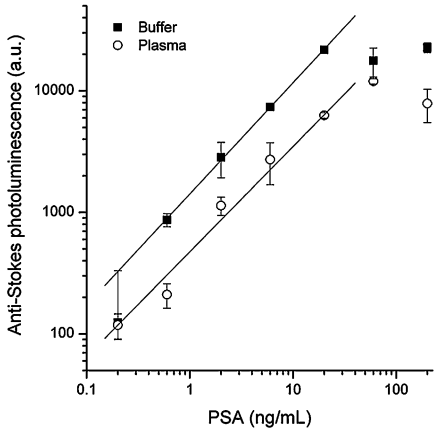

Figure 20. Standard curves in buffer and plasma for PSA in array-in-well assay (**III**).

5.4 Multiplex serodiagnostics (IV)

5.4.1 Optimizing protein immobilization with non-contact printer

To optimize the printing conditions for all immobilized proteins (B19-VLPs; C02 and C05 hexons; hIgG; anti-hIgG; and HSA) different printing buffer compositions, various protein concentrations along with different manufacturer's streptavidin-coated normal and high-capacity microtiter 96-well plates were tested with the non-contact Nano-Plotter printing instrument (data not shown). When using white normal capacity streptavidin-coated microtiter well plates, the biotinylated B19-VLP spot morphology was not optimal. The B19-VLPs accumulated at the outer boundary of a spot, causing a donut-shaped spot (Figure 21a). The reason for this might be that the biotinylated B19-VLP stock solution contained free biotin molecules (~ 250 Da), blocking the central area of the spot and causing the larger biotinylated B19-VLPs (VP2 ~ 60 kDa) to bind to the outer area. The hypothesis was tested by adding free biotin to the biotinylated C05 hexon stock. The added free biotin in the printing buffer blocked the binding sites and biotinylated C05 hexon formed donut spots (Figure 21b). The B19-VLP stock was purified with Amicon Ultra-0.5 mL 100 K devices (Millipore, MA, USA), after which, the intensity was more evenly distributed within the spot (Figure 21c) suggesting that the original biotinylated VLP stock contained free biotin.

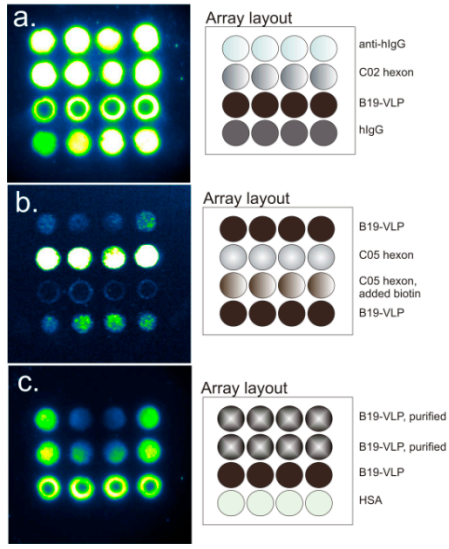

Figure 21. Array-in-well images (left) and array layouts (right) for the protein immobilization optimization step. (a) Biotinylated B19-VLP stock containing free biotin caused donut-shaped spots (b) Added free biotin on hAdV C05 hexon printing solution caused donut-shaped spots (c) Additional purification of biotinylated B19-VLP stock improved spot morphology (**unpublished**).

5.4.2 Serodiagnostic array-in-well assay

The array-in-well assay results were compared with the reference B19V IgG and hAdV IgG EIA assays. In the developed serological array-in-well assay, the hAdV hexon spots gave a positive result with four samples that were tested negative with the reference in-house hAdV IgG EIA assay. This might be due to the different serum sample dilutions used in the array-in-well assay (1/200) and reference assay (1/1000). Three of these serum samples were from children, of which two were borderline cases in the reference hAdV IgG assay. The fourth serum was the second sample from an adult with two subsequent serum samples included in this study. The first sample gave a negative result both in the array-in-well assay and in the reference hAdV IgG assay. The second sample, however, gave a low positive result (C05 and C02-specific spot signal levels were 2000 and 1550, respectively) in the multiplex assay and a negative result in the reference assay. The B19V serum IgG responses had a 100% concordance between the reference EIA and the array-in-well assay.

Plate variations, i.e., inter-assay imprecisions were determined using six serum samples and the same batch of reagents on different days (Table 4). The intra-assay imprecision was determined using six replicates of the serum sample in each of the three plates (Table 5). The paired serum samples (n = 17) gave consistent results in the B19V IgG and hAdV IgG reference assays. Also the specific anti-hIgG spot signal levels were consistent between the paired serum samples. However, the second serum sample from the paired sample pair had a positive hAdV result in the multiplex assay and a negative result in the reference assay, as discussed earlier. Three serum samples showed B19V-specific IgG seroconversion in the array-in-well assay and in the reference assay. The multiplex array-in-well was also able to detect the IgG seroconversion in these three serum samples. The printed spots were uniform in shape and able to discriminate B19V and hAdV negative and positive specimens. As shown in Figure 22, the B19V and hAdV negative samples were not, to any significant degree, bound to the B19-VLP spots and hAdV hexon spots, respectively. In addition, the hAdV C02 and C05 hexon specific spot signals correlated in both negative and positive serum samples (Figure 23). The specific mean spot signal intensities for the hIgG and anti-hIgG controls were 11400–23600 and 20600–50900, respectively. The antigen specific mean spot signal intensities were 2400–22000, 7500–60400, 4500–57500 for the B19-VLP, C02, and C05, respectively.

Table 4. Inter-assay imprecisions for three plates with six serum samples (sample ID 1-6). For HSA, the average spot signals (±SD) are presented. For hIgG, anti-hIgG, B19-VLP, hAdV C05, and C02 mean specific signals (±SD) are presented (**IV**).

#	HSA	hIgG	anti-hIgG	B19-VLP	C05	C02
1	1154 (±100)	18269 (±2601)	34805 (±7615)	767 (±73)	195 (±126)	122 (±95)
2	2003 (±215)	18618 (±3149)	33411 (±7051)	281 (±99)	37280 (±5029)	36617 (±6605)
3	2171 (±145)	19799 (±2923)	32065 (±5190)	471 (±72)	44009 (±2994)	42739 (±3606)
4	1975 (±191)	18021 (±3543)	32704 (±8299)	373 (±190)	35491 (±4846)	33663 (±4796)
5	2547 (±266)	19933 (±3582)	37043 (±8282)	6653 (±967)	49540 (±3736)	50469 (±5572)
6	1898 (±199)	20486 (±3905)	34944 (±9449)	5879 (±1836)	27505 (±3068)	24337 (±3910)

sample ID

Table 5. Intra-assay variations. In each plate (1-3) one serum sample was included in six replicates as an internal control. The mean specific signals (±SD) are presented (**IV**).

#	hIgG	anti-hIgG	B19-VLP	C02	C05
1	14749 (±3720)	23308 (±3034)	228 (±269)	28605 (±3371)	29952 (±4156)
2	20407 (±5598)	36295 (±3918)	499 (±348)	46249 (±5174)	46588 (±6110)
3	21825 (±3606)	43707 (±11630)	6784 (±3221)	53715 (±5905)	51991 (±6649)

plate ID

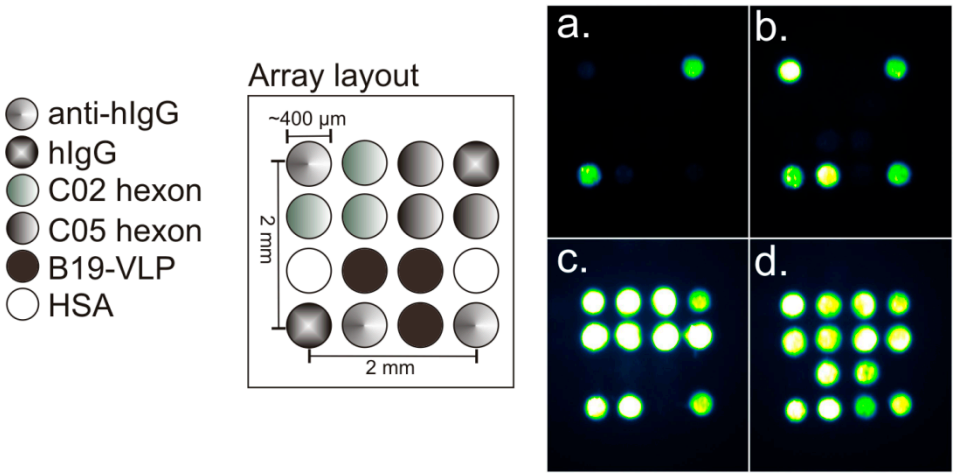

Figure 22. Fluorescence images (right) and array layout (left) of the multiplex assay probed with human sera. (a) An array well without serum sample (reagent background), (b) B19V IgG and adenovirus IgG negative sample, (c) B19V IgG negative and adenovirus IgG positive sample, (d) B19V IgG and adenovirus IgG positive sample (**IV**).

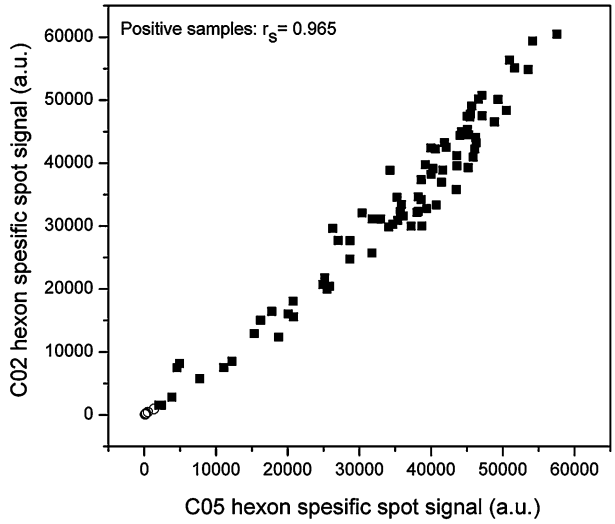

Figure 23. Correlation of hAdV C02 and C05 hexon spot signal intensities. Adenovirus positive n = 81 (black square) and negative serum samples n= 8 (white circle) (**unpublished**).

The serodiagnostic array-in-well assay was simultaneously able to detect antigen-specific IgG responses against B19V, C02, and C05 as well as separate the positive and negative sample populations according to the cut-off values (Figure 24). The cut-off values were calculated from the reagent background wells. The plate specific cut-off values for the B19V were 1154, 1299, and 1489 in plates 1 to 3, respectively. The plate and analyte-specific cut-off values were calculated also for the C05 (957, 1236, and 1480 in plates 1 to 3, respectively) and C02 (877, 1236, and 1140).

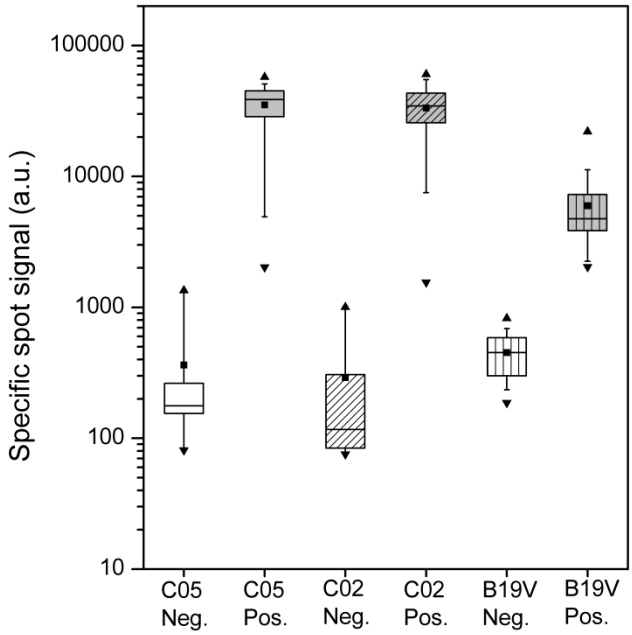

Figure 24. Serological array-in-well assay results for the hAdV (C05 and C02) IgG and B19V IgG negative and positive serum samples. The boxes represent interquartile range (25–75%); the whiskers denote 5th and 95th percentiles; the square and horizontal lines inside the boxes show mean and median, respectively; and the triangles show minimum and maximum specific spot signals for hAdV negative (Neg.), 8 patients in the groups; hAdV positive (Pos.), 81 patients in the groups; B19V negative group (Neg.), 44 patients; and B19V positive group (Pos.), 45 patients (**IV**).

6 DISCUSSION

6.1 UCPs and array-in-well assay detection (I-IV)

The aim of this study was to develop different multiplex bioaffinity assays in a 96-well-plate format based on the novel upconverting phosphor reporter technology. In this study, all the developed multiplex array-in-well assays (**I-IV**) were carried out on 96-well microtiter plates. This allowed the use of common laboratory equipment, and an easy assay performance. In addition, the array approach allowed the simultaneous testing of small sample volumes for multiple different analytes during the same day. The microtiter plates also enable the analysis of 96 samples at one time. When necessary, it is also possible to add more spots per well. This would further enhance the multiplexing capability, and enable even more target analytes to be included in one assay.

In this study, UCP label technology was used for the array-in-well assay detection. A significant advantage with the UCP reporter technique in analyte detection is that in heterogeneous assays the background fluorescence of the solid-phase material or sample matrix does not cause a similar problem as in time-resolved and conventional fluorescence. Another advantage is that autofluorescence, which commonly limits the assay sensitivity, can be avoided. The UCPs (**I-IV**) were hexagonal shaped single-crystal particles. The efficiency of upconversion luminescence is mainly affected by the choice of the host material as well as the structure and size of the crystal. The size and shape can be controlled by the optimization of the reaction conditions. The hexagonal structure of the $NaYF_4$:$Yb^{3+}Er^{3+}$ material is known to be a 10 times more efficient upconverting material than the cubic one (Krämer *et al.*, 2004).

In Study **I**, a desktop prototype for anti-Stokes photoluminescence imaging on a solid surface was constructed. The UCP-imager was constructed of a laser diode light source, conventional optics, CCD-camera for capturing the images and a plate Chameleon moving stage. The instrumentation for the UCPs is simpler and lower-cost than instrumentation employed in time-resolved fluoroimmunometric assays or the device used for array scanning. When using UCPs, continuous excitation and measurement can be used and no time-resolved measurement is needed. In Studies **II-IV**, white 96-well plates were used. The advantage of using the white plates instead of the transparent plates is that a shorter exposure time can be used because of a surface enhanced anti-Stokes photoluminescence from white well plate compared to transparent well plates making the assay process more user-friendly (Kuningas *et al.*, 2005a).

Usually, CCD-based assays have a narrower dynamic range compared to the assays carried out via PMT-equipped detection instruments because in the CCD detector the maximum value for a particular pixel is 65535. The LOD is a very important factor affecting the test performance when diagnostic assays are developed. Both the

detection technology and the imaging-based instrument affect the assay performance. A low background signal is crucial for the detection and analysis, as it affects the SNR. The high nonspecific binding of the UCNP label limited the assay sensitivity in Study **III**. The high background signal originating from the UCNP bound outside the specific spots could be minimized by optimizing, e.g., the UCNP antibody coating protocol and the assay buffer composition. In Study **III**, the dynamic range of the quantitative multianalyte immunoassay could be widened by using different exposure times with the imager. The dynamic range of the TSH in multinalyte array-in-well assay could be widened by combining different exposure times (0.2 s, 1 s, and 5 s). This was possible because of the low background signal and high photostability inherent to UCP technology. In Study **IV**, two different exposure times (1 s and 2 s) were also tested with the serum sample dilution series. A wider dynamic range was obtained with the shorter exposure time. In the future, the multiplex assays utilizing UCP technology could be measured with different exposure times. This would be useful in cases where both high and low intensity spots are measured in the same array.

The homogenous excitation of the whole array area - i.e., all spot positions - is also very important when attempting to minimize detection imprecision. An uneven excitation could have a dramatic effect on the reproducibility of the array results. To control this, it is advantageous to print replicate spots in the array well. Except in Study **III**, two to three replicate spots were printed in each array well (**I**, **II**, **IV**).

Homogenous spots and the reproducibility should be achieved in array-based assays. The spotting artifacts, such as irregular spot shapes (e.g., donut spots) need to be avoided because they cause very high intraspot standard deviation values (Pappaert *et al.*, 2006). This makes it difficult to analyze the signal, because the intensity is unevenly distributed throughout the spot. The outer border has higher intensity/pixel ratio than the spot center. In this study, the spots were manually analyzed and the measured spot area was specially selected. It is even more important to have regular round shape spots when the array data is automatically analyzed. In Study **IV**, the spotted biotinylated B19-VLP had a donut shape. Usually, the donut spots can be avoided by optimizing the spotting conditions. Guo and Zhu (2007) demonstrated that protein molecules preferentially accumulate at air/water interfaces. Detergents like Triton X-100 lower the surface tension of the spotting buffer and can be used to reduce this effect (Guo and Zhu, 2007). In Study **IV**, the free biotin molecules blocked the central area of the spot and the large biotinylated B19-VLPs were bound at the outer area of the spot. After an additional purification step, the printed B19-VLP spots showed more evenly distributed intensities within the spot.

The binding capacity of the solid-phase also affects the assay dynamic range. The spot (~200–1000 µm in diameter, **I-IV**) has lower binding capacity compared to the whole-well area (~6 mm in diameter). This might limit the dynamic range of the multianalyte assay. In Study **III**, the scanning (7 x 7 raster) measurement with the plate reader

equipped with PMT did not increase the linear range of the multianalyte assays. This means that the wide dynamic range of the reference assays measured with the plate reader does not originate solely from different measurement technology but the binding capacity of the solid-phase also affects the dynamic range. The plate reader was not optimal for the scanning of the arrays as the resolution was not adequate. There are several challenges to overcome when using the planar array detection. This detection technique is sensitive to inhomogeneities and/or variations in probe concentration, photobleaching of the probe, background fluorescence, and changes in the light source intensity.

6.2 Adenovirus genotyping assay (I-II)

The hAdV genotype-specific analysis is important for epidemiological studies to provide information on the incidence and distribution of infections by individual hAdV types. Genotype identification is also necessary for the detection of new strains and for understanding hAdV pathogenesis. In Study **II**, the hAdV genotyping assay was developed to better understand the epidemiology of clinical adenovirus infections in Finland.

6.2.1 Probe design and real-time quantitative PCR

The conserved region in the hAdV hexon sequence was chosen as the target for the hAdV genotyping assay. Through this sequence region, all the hAdV members belonging to groups A to F were targeted. An asymmetric real-time qPCR with Syber Green I dye was established for the amplification of the conserved hAdV hexon sequence region. The sensitive PCR method was able to detect the C02 genotype at concentrations of fewer than 10 copies per qPCR reaction (**I, II**).

A melting curve analysis was also included after the PCR amplification. Within the same hAdV genotype the melting temperature showed variations, and the melting temperatures of different hAdV types overlapped. The melting temperature analysis gave only a proximal estimation of the hAdV type. Also, the qPCR showed random non-specific late amplification of hAdV negative specimens or specimens infected with other viruses (**II**). The developed PCR method alone was not specific enough for hAdV genotyping. However, we combined the sensitive PCR method to a specific post-PCR oligonucleotide array-in-well hybridization assay to detect and genotype the hAdVs. The assay was specific for hAdV types, no hybridization signal was detected among the hAdV negative specimens or specimens infected with other viruses.

The 5'-terminus amino-modified capture probes used in Studies **I** and **II** contained three additional T/C nucleotides at the 5'end that could be utilized to increase the probes' hybridization efficiency by functioning as a spacer. Probe affinity is an important factor affecting the probe-target hybridization and the affinity should be as high as possible. The probe-target affinity was predicted using the calculated Gibbs free energy (ΔG) values of the probes. The thermodynamic behavior of the designed

probes (**I**) was evaluated by calculating the ΔG change of the probe-target hybrid. The designed oligonucleotides (**I**) showed a correlation between the hybridization intensity and ΔG values of the oligonucleotides. It is not always possible to design a single probe that would perfectly match within the genotype, but utilizing array technology, it is feasible to increase the number of probes to identify one genotype. Instead of using only one perfectly matched probe for one targeted hAdV type a combination of the specific oligonucleotide probes were used to give a specific hybridization pattern for each targeted hAdV type. Study (**I**) demonstrated that the array-in-well assay platform was suitable for the detection and genotyping of hAdV types in clinical nasopharyngeal samples. The hAdV type C02 was the most prevalent type among the 55 clinical nasopharyngeal samples (26% of the samples). The other types, in decreasing order, were B03, C01, E04, C06 and C05. The detected types are the most common hAdV types previously shown to cause respiratory tract infections in children (Qurei *et al.*, 2012).

6.2.2 Epidemiological study (II)

During the study period in the autumn of 2010, an outbreak of hAdV type B03 infections occurred. After this, only sporadic cases were detected. The type B03 was found in specimens from both children and adults. It was commonly associated with conjunctivitis (n = 79; 68%), and respiratory diseases (40; 47%). Genome type diversity, especially within hAdV type B03, is a well-known phenomenon observed in different parts of the world. A study conducted in Korea from 1990 to 2000 identified seven type B03 genome variants among the children during outbreaks of lower respiratory tract infections (Kim *et al*., 2003). Landry *et al*., 2009, reported two new genome B03 variant types (e.g., hAdV3a50 and hAdV3a51) and Selvaraju *et al*., 2011 reported four B03 genome variants, including previously reported hAdV-3a2 and hAdV3a50, and two novel variants based on the unique *Bgl*II and *Bst*EII profiles (Landry *et al.*, 2009; Selvaraju *et al.*, 2011). The new hAdV variant types are commonly classified on the basis of the restriction endonucleases found from various bacterial strains. These new genetic variant types could be a reason for the high incidence of B03 infections during the autumn of 2010 observed in this study. However, only a minor part of the detected B03 types were sequenced and no comprehensive sequence information on B03 types was obtained. Although group C hAdV types are common, especially among the children, other epidemiological studies have also reported high hAdV type B03 prevalence among the hospitalized children in Southern Palestine (Qurei *et al*., 2012), and also among both children and adults in the USA (Gray *et al.*, 2007; Selvaraju *et al*., 2011).

The predominant hAdV genotypes differ between countries or regions and change over time. In 2006 and 2007, the hAdV type B14 emerged as a significant contributor to acute respiratory disease and severe pneumonias in the USA and in military recruit training centers across the USA (Metzgar *et al.*, 2009; Tate *et al*., 2009). The hAdV type B14 has also emerged in Europe (Carr *et al*., 2011; O'Flanagan *et al*., 2011; Parcell *et al*., 2014). In this study, the array was not able to discriminate clinically

important hAdV type B14 from the types 11, 16, 34, and 35 belonging to group B because of the sequence similarity in the amplified hexon gene region. In this study, neither B14 nor B11, indistinguishable in the array-in-well assay, was detected among the clinical specimens. The targeted hexon gene sequence region needs to be changed if a specific probe for type B14 is designed. Since the B14 type was not present in the study population during this four year study period 2009-2012 in Finland, a redesign of the assay was not necessary at this time.

In Study (**II**), not all the prototype strains were available for genotyping. However, *in silico* analyses based on the probe-target thermodynamic ΔG values were performed to predict the binding efficiency between the probe and target. These analyses gave a specific pattern for most of the targeted genotypes. As expected, F40 was not differentiated from F41 just as B14 was not be differentiated from B11. Therefore, the samples need to be sequenced to reveal the exact type. Although the assay has some limitations, the developed hAdV genotyping assay has a wider type selection than many other published hAdV typing assays (López-Campos *et al*., 2007; Washington *et al.*, 2010). A reverse line blot hybridization method with even an broader hAdV type selection has been reported (Cao *et al*., 2011). The probes used in this study were suitable for the detection and typing of the most common and clinically relevant adenovirus types circulating in Finland. The array-in-well hybridization assay offered a robust multiplex platform for a rapid, high throughput typing of clinically relevant hAdV genotypes in different specimen types. In addition, there is scarce data on the hAdV epidemiology in Finland. Epidemiologically, the typing results gave a comprehensive picture of prevalent hAdV types in Finland during the four year study period (**unpublished**).

6.3 Quantitative multianalyte immunoassay (III)

Study **III** demonstrated a capability to perform a quantitative multiplex immunoassay using UCNP reporter technology and imaging detection. The assay specificity is a very important issue that should always be evaluated when developing multiplex assays (Gonzalez *et al.*, 2008). In multiplex immunoassay, cross-reactivity between antibodies and different proteins may cause major problems (Juncker *et al.*, 2014; Templin *et al*., 2002). Antibodies validated for singleplex immunoassays may display cross-reactivity with other proteins in multiplex formats; cross-reactivity reduces assay specificity and sensitivity leading to false interpretations of the positive and negative results. In this study, the possible cross-reactivities were tested with the single analyte array-in-wells, the analytes (PSA, TSH, and LH) were incubated with a cocktail of secondary antibody-coated UCNPs with no cross-reactions detected, so the analytes bound correctly only to the corresponding spots.

The multiplex immunoassay was carried out in a buffer, but to evaluate the possible matrix effect, a biological sample was tested in a single-analyte array-in-well assay for PSA. With the plasma sample the obtained detection limit was six times worse than detection limit obtained in buffer. This might be due to the formation of

nonimmunoreactive complexes of PSA to PSA-binding proteins present in the plasma sample. This is usually the main reason for compromised assay performance in plasma (Wu *et al.*, 2004).

The nonspecific binding of the antibody-coated UCNPs limited the assay sensitivity. In addition, the surface chemistry used for the biofunctionalization of the UCNPs as well as the assay conditions, such as the buffer used, may affect colloidal stability of the UCNPs during the assay. This can increase the background signal originating from the nonspecific binding of the UCNPs, which cannot be completely eliminated, but this inherent characteristic of antibodies can be minimized by the careful optimization of antibody combinations and assay conditions. (Ellington *et al*., 2010). By carefully choosing the antibodies used in the assay and optimizing the coating protocol of the UCNPs for each of the antibodies, the nonspecific binding could be further reduced.

The assay sensitivity (i.e., LOD) can be defined as the lowest concentration of the analyte that can be consistently measured. Comparison of different multiplex assay performances is not reliable if different models, antibodies, and detection technologies are used (Nielsen and Geierstanger, 2004). In some cases, the multianalyte protein assays may lack the adequate assay sensitivity compared to the traditional ELISAs (Copeland *et al.*, 2004). However, assays that have a high analytical performance by reaching an excellent assay sensitivity and wide linear range have been reported (Bruls *et al.*, 2009; Zong *et al.*, 2012). Bruls *et al*., 2009, have developed a rapid (total assay time a few minutes) multiplex immunoassay, which was able to detect drugs of abuse in subnanogram per milliliter in saliva and cardiac troponin I in subpicomole per liter levels in blood serum/plasma by using magnetic nanoparticle labels. Zong *et al*., 2012, developed a sensitive chemiluminescence immunoassay for the detection of tumor marker panel. This cancer screening assay reached wide linear ranges over 5 orders of magnitude as well as low detection limits.

In the multiplex immunoassay, the obtained LODs and dynamic ranges for LH and PSA were in clinically relevant ranges. Also, the multiplex immunoassay sensitivities for LH and PSA were comparable with the existing singleplex time-resolved immunofluorometric assays (Eriksson *et al.*, 2000; Stenman *et al.*, 1985). The sensitivity of the PSA assay was in the same range as that obtained in the previously published array-in-well multianalyte assay (Wiese *et al*., 2001) The LOD for TSH should have been over one order of magnitude lower to be suitable for the detection of overactive thyroid, i.e., the measurement of hyperthyroidism. TSH is known to be a very demanding analyte, requiring ultrahigh assay sensitivities and a very wide dynamic range. Earlier developed spot-based singleplex immunoassay for TSH demonstrated that using the antibody fragments as capture molecules instead of the whole monoclonal antibody can improve the assay sensitivity (Ylikotila *et al*., 2005). A very sensitive spot-based immunoassay for TSH was carried out by using a site-specifically biotinylated recombinant Fab fragment spotted (spot diameter 2.5 mm) on the bottom of streptavidin-coated 96-well microtiter plate.

The developed multiplex immunoassay platform showed potential for developing customized quantitative assays for protein biomarkers in plasma samples. The technology could be applied to, e.g., the cardiac marker multiplex assay, drug discovery, and other biomarker panels where more effective diagnosis is needed.

6.4 Serological array-in-well assay (IV)

Serological assays are used to measure disease-associated virus-specific IgM and IgG antibodies present in patients' serum during and after acute infection. In Study **IV**, a serological array-in-well assay was developed for the detection presence of B19V IgG, and hAdV IgG antibodies as well as total hIgG responses in serum samples simultaneously.

The hAdV C02 and C05 hexon specific spot signal intensities correlated with each other. C02 and C05 hexon antigen cross-reactivity was expected, because both of these viruses belong to group C and their hexon antigens show relatively high homology (86%) at the amino acid sequence level (Chroboczek *et al.*, 1992). This suggests that the epitopes in the hexon protein within at least hAdV types C02 and C05 are highly conserved. The inclusion of both C02 and C05 hexon antigens in the array offers a good control for the reproducibility of the antigen preparation process (e.g., hexon production, purification, labeling, and printing steps).

For each plate the analyte specific cut-off values were calculated and, based on these values, all the B19V samples showed 100% correlation with the reference B19V IgG assay. However, four serum samples (three from children and one from an adult) had a low hAdV IgG positive result in the array-in-well assay and a negative result in the reference hAdV IgG assay. This was not unexpected, because of the different serum sample dilutions used in these two assays. The four serum samples should have been tested in the array-in-well assay using a more diluted sample. One option could be that, in the future, more than one serum sample dilution is used in the array-in-well assay. By using both 1/200 and 1/1000 serum sample dilution the low-abundance and high-abundance antibodies could be detected. This would be useful when utilizing high multiplex degree arrays.

A limitation of the developed serological assay was that the amount of IgG antibodies bound to the surface of the specific antigen spot and control anti-hIgG spot was not quantified. There is no commonly used standard method to perform this task. However, a few studies have used either a linear (Mezzasoma *et al*., 2002) or non-linear (Yu *et al*., 2013) calibration method for quantifying antibody binding to the array surface. These assays take into account the fact that antibody concentrations vary in serum. The nonlinear standard curve method is based on a known amount of IgG standards printed on an array (Yu *et al*., 2013). The IgG antibodies bound to the spot can then calculated on the basis of standard curve. This method has an advantage compared to the standard curve method: it improves the linear dynamic range and

reduces assay variation. In the future, the serological array-in-well assay could be improved by including the quantification of the bound antibodies.

The serological array-in-well assay was feasible and correlated well with the results of the reference assay also in terms of defining B19V IgG seroconversions. Although the screening of anti-B19V antibodies especially in pregnant women has greater clinical importance, the detection of highly prevalent antibodies to hAdV served as a suitable control for virus-specific antibody response. The developed multiplex serodiagnostic model assay provides an important tool for the improved detection and screening of a wider panel of virus-specific antibody responses.

7 CONCLUSIONS

The interest in developing new and fast screening tools based on DNA- and protein arrays to detect and type a wide range of different biomarkers and pathogens is increasing. In this study, a high-quality spotting method for oligonucleotide and protein array-in-well is employed. The study verifies the advantages and potential of the UCP-based reporter technology in different multiplex bioaffinity model assays. Compared to many other widely used approaches, the UCP technology provides a fluorescence imaging system that is both low-cost and produces less background signal. Another advantage of utilizing UCPs is that continuous excitation and measurement can be used and no time-resolved measurement is needed. One of the main achievements of this study was the development of the hAdV genotyping assay, which has been used as a research tool in the epidemiological study of hAdV types circulating in Finland.

The main conclusions based on the studies are presented below.

I In this study, the developed oligonucleotide array-in-well approach utilizing upconverting phosphor reporter technology and the novel instrumentation for UCP imaging was demonstrated to be applicable to multianalyte studies. A desktop prototype of anti-Stokes photoluminescence imaging device based on laser diode excitation and CCD image sensor was constructed for multiplex testing. An oligonucleotide array-in-well assay was based on DNA amplification by the quantitative real-time PCR method using primers directed at the conserved hexon gene region of the hAdVs. A post-PCR high-throughput oligonucleotide hybridization assay was able to reveal the hAdV type in prototype strains and clinical nasopharyngeal specimens.

II The technically improved hAdV oligonucleotide array-in-well genotyping assay was used for the multiplex, rapid and accurate detection of clinically relevant hAdV genotypes in different specimen types. The hAdV negative and positive specimens as well as specimens containing other viruses than hAdV were analyzed with the array-in-well hybridization assay. During the one year study period, an outbreak of hAdV type B03 occurred in autumn 2010. Epidemiological information on hAdV types circulating in Finland is scarce, and this assay offered a robust multiplex platform for epidemiological studies.

III Antibody-based arrays represent a powerful approach for a large-scale characterization of candidate antigens. In this study, a multiplex immunoassay for three model analytes (PSA, TSH, and LH) was developed. The biotinylated antibodies were printed in an array format on the bottom of microtiter wells, and the captured target analytes were detected with secondary antibody-coated UCNPs. The array was imaged and the standard curves for each analyte were quantified from the images. Based on the multianalyte assay standard curves, all

the LODs except TSH were in clinically relevant range. The multianalyte immunoassay results were also comparable with the reference assays and single analyte array-in-well assays.

IV The serodiagnostic array-in-well assay offers a high-throughput method for the detection of virus-specific antibodies in serum. In this study, three different viral antigens (B19-VLP, hAdV C02, and C05 hexons) along with controls were printed in the same array well. Parallel serodiagnostic analyses were carried out by using one serum sample dilution. The developed assay was able to discriminate B19V and adenovirus IgG negative and positive patient populations. In addition, the results for B19V serology showed an excellent correlation with the commercial reference IgG EIA. Both the C02 and C05 were chosen because the population in Finland have high seroprevalence against these hAdV types and because it was necessary to get at least one virus-specific signal. The array-in-well assay offers a great potential for the future development of multiplex serodiagnostic assays in clinical virology.

Multiplex assays based on arrays are high-throughput platforms suitable for variable fields in clinical diagnostics. In the future, DNA-arrays may compete with the very high-throughput sequencing (e.g., next generation sequencing) methods, which increase sequence throughput by laying DNA fragments on a single chip and sequencing all these fragments in parallel yielding millions of DNA sequence reads in a single run. However, the high-throughput sequencing is still expensive and the results are more complex to analyze than array-based intensity results. In addition, the protein-based multiplex assays show great potential to improve the clinical diagnostic assay performance. Especially, the detection of the host antibody responses to multiple infectious diseases simultaneously in one array well could offer a reliable high-throughput clinical diagnostic tool in the future. Furthermore, protein arrays can be used to simultaneously analyze multiple biomarkers to a target disease providing a more accurate diagnostic result with smaller sample volume needed.

8 ACKNOWLEDGEMENTS

This study was carried out at the Department of Virology and Department of Biochemistry in the Division of Biotechnology, University of Turku, during the years 2009–2014. Financial support from the National Doctoral Programme of Advanced Diagnostic Technologies and Applications (DIA-NET), the Finnish Funding Agency for Technology and Innovation, University of Turku, Virustautien Tutkimussäätiö, Emil Aaltonen foundation, and the Academy of Finland is gratefully acknowledged.

I wish to thank the former and current Heads of the Department of Virology, Professor Timo Hyypiä, Docent Veijo Hukkanen, and Professor Ilkka Julkunen, for providing an enthusiastic scientific atmosphere. I thank also Professor Emeritus Timo Lövgren, Professor Kim Pettersson and Professor Tero Soukka for giving me the opportunity to carry out my PhD studies also at the Department of Biochemistry in the Division of Biotechnology. It has been enjoyable to work at both departments.

I owe my sincere gratitude to my supervisors Professor Tero Soukka and Docent Matti Waris for their support, encouraging attitude, and faith in my research throughout my thesis project. Tero has provided innovative ideas, which became fruitful research projects. He has also great passion towards science, and wide knowledge in all branches of molecular biotechnology. Matti has provided scientific expertise and outstanding knowledge in virus diagnostics. It has been a truly richness and my privilege to have you both as my supervisors.

My thesis committee advisors Docent Veijo Hukkanen and Dr. Petri Saviranta are thanked for their comments and encouragement during my thesis project.

I wish to thank my esteemed pre-examiners Docent Hannimari Kallio-Kokko and Professor Matti Karp for reviewing this thesis. I am grateful for their valuable comments to improve the thesis. I am also grateful to Anu Toivonen for reviewing the language of the thesis.

I warmly thank my co-authors Timo Valta, Maija Karp, Liisa Hattara, Emilia Palo (née Harju), Professor Jorma Hölsä, Dr. Petri Saviranta, Riikka Arppe, Henna Päkkilä, Satu Lahtinen, Niina Salminen, Dr. Mika Lastusaari, Siina Alaranta, Susanne Lahdenperä, Dr. Benedict Arku, and Professor Klaus Hedman for their contribution. The manuscripts would not have been possible without your help. I especially want to acknowledge Henna for sharing the responsibility of the quantitative multianalyte immunoassay project, and for her friendship. Liisa and Susanne are thanked for their precious work related to spotting and joyful moments related to scientific and personal life. I am grateful to Emilia, Satu and Riikka for their hard work preparing the upconverting phosphor particles used in this thesis. I also acknowledge Juho Terrijärvi and Mikko Pyykkö on their technical help with the UCP imaging device. I wish to thank Tiina Ylinen at the Department of Virology for her valuable laboratory

assistance with adenovirus genotyping assay. It has also been my privilege to work with Professor Klaus Hedman, who is such an expert in clinical virology.

I wish to thank Docent Tytti Vuorinen for providing valuable clinical samples from the Diagnostic Service Unit of the Department of Virology.

I want to thank the present and previous staff at the Department of Virology and Department of Biochemistry in the Division of Biotechnology for technical and secretarial assistance, you all are gratefully acknowledged.

I would like to thank my present and previous colleagues at Department of Biochemistry in the Division of Biotechnology, especially, Tanja Savukoski, Henna Päkkilä, Riikka Arppe, Satu Lahtinen, Tiina Myyryläinen, Heidi Hyytiä, Dr. Ulla Karhunen, Dr. Ari Lehmusvuori, Dr. Tuomas Huovinen, Riina-Minna Väänänen, Dr. Mari Peltola, Dr. Johanna Vuojola, Susanne Lahdenperä, Dr. Terhi Riuttamäki, Marja-Leena Järvenpää, and Marika Nummela for both scientific and non-scientific discussions, fun memories of congress trips along with important peer support.

I want to thank the former DIA-NET Doctoral Programme coordinators Dr. Mari Peltola, and Dr. Johanna Vuojola for providing technical help during the thesis writing process, arranging scientific and social events, and giving their support during the thesis project.

Special thanks to Dr. Michaela Nygårdas, Dr. Laura Kakkola, and Henrik Paavilainen for creating a pleasant atmosphere during the final phase of thesis writing. It was nice to join your office although the “Pimeähuone” was very efficient place to write the thesis. I also owe thanks to Henrik who helped me with Word formatting problems. Warm thanks go to Michaela for her friendship and practical tips during the final phase of the thesis project. I thank Riikka Österback and Dr. Piritta Peri for their friendly scientific and not so scientific advices.

I am extremely grateful to my dear biochemist friends: Anni, Hanna, Jenni, Joanna, Marika, Marja-Leena, Päivikki, Sari and Tanja. Thanks go also to the spouses. We have had fun during these years: all the parties, summer festivals, trips from Malaysia to the USA, and moments together have been valuable. I am also grateful your support. You all are very important to me. Special thanks go to Tanja for sharing the final steps of completing this thesis.

A warm thanks also to my two wonderful “old” friends Minna and Sanna who have been in life since childhood. Although we see each other rarely, you are still important to me. We are the gang of three from Kärki.

Suuret kiitokset äidille ja isälle, kun olette aina jaksaneet tukea, kannustaa ja uskoa. On ollut tärkeää päästä välillä "lataamaan akkuja" Seinäjoelle. Kiitos mummulle sekä veljille Mikolle perheineen ja Juhalle, onneksi olette olemassa. Olette kaikki valtavan tärkeitä!

Finally, my dearest thanks go to Vesa for his love, hugs & kisses, and for keeping me fed by making spicy omelettes for me. Thank you "Ma Vee" for your support during the years.

Turku, May 2014

Minna Ylihärsilä

9 REFERENCES

Ádám, E., Lengyel, A., Takács, M., Erdei, J., Fachet, J., Nász, I. (1986) Grouping of monoclonal antibodies to adenovirus hexons by their cross-reactivity. *Arch Virol* **87**, 61-71.

Afanassiev, V., Hanemann, V., Wolfl, S. (2000) Preparation of DNA and protein micro arrays on glass slides coated with an agarose film. *Nucleic Acids Res* **28**, E66.

Ahmed Ebbiary, N.A., Lenton, E.A., Cooke, I.D. (1994) Hypothalamic-pituitary ageing: progressive increase in FSH and LH concentrations throughout the reproductive life in regularly menstruating women. *Clin Endocrinol (Oxf)* **41**, 199-206.

Alexandre, I., Hamels, S., Dufour, S., Collet, J., Zammatteo, N., De Longueville, F., Gala, J.L., Remacle, J. (2001) Colorimetric silver detection of DNA microarrays. *Anal Biochem* **295**, 1-8.

Allander, T., Andreasson, K., Gupta, S., Bjerkner, A., Bogdanovic, G., Persson, M.A., Dalianis, T., Ramqvist, T., Andersson, B. (2007) Identification of a third human polyomavirus. *J Virol* **81**, 4130-4136.

Allander, T., Tammi, M.T., Eriksson, M., Bjerkner, A., Tiveljung-Lindell, A., Andersson, B. (2005) Cloning of a human parvovirus by molecular screening of respiratory tract samples. *Proc Natl Acad Sci U S A* **102**, 12891-12896.

Almgren, M., Atkinson, R., He, J., Hilding, A., Hagman, E., Wolk, A., Thorell, A., Marcus, C., Näslund, E., Östenson, C.G., Schalling, M., Lavebratt, C. (2012) Adenovirus-36 is associated with obesity in children and adults in Sweden as determined by rapid ELISA. *PLoS One* **7**, e41652.

Anderson, L.J., Tsou, C., Parker, R.A., Chorba, T.L., Wulff, H., Tattersall, P., Mortimer, P.P. (1986) Detection of antibodies and antigens of human parvovirus B19 by enzyme-linked immunosorbent assay. *J Clin Microbiol* **24**, 522-526.

Arppe, R., Salovaara, O., Mattsson, L., Lahtinen, S., Valta, T., Riuttamäki, T., Soukka, T. (2013) High gradient magnetic separation of upconverting lanthanide nanophosphors based on their intrinsic paramagnetism. *Journal of Nanoparticle Research* **15**:1883.

Artieda, J., Piñeiro, L., González, M., Muñoz, M., Basterrechea, M., Iturzaeta, A., Cilla, G. (2009) A swimming pool-related outbreak of pharyngoconjunctival fever in children due to adenovirus type 4, Gipuzkoa, Spain, 2008. *Euro Surveill* **14**, 6-8.

Auzel, F. (2004) Upconversion and anti-Stokes processes with f and d ions in solids. *Chem Rev* **104**, 139-173.

Avellón, A., Peréz, P., Aguilar, J.C., Lejarazu, R., Echevarría, J.E. (2001) Rapid and sensitive diagnosis of human adenovirus infections by a generic polymerase chain reaction. *J Virol Methods* **92**, 113-120.

Avseenko, N.V., Morozova, T.Y., Ataullakhanov, F.I., Morozov, V.N. (2002) Immunoassay with multicomponent protein microarrays fabricated by electrospray deposition. *Anal Chem* **74**, 927-933.

Aybay, C. (2003) Differential binding characteristics of protein G and protein A for Fc fragments of papain-digested mouse IgG. *Immunol Lett* **85**, 231-235.

Bacarese-Hamilton, T., Mezzasoma, L., Ingham, C., Ardizzoni, A., Rossi, R., Bistoni, F., Crisanti, A. (2002) Detection of allergen-specific IgE on microarrays by use of signal amplification techniques. *Clin Chem* **48**, 1367-1370.

Bagwe, R.P., Yang, C., Hilliard, L.R., Tan, W. (2004) Optimization of dye-doped silica nanoparticles prepared using a reverse microemulsion method. *Langmuir* **20**, 8336-8342.

Balada-Llasat, J.M., LaRue, H., Kelly, C., Rigali, L., Pancholi, P. (2011) Evaluation of commercial ResPlex II v2.0, MultiCode-PLx, and xTAG respiratory viral panels for the diagnosis of respiratory viral infections in adults. *J Clin Virol* **50**, 42-45.

Balen, A.H., Conway, G.S., Kaltsas, G., Techatrasak, K., Manning, P.J., West, C., Jacobs, H.S. (1995) Polycystic ovary syndrome: the spectrum of the disorder in 1741 patients. *Hum Reprod* **10**, 2107-2111.

Bally, M., Halter, M., Vörös, J., Grandin, H.M. (2006) Optical microarray biosensing techniques. *Surface and Interface Analysis* **38**, 1442-1458.

Barbulovic-Nad, I., Lucente, M., Sun, Y., Zhang, M., Wheeler, A.R., Bussmann, M. (2006) Bio-microarray fabrication techniques--a review. *Crit Rev Biotechnol* **26**, 237-259.

Barraza, E.M., Ludwig, S.L., Gaydos, J.C., Brundage, J.F. (1999) Reemergence of adenovirus type 4 acute respiratory disease in military trainees: report of an outbreak during a lapse in vaccination. *J Infect Dis* **179**, 1531-1533.

Beier, M., Hoheisel, J.D. (1999) Versatile derivatisation of solid support media for covalent bonding on DNA-microchips. *Nucleic Acids Res* **27**, 1970-1977.

Belosludtsev, Y., Iverson, B., Lemeshko, S., Eggers, R., Wiese, R., Lee, S., Powdrill, T., Hogan, M. (2001) DNA microarrays based on noncovalent oligonucleotide attachment and hybridization in two dimensions. *Anal Biochem* **292**, 250-256.

Bernal, J., Guadano-Ferraz, A., Morte, B. (2003) Perspectives in the study of thyroid hormone action on brain development and function. *Thyroid* **13**, 1005-1012.

Berthet, N., Paulous, S., Coffey, L.L., Frenkiel, M.P., Moltini, I., Tran, C., Matheus, S., Ottone, C., Ungeheuer, M.N., Renaudat, C., Caro, V., Dussart, P., Gessain, A., Despres, P. (2013) Resequencing microarray method for molecular diagnosis of human arboviral diseases. *J Clin Virol* **56**, 238-243.

Biere, B., Schweiger, B. (2010) Human adenoviruses in respiratory infections: sequencing of the hexon hypervariable region reveals high sequence variability. *J Clin Virol* **47**, 366-371.

Bouguelia, S., Roupioz, Y., Slimani, S., Mondani, L., Casabona, M.G., Durmort, C., Vernet, T., Calemczuk, R., Livache, T. (2013) On-chip microbial culture for the specific detection of very low levels of bacteria. *Lab Chip* **13**, 4024-4032.

Bruls, D.M., Evers, T.H., Kahlman, J.A., van Lankvelt, P.J., Ovsyanko, M., Pelssers, E.G., Schleipen, J.J., de Theije, F.K., Verschuren, C.A., van der Wijk, T., van

Zon, J.B., Dittmer, W.U., Immink, A.H., Nieuwenhuis, J.H., Prins, M.W. (2009) Rapid integrated biosensor for multiplexed immunoassays based on actuated magnetic nanoparticles. *Lab Chip* **9**, 3504-3510.

Burgess, S.T., Kenyon, F., O'Looney, N., Ross, A.J., Chong Kwan, M., Beattie, J.S., Petrik, J., Ghazal, P., Campbell, C.J. (2008) A multiplexed protein microarray for the simultaneous serodiagnosis of human immunodeficiency virus/hepatitis C virus infection and typing of whole blood. *Anal Biochem* **382**, 9-15.

Cannon, G.A., Carr, M.J., Yandle, Z., Schaffer, K., Kidney, R., Hosny, G., Doyle, A., Ryan, J., Gunson, R., Collins, T., Carman, W.F., Connell, J., Hall, W.W. (2010) A low density oligonucleotide microarray for the detection of viral and atypical bacterial respiratory pathogens. *J Virol Methods* **163**, 17-24.

Cao, Y., Kong, F., Zhou, F., Xiao, M., Wang, Q., Duan, Y., Kesson, A.M., McPhie, K., Gilbert, G.L., Dwyer, D.E. (2011) Genotyping of human adenoviruses using a PCR-based reverse line blot hybridisation assay. *Pathology* **43**, 488-494.

Cao, Y.C., Jin, R., Mirkin, C.A. (2002) Nanoparticles with Raman spectroscopic fingerprints for DNA and RNA detection. *Science* **297**, 1536-1540.

Cao, Y.C., Jin, R., Nam, J.M., Thaxton, C.S., Mirkin, C.A. (2003) Raman dye-labeled nanoparticle probes for proteins. *J Am Chem Soc* **125**, 14676-14677.

Carr, M.J., Kajon, A.E., Lu, X., Dunford, L., O'Reilly, P., Holder, P., De Gascun, C.F., Coughlan, S., Connell, J., Erdman, D.D., Hall, W.W. (2011) Deaths associated with human adenovirus-14p1 infections, Europe, 2009-2010. *Emerg Infect Dis* **17**, 1402-1408.

Cha, T., Guo, A., Jun, Y., Pei, D., Zhu, X.Y. (2004) Immobilization of oriented protein molecules on poly(ethylene glycol)-coated Si(111). *Proteomics* **4**, 1965-1976.

Chen, S.P., Huang, Y.C., Chiu, C.H., Wong, K.S., Huang, Y.L., Huang, C.G., Tsao, K.C., Lin, T.Y. (2013) Clinical features of radiologically confirmed pneumonia due to adenovirus in children. *J Clin Virol* **56**, 7-12.

Chen, Z., Tabakman, S.M., Goodwin, A.P., Kattah, M.G., Daranciang, D., Wang, X., Zhang, G., Li, X., Liu, Z., Utz, P.J., Jiang, K., Fan, S., Dai, H. (2008) Protein microarrays with carbon nanotubes as multicolor Raman labels. *Nat Biotechnol* **26**, 1285-1292.

Chrisey, L.A., Lee, G.U., O'Ferrall, C.E. (1996) Covalent attachment of synthetic DNA to self-assembled monolayer films. *Nucleic Acids Res* **24**, 3031-3039.

Chroboczek, J., Bieber, F., Jacrot, B. (1992) The sequence of the genome of adenovirus type 5 and its comparison with the genome of adenovirus type 2. *Virology* **186**, 280-285.

Chuang, Y., Chiu, C.H., Wong, K.S., Huang, J.G., Huang, Y.C., Chang, L.Y., Lin, T.Y. (2003) Severe adenovirus infection in children. *J Microbiol Immunol Infect* **36**, 37-40.

Clewley, J.P. (2004) A role for arrays in clinical virology: fact or fiction? *Journal of Clinical Virology* **29**, 2-12.

Cohen, B.J., Buckley, M.M. (1988) The prevalence of antibody to human parvovirus B19 in England and Wales. *J Med Microbiol* **25**, 151-153.

Coiras, M.T., Aguilar, J.C., García, M.L., Casas, I., Pérez-Breña, P. (2004) Simultaneous detection of fourteen respiratory viruses in clinical specimens by two multiplex reverse transcription nested-PCR assays. *J Med Virol* **72**, 484-495.

Copeland, S., Siddiqui, J., Remick, D. (2004) Direct comparison of traditional ELISAs and membrane protein arrays for detection and quantification of human cytokines. *J Immunol Methods* **284**, 99-106.

Coppée, J.Y. (2008) Do DNA microarrays have their future behind them? *Microbes Infect* **10**, 1067-1071.

Corstjens, P.L., Li, S., Zuiderwijk, M., Kardos, K., Abrams, W.R., Niedbala, R.S., Tanke, H.J. (2005) Infrared up-converting phosphors for bioassays. *IEE Proc Nanobiotechnol* **152**, 64-72.

Cossart, Y.E., Field, A.M., Cant, B., Widdows, D. (1975) Parvovirus-like particles in human sera. *Lancet* **1**, 72-73.

Cretich, M., Reddington, A., Monroe, M., Bagnati, M., Damin, F., Sola, L., Unlu, M.S., Chiari, M. (2011) Silicon biochips for dual label-free and fluorescence detection: Application to protein microarray development. *Biosens Bioelectron* **26**, 3938–3943.

Csáki, A., Möller, R., Straube, W., Köhler, J.M., Fritzsche, W. (2001) DNA monolayer on gold substrates characterized by nanoparticle labeling and scanning force microscopy. *Nucleic Acids Res* **29**, E81.

D'Angelo, L.J., Hierholzer, J.C., Keenlyside, R.A., Anderson, L.J., Martone, W.J. (1979) Pharyngoconjunctival fever caused by adenovirus type 4: report of a swimming pool-related outbreak with recovery of virus from pool water. *J Infect Dis* **140**, 42-47.

Dabbousi, B.O., Rodriguez-Viejo, J., Mikulec, F.V., Heine, J.R., Mattoussi, H., Ober, R., Jensen, K.F., Bawendi, M.G. (1997) (CdSe)ZnS Core-Shell Quantum Dots: Synthesis and Characterization of a Size Series of Highly Luminescent Nanocrystallites. *J. Phys. Chem. B* **101**, 9463-9475.

Dankbar, D.M., Dawson, E.D., Mehlmann, M., Moore, C.L., Smagala, J.A., Shaw, M.W., Cox, N.J., Kuchta, R.D., Rowlen, K.L. (2007) Diagnostic microarray for influenza B viruses. *Anal Chem* **79**, 2084-2090.

Dawson, E.D., Moore, C.L., Smagala, J.A., Dankbar, D.M., Mehlmann, M., Townsend, M.B., Smith, C.B., Cox, N.J., Kuchta, R.D., Rowlen, K.L. (2006) MChip: a tool for influenza surveillance. *Anal Chem* **78**, 7610-7615.

del Mar Mosquera, M., de Ory, F., Moreno, M., Echevarria, J.E. (2002) Simultaneous detection of measles virus, rubella virus, and parvovirus B19 by using multiplex PCR. *J Clin Microbiol* **40**, 111-116.

Delehanty, J.B., Ligler, F.S. (2003) Method for printing functional protein microarrays. *Biotechniques* **34**, 380-385.

Driskell, J.D., Zhu, Y., Kirkwood, C.D., Zhao, Y., Dluhy, R.A., Tripp, R.A. (2010) Rapid and sensitive detection of rotavirus molecular signatures using surface enhanced Raman spectroscopy. *PLoS One* **5**, 1-9.

Dufva, M. (2005) Fabrication of high quality microarrays. *Biomol Eng* **22**, 173-184.

Dufva, M. (2009) Introduction to microarray. *DNA Microarrays for Biomedical Research: Methods and Protocols* **529**, 1-22.

Dunbar, S.A. (2006) Applications of Luminex xMAP technology for rapid, high-throughput multiplexed nucleic acid detection. *Clin Chim Acta* **363**, 71-82.

Eastman, P.S., Ruan, W., Doctolero, M., Nuttall, R., de Feo, G., Park, J.S., Chu, J.S., Cooke, P., Gray, J.W., Li, S., Chen, F.F. (2006) Qdot nanobarcodes for multiplexed gene expression analysis. *Nano Lett* **6**, 1059-1064.

Ebner, K., Pinsker, W., Lion, T. (2005) Comparative sequence analysis of the hexon gene in the entire spectrum of human adenovirus serotypes: phylogenetic, taxonomic, and clinical implications. *J Virol* **79**, 12635-12642.

Ebner, K., Rauch, M., Preuner, S., Lion, T. (2006) Typing of human adenoviruses in specimens from immunosuppressed patients by PCR-fragment length analysis and real-time quantitative PCR. *J Clin Microbiol* **44**, 2808-2815.

Ekins, R., Chu, F. (1992) Multianalyte microspot immunoassay. The microanalytical 'compact disk' of the future. *Ann Biol Clin (Paris)* **50**, 337-353.

Ekins, R., Chu, F., Biggart, E. (1990) Multispot, multianalyte, immunoassay. *Ann Biol Clin (Paris)* **48**, 655-666.

Ekins, R.P. (1989) Multi-analyte immunoassay. *J Pharm Biomed Anal* **7**, 155-168.

Ellington, A.A., Kullo, I.J., Bailey, K.R., Klee, G.G. (2010) Antibody-based protein multiplex platforms: technical and operational challenges. *Clin Chem* **56**, 186-193.

Elnifro, E.M., Ashshi, A.M., Cooper, R.J., Klapper, P.E. (2000) Multiplex PCR: Optimization and Application in Diagnostic Virology. *Clinical Microbiology reviews* **13**, 559-570.

Enders, M., Schalasta, G., Baisch, C., Weidner, A., Pukkila, L., Kaikkonen, L., Lankinen, H., Hedman, L., Söderlund-Venermo, M., Hedman, K. (2006) Human parvovirus B19 infection during pregnancy--value of modern molecular and serological diagnostics. *J Clin Virol* **35**, 400-406.

Erfurth, F., Tretyakov, A., Nyuyki, B., Mrotzek, G., Schmidt, W.D., Fassler, D., Saluz, H.P. (2008) Two-laser, large-field hyperspectral microarray scanner for the analysis of multicolor microarrays. *Anal Chem* **80**, 7706-7713.

Eriksson, S., Vehniäinen, M., Jansen, T., Meretoja, V., Saviranta, P., Pettersson, K., Lövgren, T. (2000) Dual-label time-resolved immunofluorometric assay of free and total prostate-specific antigen based on recombinant Fab fragments. *Clin Chem* **46**, 658-666.

Espina, V., Mehta, A.I., Winters, M.E., Calvert, V., Wulfkuhle, J., Petricoin, E.F., 3rd, Liotta, L.A. (2003) Protein microarrays: molecular profiling technologies for clinical specimens. *Proteomics* **3**, 2091-2100.

Espina, V., Woodhouse, E.C., Wulfkuhle, J., Asmussen, H.D., Petricoin, E.F., 3rd, Liotta, L.A. (2004) Protein microarray detection strategies: focus on direct detection technologies. *J Immunol Methods* **290**, 121-133.

Fan, J.B., Gunderson, K.L., Bibikova, M., Yeakley, J.M., Chen, J., Wickham Garcia, E., Lebruska, L.L., Laurent, M., Shen, R., Barker, D. (2006) Illumina universal bead arrays. *Methods Enzymol* **410**, 57-73.

Fernandez-Lafuente, R., Rosell, C.M., Rodriguez, V., Santana, C., Soler, G., Bastida, A., Guisán, J.M. (1993) Preparation of activated supports containing low pK amino groups. A new tool for protein immobilization via the carboxyl coupling method. *Enzyme Microb Technol* **15**, 546-550.

Feron, D., Charlier, C., Gourain, V., Garderet, L., Coste-Burel, M., Le Pape, P., Weigel, P., Jacques, Y., Hermouet, S., Bigot-Corbel, E. (2013) Multiplexed infectious protein microarray immunoassay suitable for the study of the specificity of monoclonal immunoglobulins. *Anal Biochem* **433**, 202-209.

Franken, P.A., Hill, A.E., Peters, C.W., Weinreich, G. (1961) Generation of optical harmonics. *Phys. Rev. Lett.* **7**, 118-119.

Fraser, C., Donnelly, C.A., Cauchemez, S., Hanage, W.P., Van Kerkhove, M.D., Hollingsworth, T.D., Griffin, J., Baggaley, R.F., Jenkins, H.E., Lyons, E.J., Jombart, T., Hinsley, W.R., Grassly, N.C., Balloux, F., Ghani, A.C., Ferguson, N.M., Rambaut, A., Pybus, O.G., Lopez-Gatell, H., Alpuche-Aranda, C.M., Chapela, I.B., Zavala, E.P., Guevara, D.M., Checchi, F., Garcia, E., Hugonnet, S., Roth, C., Collaboration, W.H.O.R.P.A. (2009) Pandemic potential of a strain of influenza A (H1N1): early findings. *Science* **324**, 1557-1561.

Gaynor, A.M., Nissen, M.D., Whiley, D.M., Mackay, I.M., Lambert, S.B., Wu, G., Brennan, D.C., Storch, G.A., Sloots, T.P., Wang, D. (2007) Identification of a novel polyomavirus from patients with acute respiratory tract infections. *PLoS Pathog* **3**, 595-604.

Gehring, A.G., Albin, D.M., Reed, S.A., Tu, S.I., Brewster, J.D. (2008) An antibody microarray, in multiwell plate format, for multiplex screening of foodborne pathogenic bacteria and biomolecules. *Anal Bioanal Chem* **391**, 497-506.

Ginocchio, C.C. (2011) Strengths and weaknesses of FDA-approved/cleared diagnostic devices for the molecular detection of respiratory pathogens. *Clin Infect Dis* **52** Suppl 4, S312-325.

Giorgio, E., De Oronzo, M.A., Iozza, I., Di Natale, A., Cianci, S., Garofalo, G., Giacobbe, A.M., Politi, S. (2010) Parvovirus B19 during pregnancy: a review. *J Prenat Med* **4**, 63-66.

Golden, J.P., Ligler, F.S. (2002) A comparison of imaging methods for use in an array biosensor. *Biosens Bioelectron* **17**, 719-725.

Gonzalez, R.M., Seurynck-Servoss, S.L., Crowley, S.A., Brown, M., Omenn, G.S., Hayes, D.F., Zangar, R.C. (2008) Development and validation of sandwich ELISA microarrays with minimal assay interference. *J Proteome Res* **7**, 2406-2414.

Gray, G.C., McCarthy, T., Lebeck, M.G., Schnurr, D.P., Russell, K.L., Kajon, A.E., Landry, M.L., Leland, D.S., Storch, G.A., Ginocchio, C.C., Robinson, C.C., Demmler, G.J., Saubolle, M.A., Kehl, S.C., Selvarangan, R., Miller, M.B., Chappell, J.D., Zerr, D.M., Kiska, D.L., Halstead, D.C., Capuano, A.W., Setterquist, S.F., Chorazy, M.L., Dawson, J.D., Erdman, D.D. (2007) Genotype prevalence and risk factors for severe clinical adenovirus infection, United States 2004-2006. *Clin Infect Dis* **45**, 1120-1131.

Gray, J.J. (2004) The interaction of proteins with solid surfaces. *Curr Opin Struct Biol* **14**, 110-115.

Guo, A., Zhu, X.-Y., (2007). The critical role of surface chemistry in protein microarrays, in: Predki, P.F. (Ed.), *Functional Protein Microarrays in Drug Discovery*. CRC Press, pp. 53-71.

Guo, L., Gonzalez, R., Zhou, H., Wu, C., Vernet, G., Wang, Z., Wang, J. (2012) Detection of three human adenovirus species in adults with acute respiratory infection in China. *Eur J Clin Microbiol Infect Dis* **31**, 1051-1058.

Guo, Z., Guilfoyle, R.A., Thiel, A.J., Wang, R., Smith, L.M. (1994) Direct fluorescence analysis of genetic polymorphisms by hybridization with oligonucleotide arrays on glass supports. *Nucleic Acids Res* **22**, 5456-5465.

Gutmann, O., Niekrawietz, R., Kuehlewein, R., Steinert, C.P., Reinbold, S., De Heij, B., Daub, M., Zengerle, R. (2004) Non-contact production of oligonucleotide microarrays using the highly integrated TopSpot nanoliter dispenser. *Analyst* **129**, 835-840.

Haab, B.B., Dunham, M.J., Brown, P.O. (2001) Protein microarrays for highly parallel detection and quantitation of specific proteins and antibodies in complex solutions. *Genome Biol* **2**, 1-13.

Haase, M., Schäfer, H. (2011) Upconverting nanoparticles. *Angew Chem Int Ed Engl* **50**, 5808-5829.

Hacia, J.G., Fan, J.B., Ryder, O., Jin, L., Edgemon, K., Ghandour, G., Mayer, R.A., Sun, B., Hsie, L., Robbins, C.M., Brody, L.C., Wang, D., Lander, E.S., Lipshutz, R., Fodor, S.P., Collins, F.S. (1999) Determination of ancestral alleles for human single-nucleotide polymorphisms using high-density oligonucleotide arrays. *Nat Genet* **22**, 164-167.

Hall, D.A., Ptacek, J., Snyder, M. (2007) Protein microarray technology. *Mech Ageing Dev* **128**, 161-167.

Hall, J.E., Taylor, A.E., Hayes, F.J., Crowley, W.F., Jr. (1998) Insights into hypothalamic-pituitary dysfunction in polycystic ovary syndrome. *J Endocrinol Invest* **21**, 602-611.

Hardman, R. (2006) A toxicologic review of quantum dots: toxicity depends on physicochemical and environmental factors. *Environ Health Perspect* **114**, 165-172.

Heegaard, E.D., Brown, K.E. (2002) Human parvovirus B19. *Clin Microbiol Rev* **15**, 485-505.

Heer, S., Kömpe, K., Güdel, H.-U., Haase, M. (2004) Highly Efficient Multicolour Upconversion Emission in Transparent Colloids of Lanthanide-Doped NaYF4 Nanocrystals. *Advanced Materials* **16**, 2102-2105.

Heller, M.J. (2002) DNA Microarray Technology: Devices, Systems, and Applications. *Annu. Rev. Biomed. Eng.* **4**, 129-153.

Hierholzer, J.C. (1992) Adenoviruses in the immunocompromised host. *Clin Microbiol Rev* **5**, 262-274.

Hierholzer, J.C., Johansson, K.H., Anderson, L.J., Tsou, C.J., Halonen, P.E. (1987) Comparison of monoclonal time-resolved fluoroimmunoassay with

monoclonal capture-biotinylated detector enzyme immunoassay for adenovirus antigen detection. *J Clin Microbiol* **25**, 1662-1667.

Hlady, V.V., Buijs, J. (1996) Protein adsorption on solid surfaces. *Curr Opin Biotechnol* **7**, 72-77.

Hodneland, C.D., Lee, Y.S., Min, D.H., Mrksich, M. (2002) Selective immobilization of proteins to self-assembled monolayers presenting active site-directed capture ligands. *Proc Natl Acad Sci U S A* **99**, 5048-5052.

Hoke, C.H., Jr., Snyder, C.E., Jr. (2013) History of the restoration of adenovirus type 4 and type 7 vaccine, live oral (Adenovirus Vaccine) in the context of the Department of Defense acquisition system. *Vaccine* **31**, 1623-1632.

Hong, S., Li, X. (2013) Optimal Size of Gold Nanoparticles for Surface-Enhanced Raman Spectroscopy under Different Conditions. *Journal of Nanomaterials* **2013**, 1-9.

Honkinen, M., Lahti, E., Österback, R., Ruuskanen, O., Waris, M. (2012) Viruses and bacteria in sputum samples of children with community-acquired pneumonia. *Clin Microbiol Infect* **18**, 300-307.

Houk, C.P., Kunselman, A.R., Lee, P.A. (2009) Adequacy of a single unstimulated luteinizing hormone level to diagnose central precocious puberty in girls. *Pediatrics* **123**, e1059-1063.

Huang, G., Yu, D., Zhu, Z., Zhao, H., Wang, P., Gray, G.C., Meng, L., Xu, W. (2013) Outbreak of febrile respiratory illness associated with human adenovirus type 14p1 in Gansu Province, China. *Influenza Other Respir Viruses* **7**, 1048-1054.

Hyppänen, I., Hölsä, J., Kankare, J., Lastusaari, M., Pihlgren, L., Soukka, T. (2009) Preparation and Up-Conversion Luminescence Properties of NaYF4:Yb3+,Er3+ Nanomaterials. *Terrae Rarae* **16**, 1-6.

Jin, Y., Zhang, R.F., Xie, Z.P., Yan, K.L., Gao, H.C., Song, J.R., Yuan, X.H., Hou, Y.D., Duan, Z.J. (2013) Prevalence of adenovirus in children with acute respiratory tract infection in Lanzhou, China. *Virol J* **10**, 271-278.

Jonkheijm, P., Weinrich, D., Schroder, H., Niemeyer, C.M., Waldmann, H. (2008) Chemical strategies for generating protein biochips. *Angew Chem Int Ed Engl* **47**, 9618-9647.

Joos, B., Kuster, H., Cone, R. (1997) Covalent attachment of hybridizable oligonucleotides to glass supports. *Anal Biochem* **247**, 96-101.

Jun, B.H., Kim, J.H., Park, H., Kim, J.S., Yu, K.N., Lee, S.M., Choi, H., Kwak, S.Y., Kim, Y.K., Jeong, D.H., Cho, M.H., Lee, Y.S. (2007) Surface-enhanced Raman spectroscopic-encoded beads for multiplex immunoassay. *J Comb Chem* **9**, 237-244.

Juncker, D., Bergeron, S., Laforte, V., Li, H. (2014) Cross-reactivity in antibody microarrays and multiplexed sandwich assays: shedding light on the dark side of multiplexing. *Current Opinion in Chemical Biology* **18**, 29-37.

Järås, K., Adler, B., Tojo, A., Malm, J., Marko-Varga, G., Lilja, H., Laurell, T. (2012) Porous silicon antibody microarrays for quantitative analysis: measurement of free and total PSA in clinical plasma samples. *Clin Chim Acta* **414**, 76-84.

Kaikkonen, L., Lankinen, H., Harjunpää, I., Hokynar, K., Söderlund-Venermo, M., Oker-Blom, C., Hedman, L., Hedman, K. (1999) Acute-phase-specific

heptapeptide epitope for diagnosis of parvovirus B19 infection. *J Clin Microbiol* **37**, 3952-3956.

Kaikkonen, L., Söderlund-Venermo, M., Brunstein, J., Schou, O., Panum Jensen, I., Rousseau, S., Caul, E.O., Cohen, B., Valle, M., Hedman, L., Hedman, K. (2001) Diagnosis of human parvovirus B19 infections by detection of epitope-type-specific VP2 IgG. *J Med Virol* **64**, 360-365.

Kaneko, H., Iida, T., Ishiko, H., Ohguchi, T., Ariga, T., Tagawa, Y., Aoki, K., Ohno, S., Suzutani, T. (2009) Analysis of the complete genome sequence of epidemic keratoconjunctivitis-related human adenovirus type 8, 19, 37 and a novel serotype. *J Gen Virol* **90**, 1471-1476.

Kang, L.H., Oh, S.H., Park, J.W., Won, Y.J., Ryu, S., Paik, S.Y. (2013) Simultaneous detection of waterborne viruses by multiplex real-time PCR. *J Microbiol* **51**, 671-675.

Kaplan, M.M. (1999) Clinical perspectives in the diagnosis of thyroid disease. *Clin Chem* **45**, 1377-1383.

Karagiannis, A., Harsoulis, F. (2005) Gonadal dysfunction in systemic diseases. *Eur J Endocrinol* **152**, 501-513.

Kaufmann, B., Simpson, A.A., Rossmann, M.G. (2004) The structure of human parvovirus B19. *Proc Natl Acad Sci U S A* **101**, 11628-11633.

Kim, I., Junejo, I.-u.-R., Lee, M., Lee, S., Lee, E.K., Chang, S.-I., Choo, J. (2012) SERS-based multiple biomarker detection using a gold-patterned microarray chip. *Journal of Molecular Structure* **1023**, 197-203.

Kim, S.R., Ki, C.S., Lee, N.Y. (2009) Rapid detection and identification of 12 respiratory viruses using a dual priming oligonucleotide system-based multiplex PCR assay. *J Virol Methods* **156**, 111-116.

Kim, Y.J., Hong, J.Y., Lee, H.J., Shin, S.H., Kim, Y.K., Inada, T., Hashido, M., Piedra, P.A. (2003) Genome type analysis of adenovirus types 3 and 7 isolated during successive outbreaks of lower respiratory tract infections in children. *J Clin Microbiol* **41**, 4594-4599.

Kimura, N., Oda, R., Inaki, Y., Suzuki, O. (2004) Attachment of oligonucleotide probes to poly carbodiimide-coated glass for microarray applications. *Nucleic Acids Res* **32**, e68.

Kingsmore, S.F. (2006) Multiplexed protein measurement: technologies and applications of protein and antibody arrays. *Nat Rev Drug Discov* **5**, 310-320.

Kneipp, K., Kneipp, H., Itzkan, I., Dasari, R.R., Feld, M.S. (1999) Ultrasensitive chemical analysis by Raman spectroscopy. *Chem Rev* **99**, 2957-2976.

Koopmans, M., de Bruin, E., Godeke, G.J., Friesema, I., van Gageldonk, R., Schipper, M., Meijer, A., van Binnendijk, R., Rimmelzwaan, G.F., de Jong, M.D., Buisman, A., van Beek, J., van de Vijver, D., Reimerink, J. (2012) Profiling of humoral immune responses to influenza viruses by using protein microarray. *Clin Microbiol Infect* **18**, 797-807.

Korada, M., Pearce, M.S., Avis, E., Turner, S., Cheetham, T. (2009) TSH levels in relation to gestation, birth weight and sex. *Horm Res* **72**, 120-123.

Kosobrodova, E., Mohamed, A., Su, Y., Kondyurin, A., dos Remedios, C.G., McKenzie, D.R., Bilek, M.M.M. (2014) Cluster of differentiation antibody

microarrays on plasma immersion ion implanted polycarbonate. *Materials Science and Engineering: C* **35**, 434-440.

Krishna, N.K., Cunnion, K.M. (2012) Role of molecular diagnostics in the management of infectious disease emergencies. *Med Clin North Am* **96**, 1067-1078.

Krämer, K.W., Biner, D., Fre, G., Güdel, H.U., Hehlen, M.P., Lüthi, S.R. (2004) Hexagonal Sodium Yttrium Fluoride Based Green and Blue Emitting Upconversion Phosphors. *Chem. Mater.* **16**, 1244-1251.

Kuningas, K., Rantanen, T., Lövgren, T., Soukka, T. (2005a) Enhanced photoluminescence of up-converting phosphors in a solid phase bioaffinity assay. *Analytica Chimica Acta* **543**, 130-136.

Kuningas, K., Rantanen, T., Ukonaho, T., Lövgren, T., Soukka, T. (2005b) Homogeneous assay technology based on upconverting phosphors. *Anal Chem* **77**, 7348-7355.

Kuo, C.Y., Lee, C.Y., Kao, C.L., Hsu, Y.H. (1990) A fatal case of viral pneumonia in a child infected with adenovirus type 3. *Zhonghua Min Guo Xiao Er Ke Yi Xue Hui Za Zhi* **31**, 40-46.

Kusnezow, W., Hoheisel, J.D. (2003) Solid supports for microarray immunoassays. *J Mol Recognit* **16**, 165-176.

Kusnezow, W., Jacob, A., Walijew, A., Diehl, F., Hoheisel, J.D. (2003) Antibody microarrays: an evaluation of production parameters. *Proteomics* **3**, 254-264.

Kwon, Y., Coleman, M.A., Camarero, J.A. (2006) Selective immobilization of proteins onto solid supports through split-intein-mediated protein trans-splicing. *Angew Chem Int Ed Engl* **45**, 1726-1729.

La Rosa, A.M., Champlin, R.E., Mirza, N., Gajewski, J., Giralt, S., Rolston, K.V., Raad, I., Jacobson, K., Kontoyiannis, D., Elting, L., Whimbey, E. (2001) Adenovirus infections in adult recipients of blood and marrow transplants. *Clin Infect Dis* **32**, 871-876.

Lababidi, S. (2008) Challenges in DNA microarray studies from the regulatory perspective. *J Biopharm Stat* **18**, 183-202.

Lai, C.Y., Lee, C.J., Lu, C.Y., Lee, P.I., Shao, P.L., Wu, E.T., Wang, C.C., Tan, B.F., Chang, H.Y., Hsia, S.H., Lin, J.J., Chang, L.Y., Huang, Y.C., Huang, L.M., Taiwan Pediatric Infectious Disease, A. (2013) Adenovirus serotype 3 and 7 infection with acute respiratory failure in children in Taiwan, 2010-2011. *PLoS One* **8**, 1-7.

Lam, W.Y., Yeung, A.C., Tang, J.W., Ip, M., Chan, E.W., Hui, M., Chan, P.K. (2007) Rapid multiplex nested PCR for detection of respiratory viruses. *J Clin Microbiol* **45**, 3631-3640.

Landry, M.L., Lebeck, M.G., Capuano, A.W., McCarthy, T., Gray, G.C. (2009) Adenovirus type 3 outbreak in connecticut associated with a novel variant. *J Med Virol* **81**, 1380-1384.

Larson, D.R., Zipfel, W.R., Williams, R.M., Clark, S.W., Bruchez, M.P., Wise, F.W., Webb, W.W. (2003) Water-soluble quantum dots for multiphoton fluorescence imaging in vivo. *Science* **300**, 1434-1436.

Le Goff, G.C., Blum, L.J., Marquette, C.A. (2011) Enhanced colorimetric detection on porous microarrays using in situ substrate production. *Anal Chem* **83**, 3610-3615.

Lebeck, M.G., McCarthy, T.A., Capuano, A.W., Schnurr, D.P., Landry, M.L., Setterquist, S.F., Heil, G.L., Kilic, S., Gray, G.C. (2009) Emergent US adenovirus 3 strains associated with an epidemic and serious disease. *J Clin Virol* **46**, 331-336.

Lee, C.-S., Kim, B.-G. (2002) Improvement of protein stability in protein microarrays. *Biotechnology Letters* **24**, 839-844.

Lee, J.S., Song, J.J., Deaton, R., Kim, J.W. (2013) Assessing the detection capacity of microarrays as bio/nanosensing platforms. *Biomed Res Int* **2013**, 1-8.

Lemeshko, S.V., Powdrill, T., Belosludtsev, Y.Y., Hogan, M. (2001) Oligonucleotides form a duplex with non-helical properties on a positively charged surface. *Nucleic Acids Res* **29**, 3051-3058.

LePage, J., Peters, S., Lehotay, D.C. (2004) Assay of neonatal TSH from blood spots using the Architect i2000, an immunoassay analyzer. *Clin Biochem* **37**, 415-417.

Lévêque, N., Renois, F., Andréoletti, L. (2013) The microarray technology: facts and controversies. *Clin Microbiol Infect* **19**, 10-14.

Leveque, N., Van Haecke, A., Renois, F., Boutolleau, D., Talmud, D., Andreoletti, L. (2011) Rapid virological diagnosis of central nervous system infections by use of a multiplex reverse transcription-PCR DNA microarray. *J Clin Microbiol* **49**, 3874-3879.

Lewis, P.F., Schmidt, M.A., Lu, X., Erdman, D.D., Campbell, M., Thomas, A., Cieslak, P.R., Grenz, L.D., Tsaknardis, L., Gleaves, C., Kendall, B., Gilbert, D. (2009) A community-based outbreak of severe respiratory illness caused by human adenovirus serotype 14. *J Infect Dis* **199**, 1427-1434.

Li, L., Shimizu, H., Doan, L.T., Tung, P.G., Okitsu, S., Nishio, O., Suzuki, E., Seo, J.K., Kim, K.S., Muller, W.E., Ushijima, H. (2004) Characterizations of adenovirus type 41 isolates from children with acute gastroenteritis in Japan, Vietnam, and Korea. *J Clin Microbiol* **42**, 4032-4039.

Li, T., Guo, L., Wang, Z. (2008) Microarray based Raman spectroscopic detection with gold nanoparticle probes. *Biosens Bioelectron* **23**, 1125-1130.

Lilja, H., Christensson, A., Dahlén, U., Matikainen, M.T., Nilsson, O., Pettersson, K., Lövgren, T. (1991) Prostate-specific antigen in serum occurs predominantly in complex with alpha 1-antichymotrypsin. *Clin Chem* **37**, 1618-1625.

Lin, B., Wang, Z., Vora, G.J., Thornton, J.A., Schnur, J.M., Thach, D.C., Blaney, K.M., Ligler, A.G., Malanoski, A.P., Santiago, J., Walter, E.A., Agan, B.K., Metzgar, D., Seto, D., Daum, L.T., Kruzelock, R., Rowley, R.K., Hanson, E.H., Tibbetts, C., Stenger, D.A. (2006a) Broad-spectrum respiratory tract pathogen identification using resequencing DNA microarrays. *Genome Res* **16**, 527-535.

Lin, P.C., Ueng, S.H., Tseng, M.C., Ko, J.L., Huang, K.T., Yu, S.C., Adak, A.K., Chen, Y.J., Lin, C.C. (2006b) Site-specific protein modification through

Cu(I)-catalyzed 1,2,3-triazole formation and its implementation in protein microarray fabrication. *Angew Chem Int Ed Engl* **45**, 4286-4290.

Liotta, L.A., Espina, V., Mehta, A.I., Calvert, V., Rosenblatt, K., Geho, D., Munson, P.J., Young, L., Wulfkuhle, J., Petricoin, E.F. (2003) Protein microarrays: Meeting analytical challenges for clinical applications. *Cancer Cell* **3**, 317-325.

Liu, A., Wu, L., He, Z., Zhou, J. (2011) Development of highly fluorescent silica nanoparticles chemically doped with organic dye for sensitive DNA microarray detection. *Anal Bioanal Chem* **401**, 2003-2011.

Liu, Y., Xu, Z.Q., Zhang, Q., Jin, M., Yu, J.M., Li, J.S., Liu, N., Cui, S.X., Kong, X.Y., Wang, H., Li, H.Y., Cheng, W.X., Ma, X.J., Duan, Z.J. (2012) Simultaneous detection of seven enteric viruses associated with acute gastroenteritis by a multiplexed Luminex-based assay. *J Clin Microbiol* **50**, 2384-2389.

Liu, Y., Yu, F., Huang, H., Han, J. (2013) Development of recombinant antigen array for simultaneous detection of viral antibodies. *PLoS One* **8**, e73842.

Lochhead, M.J., Todorof, K., Delaney, M., Ives, J.T., Greef, C., Moll, K., Rowley, K., Vogel, K., Myatt, C., Zhang, X.Q., Logan, C., Benson, C., Reed, S., Schooley, R.T. (2011) Rapid multiplexed immunoassay for simultaneous serodiagnosis of HIV-1 and coinfections. *J Clin Microbiol* **49**, 3584-3590.

Lodes, M.J., Suciu, D., Wilmoth, J.L., Ross, M., Munro, S., Dix, K., Bernards, K., Stover, A.G., Quintana, M., Iihoshi, N., Lyon, W.J., Danley, D.L., McShea, A. (2007) Identification of upper respiratory tract pathogens using electrochemical detection on an oligonucleotide microarray. *PLoS One* **2**, e924.

López-Campos, G., Coiras, M., Sánchez-Merino, J.P., López-Huertas, M.R., Spiteri, I., Martin-Sanchez, F., Pérez-Breña, P. (2007) Oligonucleotide microarray design for detection and serotyping of human respiratory adenoviruses by using a virtual amplicon retrieval software. *J Virol Methods* **145**, 127-136.

Louie, J.K., Kajon, A.E., Holodniy, M., Guardia-LaBar, L., Lee, B., Petru, A.M., Hacker, J.K., Schnurr, D.P. (2008) Severe pneumonia due to adenovirus serotype 14: a new respiratory threat? *Clin Infect Dis* **46**, 421-425.

Lu, X., Erdman, D.D. (2006) Molecular typing of human adenoviruses by PCR and sequencing of a partial region of the hexon gene. *Arch Virol* **151**, 1587-1602.

Lueking, A., Horn, M., Eickhoff, H., Bussow, K., Lehrach, H., Walter, G. (1999) Protein microarrays for gene expression and antibody screening. *Anal Biochem* **270**, 103-111.

Lyng, H., Badiee, A., Svendsrud, D.H., Hovig, E., Myklebost, O., Stokke, T. (2004) Profound influence of microarray scanner characteristics on gene expression ratios: analysis and procedure for correction. *BMC Genomics* **5**, 10.

MacBeath, G., Schreiber, S.L. (2000) Printing proteins as microarrays for high-throughput function determination. *Science* **289**, 1760-1763.

Mahajan, S., Kumar, P., Gupta, K.C. (2006) Oligonucleotide microarrays: immobilization of phosphorylated oligonucleotides on epoxylated surface. *Bioconjug Chem* **17**, 1184-1189.

Mahony, J.B. (2008) Detection of respiratory viruses by molecular methods. *Clin Microbiol Rev* **21**, 716-747.

Majtán, T., Bukovská, G., Timko, J. (2004) DNA microarrays--techniques and applications in microbial systems. *Folia Microbiol (Praha)* **49**, 635-664.

Markham, N.R., Zuker, M. (2005) DINAMelt web server for nucleic acid melting prediction. *Nucleic Acids Res* **33**, W577-581.

Mattison, K., Corneau, N., Berg, I., Bosch, A., Duizer, E., Gutierrez-Aguirre, I., L'Homme, Y., Lucero, Y., Luo, Z., Martyres, A., Myrmel, M., O'Ryan, M., Pagotto, F., Sano, D., Svraka, S., Urzua, U., Bidawid, S. (2011) Development and validation of a microarray for the confirmation and typing of norovirus RT-PCR products. *J Virol Methods* **173**, 233-250.

McLoughlin, K.S. (2011) Microarrays for Pathogen Detection and Analysis. *Briefings in Functional Genomics* **10**, 342-353.

Mehlmann, M., Bonner, A.B., Williams, J.V., Dankbar, D.M., Moore, C.L., Kuchta, R.D., Podsiad, A.B., Tamerius, J.D., Dawson, E.D., Rowlen, K.L. (2007) Comparison of the MChip to viral culture, reverse transcription-PCR, and the QuickVue influenza A+B test for rapid diagnosis of influenza. *J Clin Microbiol* **45**, 1234-1237.

Mendoza, L.G., McQuary, P., Mongan, A., Gangadharan, R., Brignac, S., Eggers, M. (1999) High-throughput microarray-based enzyme-linked immunosorbent assay (ELISA). *Biotechniques* **27**, 778-788.

Metzgar, D., Skochko, G., Gibbins, C., Hudson, N., Lott, L., Jones, M.S. (2009) Evaluation and validation of a real-time PCR assay for detection and quantitation of human adenovirus 14 from clinical samples. *PLoS One* **4**, e7081.

Mezzasoma, L., Bacarese-Hamilton, T., Di Cristina, M., Rossi, R., Bistoni, F., Crisanti, A. (2002) Antigen Microarrays for Serodiagnosis of Infectious Diseases. *Clinical Chemistry* **48**, 121-130.

Mi, C., Tian, Z., Cao, C., Wang, Z., Mao, C., Xu, S. (2011) Novel microwave-assisted solvothermal synthesis of NaYF4:Yb,Er upconversion nanoparticles and their application in cancer cell imaging. *Langmuir* **27**, 14632-14637.

Mitrunen, K., Pettersson, K., Piironen, T., Björk, T., Lilja, H., Lövgren, T. (1995) Dual-label one-step immunoassay for simultaneous measurement of free and total prostate-specific antigen concentrations and ratios in serum. *Clin Chem* **41**, 1115-1120.

Mizuta, K., Abiko, C., Aoki, Y., Murata, T., Katsushima, N., Sakamoto, M., Itagaki, T., Hoshina, H., Ootani, K. (2006) A slow spread of adenovirus type 7 infection after its re-emergence in Yamagata, Japan, in 1995. *Microbiol Immunol* **50**, 553-558.

Mogi, T., Hatakeyama, K., Taguchi, T., Wake, H., Tanaami, T., Hosokawa, M., Tanaka, T., Matsunaga, T. (2011) Real-time detection of DNA hybridization on microarray using a CCD-based imaging system equipped with a rotated microlens array disk. *Biosens Bioelectron* **26**, 1942-1946.

Morais, S., Tortajada-Genaro, L.A., Arnandis-Chover, T., Puchades, R., Maquieira, A. (2009) Multiplexed microimmunoassays on a digital versatile disk. *Anal Chem* **81**, 5646-5654.

Moulton, K.R., Taylor, A.W., Rowlen, K.L., Dawson, E.D. (2011) ampliPHOX colorimetric detection on a DNA microarray for influenza. *J Vis Exp* **52**, e2682.

Mueller, C., Liotta, L.A., Espina, V. (2010) Reverse phase protein microarrays advance to use in clinical trials. *Mol Oncol* **4**, 461-481.

Mujawar, L.H., Maan, A.A., Khan, M.K., Norde, W., van Amerongen, A. (2013) Distribution of biomolecules in porous nitrocellulose membrane pads using confocal laser scanning microscopy and high-speed cameras. *Anal Chem* **85**, 3723-3729.

Nagl, S., Schäeferling, M., Wolfbeis, O.S. (2005) Fluorescence Analysis in Microarray Technology. *Microchimica Acta* **151**, 1-21.

Nakanishi, K., Sakiyama, T., Kumada, Y., Imamura, K., Imanaka, H. (2008) Recent Advances in Controlled Immobilization of Proteins onto the Surface of the Solid Substrate and Its Possible Application to Proteomics. *Current Proteomics* **5**, 161-175.

Nielsen, U.B., Geierstanger, B.H. (2004) Multiplexed sandwich assays in microarray format. *J Immunol Methods* **290**, 107-120.

Nilsson, C., Seppälä, M., Pettersson, K. (2001) Immunological characterization of human luteinizing hormone with special regard to a common genetic variant. *J Endocrinol* **168**, 107-116.

Nomellini, J.F., Duncan, G., Dorocicz, I.R., Smit, J. (2007) S-layer-mediated display of the immunoglobulin G-binding domain of streptococcal protein G on the surface of Caulobacter crescentus: development of an immunoactive reagent. *Appl Environ Microbiol* **73**, 3245-3253.

O'Flanagan, D., O'Donnell, J., Domegan, L., Fitzpatrick, F., Connell, J., Coughlan, S., De Gascun, C., Carr, M.J. (2011) First reported cases of human adenovirus serotype 14p1 infection, Ireland, October 2009 to July 2010. *Euro Surveill* **16**, 1-5.

Oh, T.J., Kim, C.J., Woo, S.K., Kim, T.S., Jeong, D.J., Kim, M.S., Lee, S., Cho, H.S., An, S. (2004) Development and clinical evaluation of a highly sensitive DNA microarray for detection and genotyping of human papillomaviruses. *J Clin Microbiol* **42**, 3272-3280.

Ozawa, K., Young, N. (1987) Characterization of capsid and noncapsid proteins of B19 parvovirus propagated in human erythroid bone marrow cell cultures. *J Virol* **61**, 2627-2630.

Pacini, D.L., Collier, A.M., Henderson, F.W. (1987) Adenovirus infections and respiratory illnesses in children in group day care. *J Infect Dis* **156**, 920-927.

Pappaert, K., Ottevaere, H., Thienpont, H., Van Hummelen, P., Desmet, G. (2006) Diffusion limitation: a possible source for the occurrence of doughnut patterns on DNA microarrays. *Biotechniques* **41**, 609-616.

Parcell, B.J., McIntyre, P.G., Yirrell, D.L., Fraser, A., Quinn, M., Templeton, K., Christie, S., Romanes, F. (2014) Prison and community outbreak of severe

respiratory infection due to adenovirus type 14p1 in Tayside, UK. *J Public Health (Oxf)*.

Parida, M.M. (2008) Rapid and real-time detection technologies for emerging viruses of biomedical importance. *J Biosci* **33**, 617-628.

Park, J.C., Kim, J.M., Kwon, O.J., Lee, K.R., Chai, Y.G., Oh, H.B. (2010) Development and clinical evaluation of a microarray for hepatitis C virus genotyping. *J Virol Methods* **163**, 269-275.

Pattenden, L.K., Middelberg, A.P., Niebert, M., Lipin, D.I. (2005) Towards the preparative and large-scale precision manufacture of virus-like particles. *Trends Biotechnol* **23**, 523-529.

Patterson, T.A., Lobenhofer, E.K., Fulmer-Smentek, S.B., Collins, P.J., Chu, T.M., Bao, W., Fang, H., Kawasaki, E.S., Hager, J., Tikhonova, I.R., Walker, S.J., Zhang, L., Hurban, P., de Longueville, F., Fuscoe, J.C., Tong, W., Shi, L., Wolfinger, R.D. (2006) Performance comparison of one-color and two-color platforms within the MicroArray Quality Control (MAQC) project. *Nat Biotechnol* **24**, 1140-1150.

Peiris, J.S., Lai, S.T., Poon, L.L., Guan, Y., Yam, L.Y., Lim, W., Nicholls, J., Yee, W.K., Yan, W.W., Cheung, M.T., Cheng, V.C., Chan, K.H., Tsang, D.N., Yung, R.W., Ng, T.K., Yuen, K.Y., group, S.s. (2003) Coronavirus as a possible cause of severe acute respiratory syndrome. *Lancet* **361**, 1319-1325.

Peluso, P., Wilson, D.S., Do, D., Tran, H., Venkatasubbaiah, M., Quincy, D., Heidecker, B., Poindexter, K., Tolani, N., Phelan, M., Witte, K., Jung, L.S., Wagner, P., Nock, S. (2003) Optimizing antibody immobilization strategies for the construction of protein microarrays. *Anal Biochem* **312**, 113-124.

Perraut, F., Lagrange, A., Pouteau, P., Peyssonneaux, O., Puget, P., McGall, G., Menou, L., Gonzalez, R., Labeye, P., Ginot, F. (2002) A new generation of scanners for DNA chips. *Biosens Bioelectron* **17**, 803-813.

Peterson, A.W., Heaton, R.J., Georgiadis, R.M. (2001) The effect of surface probe density on DNA hybridization. *Nucleic Acids Res* **29**, 5163-5168.

Petryayeva, E., Algar, W.R., Krull, U.J. (2013) Adapting fluorescence resonance energy transfer with quantum dot donors for solid-phase hybridization assays in microtiter plate format. *Langmuir* **29**, 977-987.

Pickett, S. (2003). Understanding and evaluating fluorescent microarray imaging instruments. *IVD Technol* **9**, 45-50.

Piironen, T., Nurmi, M., Irjala, K., Heinonen, O., Lilja, H., Lövgren, T., Pettersson, K. (2001) Measurement of circulating forms of prostate-specific antigen in whole blood immediately after venipuncture: implications for point-of-care testing. *Clin Chem* **47**, 703-711.

Piironen, T., Villoutreix, B.O., Becker, C., Hollingsworth, K., Vihinen, M., Bridon, D., Qiu, X., Rapp, J., Dowell, B., Lövgren, T., Pettersson, K., Lilja, H. (1998) Determination and analysis of antigenic epitopes of prostate specific antigen (PSA) and human glandular kallikrein 2 (hK2) using synthetic peptides and computer modeling. *Protein Sci* **7**, 259-269.

Poehling, K.A., Edwards, K.M., Weinberg, G.A., Szilagyi, P., Staat, M.A., Iwane, M.K., Bridges, C.B., Grijalva, C.G., Zhu, Y., Bernstein, D.I., Herrera, G.,

Erdman, D., Hall, C.B., Seither, R., Griffin, M.R., New Vaccine Surveillance, N. (2006) The underrecognized burden of influenza in young children. *N Engl J Med* **355**, 31-40.

Price, J.V., Jarrell, J.A., Furman, D., Kattah, N.H., Newell, E., Dekker, C.L., Davis, M.M., Utz, P.J. (2013) Characterization of influenza vaccine immunogenicity using influenza antigen microarrays. *PLoS One* **8**, e64555.

Qi, C., Zhu, W., Niu, Y., Zhang, H.G., Zhu, G.Y., Meng, Y.H., Chen, S., Jin, G. (2009) Detection of hepatitis B virus markers using a biosensor based on imaging ellipsometry. *J Viral Hepat* **16**, 822-832.

Qiu, M., Shi, Y., Guo, Z., Chen, Z., He, R., Chen, R., Zhou, D., Dai, E., Wang, X., Si, B., Song, Y., Li, J., Yang, L., Wang, J., Wang, H., Pang, X., Zhai, J., Du, Z., Liu, Y., Zhang, Y., Li, L., Wang, J., Sun, B., Yang, R. (2005) Antibody responses to individual proteins of SARS coronavirus and their neutralization activities. *Microbes Infect* **7**, 882-889.

Qurei, L., Seto, D., Salah, Z., Azzeh, M. (2012) A molecular epidemiology survey of respiratory adenoviruses circulating in children residing in Southern Palestine. *PLoS One* **7**, e42732.

Raddatz, S., Mueller-Ibeler, J., Kluge, J., Wäß, L., Burdinski, G., Havens, J.R., Onofrey, T.J., Wang, D., Schweitzer, M. (2002) Hydrazide oligonucleotides: new chemical modification for chip array attachment and conjugation. *Nucleic Acids Res* **30**, 4793-4802.

Rajakoski, K., Piironen, T., Pettersson, K., Lövgren, J., Karp, M. (1997) Epitope mapping of human prostate specific antigen and glandular kallikrein expressed in insect cells. *Prostate Cancer Prostatic Dis* **1**, 16-20.

Ramachandran, N., Srivastava, S., Labaer, J. (2008) Applications of protein microarrays for biomarker discovery. *Proteomics Clin Appl* **2**, 1444-1459.

Rantanen, T., Järvenpää, M.L., Vuojola, J., Arppe, R., Kuningas, K., Soukka, T. (2009) Upconverting phosphors in a dual-parameter LRET-based hybridization assay. *Analyst* **134**, 1713-1716.

Ray, S., Mehta, G., Srivastava, S. (2010) Label-free detection techniques for protein microarrays: prospects, merits and challenges. *Proteomics* **10**, 731-748.

Raymond, F., Carbonneau, J., Boucher, N., Robitaille, L., Boisvert, S., Wu, W.K., De Serres, G., Boivin, G., Corbeil, J. (2009) Comparison of automated microarray detection with real-time PCR assays for detection of respiratory viruses in specimens obtained from children. *J Clin Microbiol* **47**, 743-750.

Relógio, A., Schwager, C., Richter, A., Ansorge, W., Valcárcel, J. (2002) Optimization of oligonucleotide-based DNA microarrays. *Nucleic Acids Res* **30**, e51.

Renois, F., Talmud, D., Huguenin, A., Moutte, L., Strady, C., Cousson, J., Leveque, N., Andreoletti, L. (2010) Rapid detection of respiratory tract viral infections and coinfections in patients with influenza-like illnesses by use of reverse transcription-PCR DNA microarray systems. *J Clin Microbiol* **48**, 3836-3842.

Resch-Genger, U., Grabolle, M., Cavaliere-Jaricot, S., Nitschke, R., Nann, T. (2008) Quantum dots versus organic dyes as fluorescent labels. *Nat Methods* **5**, 763-775.

Ritari, J., Hultman, J., Fingerroos, R., Tarkkanen, J., Pullat, J., Paulin, L., Kivi, N., Auvinen, P., Auvinen, E. (2012) Detection of human papillomaviruses by polymerase chain reaction and ligation reaction on universal microarray. *PLoS One* **7**, e34211.

Robinson, C.M., Singh, G., Lee, J.Y., Dehghan, S., Rajaiya, J., Liu, E.B., Yousuf, M.A., Betensky, R.A., Jones, M.S., Dyer, D.W., Seto, D., Chodosh, J. (2013) Molecular evolution of human adenoviruses. *Sci Rep* **3**, 1-7.

Rogers, Y.H., Jiang-Baucom, P., Huang, Z.J., Bogdanov, V., Anderson, S., Boyce-Jacino, M.T. (1999) Immobilization of oligonucleotides onto a glass support via disulfide bonds: A method for preparation of DNA microarrays. *Anal Biochem* **266**, 23-30.

Rousserie, G., Sukhanova, A., Even-Desrumeaux, K., Fleury, F., Chames, P., Baty, D., Oleinikov, V., Pluot, M., Cohen, J.H., Nabiev, I. (2010) Semiconductor quantum dots for multiplexed bio-detection on solid-state microarrays. *Crit Rev Oncol Hematol* **74**, 1-15.

Rusmini, F., Zhong, Z., Feijen, J. (2007) Protein immobilization strategies for protein biochips. *Biomacromolecules* **8**, 1775-1789.

Ryabinin, V.A., Kostina, E.V., Maksakova, G.A., Neverov, A.A., Chumakov, K.M., Sinyakov, A.N. (2011) Universal oligonucleotide microarray for sub-typing of Influenza A virus. *PLoS One* **6**, e17529.

Sabanayagam, C.R., Smith, C.L., Cantor, C.R. (2000) Oligonucleotide immobilization on micropatterned streptavidin surfaces. *Nucleic Acids Res* **28**, E33.

Sabella, C., Goldfarb, J. (1999) Parvovirus B19 infections. *Am Fam Physician* **60**, 1455-1460.

Salama, K., Eltoukhy, H., Hassibi, A., El-Gamal, A. (2004) Modeling and simulation of luminescence detection platforms. *Biosens Bioelectron* **19**, 1377-1386.

Sánchez-Rodríguez, S.P., Münch-Anguiano, L., Echeverria, O., Vázquez-Nin, G., Mora-Pale, M., Dordick, J.S., Bustos-Jaimes, I. (2012) Human parvovirus B19 virus-like particles: In vitro assembly and stability. *Biochimie* **94**, 870-878.

Sandri, M.T., Riggio, D., Salvatici, M., Passerini, R., Zorzino, L., Boveri, S., Radice, D., Spolti, N., Sideri, M. (2009) Typing of human papillomavirus in women with cervical lesions: prevalence and distribution of different genotypes. *J Med Virol* **81**, 271-277.

Sassolas, A., Leca-Bouvier, B.D., Blum, L.J. (2008) DNA biosensors and microarrays. *Chem. Rev.* **108**, 109-139

Scarano, S., Mascini, M., Turner, A.P., Minunni, M. (2010) Surface plasmon resonance imaging for affinity-based biosensors. *Biosens Bioelectron* **25**, 957-966.

Schena, M., Shalon, D., Davis, R.W., Brown, P.O. (1995) Quantitative monitoring of gene expression patterns with a complementary DNA microarray. *Science* **270**, 467-470.

Schäferling, M., Nagl, S. (2006) Optical technologies for the read out and quality control of DNA and protein microarrays. *Anal Bioanal Chem* **385**, 500-517.

Sefers, S.E., Li, H., Tang, Y.W. (2011) Simultaneous detection and differentiation of respiratory syncytial virus and other respiratory viral pathogens. *Methods Mol Biol* **665**, 309-323.

Selvaraju, S.B., Kovac, M., Dickson, L.M., Kajon, A.E., Selvarangan, R. (2011) Molecular epidemiology and clinical presentation of human adenovirus infections in Kansas City children. *J Clin Virol* **51**, 126-131.

Sethi, D., Kumar, P., Gupta, K.C. (2009) Strategies for preparation of oligonucleotide biochips and their applications. *Nucleic Acids Symp Ser (Oxf)* **53**, 149-150.

Shalon, D., Smith, S.J., Brown, P.O. (1996) A DNA microarray system for analyzing complex DNA samples using two-color fluorescent probe hybridization. *Genome Res* **6**, 639-645.

Shanmukh, S., Jones, L., Driskell, J., Zhao, Y., Dluhy, R., Tripp, R.A. (2006) Rapid and sensitive detection of respiratory virus molecular signatures using a silver nanorod array SERS substrate. *Nano Lett* **6**, 2630-2636.

Shchepinov, M.S., Case-Green, S.C., Southern, E.M. (1997) Steric factors influencing hybridisation of nucleic acids to oligonucleotide arrays. *Nucleic Acids Res* **25**, 1155-1161.

Shiver, J.W., Fu, T.M., Chen, L., Casimiro, D.R., Davies, M.E., Evans, R.K., Zhang, Z.Q., Simon, A.J., Trigona, W.L., Dubey, S.A., Huang, L., Harris, V.A., Long, R.S., Liang, X., Handt, L., Schleif, W.A., Zhu, L., Freed, D.C., Persaud, N.V., Guan, L., Punt, K.S., Tang, A., Chen, M., Wilson, K.A., Collins, K.B., Heidecker, G.J., Fernandez, V.R., Perry, H.C., Joyce, J.G., Grimm, K.M., Cook, J.C., Keller, P.M., Kresock, D.S., Mach, H., Troutman, R.D., Isopi, L.A., Williams, D.M., Xu, Z., Bohannon, K.E., Volkin, D.B., Montefiori, D.C., Miura, A., Krivulka, G.R., Lifton, M.A., Kuroda, M.J., Schmitz, J.E., Letvin, N.L., Caulfield, M.J., Bett, A.J., Youil, R., Kaslow, D.C., Emini, E.A. (2002) Replication-incompetent adenoviral vaccine vector elicits effective anti-immunodeficiency-virus immunity. *Nature* **415**, 331-335.

Siegl, G., Bates, R.C., Berns, K.I., Carter, B.J., Kelly, D.C., Kurstak, E., Tattersall, P. (1985) Characteristics and taxonomy of Parvoviridae. *Intervirology* **23**, 61-73.

Sinclair, M.B., Timlin, J.A., Haaland, D.M., Werner-Washburne, M. (2004) Design, construction, characterization, and application of a hyperspectral microarray scanner. *Appl Opt* **43**, 2079-2088.

Sivakumar, P.M., Moritsugu, N., Obuse, S., Isoshima, T., Tashiro, H., Ito, Y. (2013) Novel microarrays for simultaneous serodiagnosis of multiple antiviral antibodies. *PLoS One* **8**, e81726.

Smith, S.R., Chhetri, M.K., Johanson, J., Radfar, N., Migeon, C.J. (1975) The pituitary-gonadal axis in men with protein-calorie malnutrition. *J Clin Endocrinol Metab* **41**, 60-69.

Sotlar, K., Diemer, D., Dethleffs, A., Hack, Y., Stubner, A., Vollmer, N., Menton, S., Menton, M., Dietz, K., Wallwiener, D., Kandolf, R., Bultmann, B. (2004) Detection and typing of human papillomavirus by e6 nested multiplex PCR. *J Clin Microbiol* **42**, 3176-3184.

Soukka, T., Kuningas, K., Rantanen, T., Haaslahti, V., Lövgren, T. (2005) Photochemical characterization of up-converting inorganic lanthanide phosphors as potential labels. *J Fluoresc* **15**, 513-528.

Soukka, T., Rantanen, T., Kuningas, K. (2008) Photon upconversion in homogeneous fluorescence-based bioanalytical assays. *Ann N Y Acad Sci* **1130**, 188-200.

Stenman, U.H., Alfthan, H., Koskimies, A., Seppälä, M., Pettersson, K., Lövgren, T. (1985) Monitoring the LH surge by ultrarapid and highly sensitive immunofluorometric assay. *Ann N Y Acad Sci* **442**, 544-550.

Storch, G.A. (2000) Diagnostic virology. *Clin Infect Dis* **31**, 739-751.

Sullivan, N.J., Sanchez, A., Rollin, P.E., Yang, Z.Y., Nabel, G.J. (2000) Development of a preventive vaccine for Ebola virus infection in primates. *Nature* **408**, 605-609.

Sun, H., Chen, G.Y., Yao, S.Q. (2013) Recent advances in microarray technologies for proteomics. *Chem Biol* **20**, 685-699.

Sun, X.L., Stabler, C.L., Cazalis, C.S., Chaikof, E.L. (2006) Carbohydrate and protein immobilization onto solid surfaces by sequential Diels-Alder and azide-alkyne cycloadditions. *Bioconjug Chem* **17**, 52-57.

Susi, P., Hattara, L., Waris, M., Luoma-aho, T., Siitari, H., Hyypiä, T., Saviranta, P. (2009) Typing of Enteroviruses by Use of Microwell Oligonucleotide Arrays. *J Clin Microbiol* **47**, 1863-1870.

Suyver, J.F., Aebischer, A., Biner, D., Gerner, P., Grimm, J., Heer, S., Krämer, K.W., Reinhard, C., Güdel, H.U. (2005) Novel materials doped with trivalent lanthanides and transition metal ions showing near-infrared to visible photon upconversion. *Optical Materials* **27**, 1111-1130.

Söderlund, M., Brown, C.S., Cohen, B.J., Hedman, K. (1995a) Accurate serodiagnosis of B19 parvovirus infections by measurement of IgG avidity. *J Infect Dis* **171**, 710-713.

Söderlund, M., Brown, C.S., Spaan, W.J., Hedman, L., Hedman, K. (1995b) Epitope type-specific IgG responses to capsid proteins VP1 and VP2 of human parvovirus B19. *J Infect Dis* **172**, 1431-1436.

Tanaka, T., Kogawa, K., Sasa, H., Nonoyama, S., Furuya, K., Sato, K. (2009) Rapid and simultaneous detection of 6 types of human herpes virus (herpes simplex virus, varicella-zoster virus, Epstein-Barr virus, cytomegalovirus, human herpes virus 6A/B, and human herpes virus 7) by multiplex PCR assay. *Biomed Res* **30**, 279-285.

Tate, J.E., Bunning, M.L., Lott, L., Lu, X., Su, J., Metzgar, D., Brosch, L., Panozzo, C.A., Marconi, V.C., Faix, D.J., Prill, M., Johnson, B., Erdman, D.D., Fonseca, V., Anderson, L.J., Widdowson, M.A. (2009) Outbreak of severe respiratory disease associated with emergent human adenovirus serotype 14 at a US air force training facility in 2007. *J Infect Dis* **199**, 1419-1426.

Taylor, S., Smith, S., Windle, B., Guiseppi-Elie, A. (2003) Impact of surface chemistry and blocking strategies on DNA microarrays. *Nucleic Acids Res* **31**, e87.

Templin, M.F., Stoll, D., Schrenk, M., Traub, P.C., Vohringer, C.F., Joos, T.O. (2002) Protein microarray technology. *Trends Biotechnol* **20**, 160-166.

Templin, M.F., Stoll, D., Schwenk, J.M., Potz, O., Kramer, S., Joos, T.O. (2003) Protein microarrays: promising tools for proteomic research. *Proteomics* **3**, 2155-2166.

Težak, Z., Ranamukhaarachchi, D., Russek-Cohen, E., Gutman, S.I. (2006) FDA perspectives on potential microarray-based clinical diagnostics. *Hum Genomics* **2**, 236-243.

Timlin, J.A., Haaland, D.M., Sinclair, M.B., Aragon, A.D., Martinez, M.J., Werner-Washburne, M. (2005) Hyperspectral microarray scanning: impact on the accuracy and reliability of gene expression data. *BMC Genomics* **6:**72.

Townsend, M.B., Dawson, E.D., Mehlmann, M., Smagala, J.A., Dankbar, D.M., Moore, C.L., Smith, C.B., Cox, N.J., Kuchta, R.D., Rowlen, K.L. (2006) Experimental evaluation of the FluChip diagnostic microarray for influenza virus surveillance. *J Clin Microbiol* **44**, 2863-2871.

Tsujimura, M., Matsushita, K., Shiraki, H., Sato, H., Okochi, K., Maeda, Y. (1995) Human parvovirus B19 infection in blood donors. *Vox Sang* **69**, 206-212.
Tsutsumi, R., Webster, N.J. (2009) GnRH pulsatility, the pituitary response and reproductive dysfunction. *Endocr J* **56**, 729-737.

Uhnoo, I., Wadell, G., Svensson, L., Johansson, M.E. (1984) Importance of enteric adenoviruses 40 and 41 in acute gastroenteritis in infants and young children. *J Clin Microbiol* **20**, 365-372.

Vainrub, A., Pettitt, B.M. (2003) Surface electrostatic effects in oligonucleotide microarrays: control and optimization of binding thermodynamics. *Biopolymers* **68**, 265-270.

van de Rijke, F., Zijlmans, H., Li, S., Vail, T., Raap, A.K., Niedbala, R.S., Tanke, H.J. (2001) Up-converting phosphor reporters for nucleic acid microarrays. *Nature biotechnology* **19**, 273-276.

van den Hoogen, B.G., de Jong, J.C., Groen, J., Kuiken, T., de Groot, R., Fouchier, R.A., Osterhaus, A.D. (2001) A newly discovered human pneumovirus isolated from young children with respiratory tract disease. *Nat Med* **7**, 719-724.

Wang, F., Deng, R., Wang, J., Wang, Q., Han, Y., Zhu, H., Chen, X., Liu, X. (2011) Tuning upconversion through energy migration in core-shell nanoparticles. *Nat Mater* **10**, 968-973.

Wang, F., Liu, X. (2009) Recent advances in the chemistry of lanthanide-doped upconversion nanocrystals. *Chem Soc Rev* **38**, 976-989.

Wang, J., Bhattacharyya, D., Bachas, L.G. (2001) Improving the activity of immobilized subtilisin by site-directed attachment through a genetically engineered affinity tag. *Fresenius J Anal Chem* **369**, 280-285.

Wang, X., Chen, J.T., Zhu, H., Chen, X., Yan, X.P. (2013a) One-step solvothermal synthesis of targetable optomagnetic upconversion nanoparticles for in vivo bimodal imaging. *Anal Chem* **85**, 10225-10231.

Wang, X., Dang, E., Gao, J., Guo, S., Li, Z. (2013b) Development of a gold nanoparticle-based oligonucleotide microarray for simultaneous detection of seven swine viruses. *J Virol Methods* **191**, 9-15.

Waris, M., Halonen, P., Ziegler, T., Nikkari, S., Obert, G. (1988) Time-resolved fluoroimmunoassay compared with virus isolation for rapid detection of respiratory syncytial virus in nasopharyngeal aspirates. *J Clin Microbiol* **26**, 2581-2585.

Washburn, A.L., Gomez, J., Bailey, R.C. (2011) DNA-encoding to improve performance and allow parallel evaluation of the binding characteristics of multiple antibodies in a surface-bound immunoassay format. *Anal Chem* **83**, 3572-3580.

Washington, C., Metzgar, D., Hazbon, M.H., Binn, L., Lyons, A., Coward, C., Kuschner, R. (2010) Multiplexed Luminex xMAP assay for detection and identification of five adenovirus serotypes associated with epidemics of respiratory disease in adults. *J Clin Microbiol* **48**, 2217-2222.

Vet, J.A., Majithia, A.R., Marras, S.A., Tyagi, S., Dube, S., Poiesz, B.J., Kramer, F.R. (1999) Multiplex detection of four pathogenic retroviruses using molecular beacons. *Proc Natl Acad Sci U S A* **96**, 6394-6399.

Vetrone, F., Boyer, J.C., Capobianco, J.A., Speghini, A., Bettinelli, M. (2004) Significance of Yb^{3+} concentration on the upconversion mechanisms in codoped Y_2O_3:Er^{3+}, Yb^{3+} nanocrystals. *J. Appl. Phys.* **96**, 661-667.

Vetrone, F., Naccache, R., Mahalingam, V., Morgan, C.G., Capobianco, J.A. (2009) The Active-Core/Active-Shell Approach: A Strategy to Enhance the Upconversion Luminescence in Lanthanide-Doped Nanoparticles. *Advanced Functional Materials* **19**, 2924-2929.

Vickers, A., Cronin, A., Roobol, M., Savage, C., Peltola, M., Pettersson, K., Scardino, P.T., Schröder, F., Lilja, H. (2010) Reducing unnecessary biopsy during prostate cancer screening using a four-kallikrein panel: an independent replication. *J Clin Oncol* **28**, 2493-2498.

Wiese, R., Belosludtsev, Y., Powdrill, T., Thompson, P., Hogan, M. (2001) Simultaneous multianalyte ELISA performed on a microarray platform. *Clin Chem* **47**, 1451-1457.

Wigand, R., Bartha, A., Dreizin, R.S., Esche, H., Ginsberg, H.S., Green, M., Hierholzer, J.C., Kalter, S.S., McFerran, J.B., Pettersson, U., Russell, W.C.,
Wadell, G. (1982) Adenoviridae: second report. *Intervirology* **18**, 169-176.

Viitala, S.M., Jääskeläinen, A.J., Kelo, E., Sirola, H., Moilanen, K., Suni, J., Vaheri, A., Vapalahti, O., Närvänen, A. (2013) Surface-activated microtiter-plate microarray for simultaneous CRP quantification and viral antibody detection. *Diagn Microbiol Infect Dis* **75**, 174-179.

Vogels, R., Zuijdgeest, D., van Rijnsoever, R., Hartkoorn, E., Damen, I., de Béthune, M.P., Kostense, S., Penders, G., Helmus, N., Koudstaal, W., Cecchini, M., Wetterwald, A., Sprangers, M., Lemckert, A., Ophorst, O., Koel, B., van Meerendonk, M., Quax, P., Panitti, L., Grimbergen, J., Bout, A., Goudsmit, J., Havenga, M. (2003) Replication-deficient human adenovirus type 35 vectors for gene transfer and vaccination: efficient human cell infection and bypass of preexisting adenovirus immunity. *J Virol* **77**, 8263-8271.

Wu, P., Zhu, L., Stenman, U.H., Leinonen, J. (2004) Immunopeptidometric assay for enzymatically active prostate-specific antigen. *Clin Chem* **50**, 125-129.

Väisänen, V., Peltola, M.T., Lilja, H., Nurmi, M., Pettersson, K. (2006) Intact free prostate-specific antigen and free and total human glandular kallikrein 2. Elimination of assay interference by enzymatic digestion of antibodies to F(ab')2 fragments. *Anal Chem* **78**, 7809-7815.

Xie, L., Yu, X.F., Sun, Z., Yang, X.H., Huang, R.J., Wang, J., Yu, A., Zheng, L., Yu, M.C., Hu, X.W., Wang, B.M., Chen, J., Pan, J.C., Liu, S.L. (2012) Two adenovirus serotype 3 outbreaks associated with febrile respiratory disease and pharyngoconjunctival fever in children under 15 years of age in Hangzhou, China, during 2011. *J Clin Microbiol* **50**, 1879-1888.

Xu, R., Gan, X., Fang, Y., Zheng, S., Dong, Q. (2007) A simple, rapid, and sensitive integrated protein microarray for simultaneous detection of multiple antigens and antibodies of five human hepatitis viruses (HBV, HCV, HDV, HEV, and HGV). *Anal Biochem* **362**, 69-75.

Yan, X., Zhong, W., Tang, A., Schielke, E.G., Hang, W., Nolan, J.P. (2005) Multiplexed flow cytometric immunoassay for influenza virus detection and differentiation. *Anal Chem* **77**, 7673-7678.

Yang, Y., Stafford, P., Kim, Y. (2011) Segmentation and intensity estimation for microarray images with saturated pixels. *BMC Bioinformatics* **12**:462.

Ylikotila, J., Välimaa, L., Vehniäinen, M., Takalo, H., Lövgren, T., Pettersson, K. (2005) A sensitive TSH assay in spot-coated microwells utilizing recombinant antibody fragments. *J Immunol Methods* **306**, 104-114.

Young, K.A., Chaffin, C.L., Molskness, T.A., Stouffer, R.L. (2003) Controlled ovulation of the dominant follicle: a critical role for LH in the late follicular phase of the menstrual cycle. *Hum Reprod* **18**, 2257-2263.

Yu, X., Schneiderhan-Marra, N., Joos, T.O. (2010) Protein microarrays for personalized medicine. *Clin Chem* **56**, 376-387.

Yu, X., Wallstrom, G., Magee, D.M., Qiu, J., Mendoza, D.E., Wang, J., Bian, X., Graves, M., LaBaer, J. (2013) Quantifying antibody binding on protein microarrays using microarray nonlinear calibration. *Biotechniques* **54**, 257-264.

Yu, X., Xu, D., Cheng, Q. (2006) Label-free detection methods for protein microarrays. *Proteomics* **6**, 5493-5503.

Zammatteo, N., Jeanmart, L., Hamels, S., Courtois, S., Louette, P., Hevesi, L., Remacle, J. (2000) Comparison between different strategies of covalent attachment of DNA to glass surfaces to build DNA microarrays. *Anal Biochem* **280**, 143-150.

Zhao, X., Nampalli, S., Serino, A.J., Kumar, S. (2001) Immobilization of oligodeoxyribonucleotides with multiple anchors to microchips. *Nucleic Acids Res* **29**, 955-959.

Zhou, J., Thompson, D.K. (2004) Microarray technology and applications in environmental microbiology. *Advances in Agronomy* **82**, 183-270.

Zhu, H., Hu, S., Jona, G., Zhu, X., Kreiswirth, N., Willey, B.M., Mazzulli, T., Liu, G., Song, Q., Chen, P., Cameron, M., Tyler, A., Wang, J., Wen, J., Chen, W., Compton, S., Snyder, M. (2006) Severe acute respiratory syndrome

diagnostics using a coronavirus protein microarray. *Proc Natl Acad Sci U S A* **103**, 4011-4016.

Zhu, H., Snyder, M. (2003) Protein chip technology. *Curr Opin Chem Biol* **7**, 55-63.

Zijlmans, H.J.M.A.A., Bonnet, J., Burton, J., Kardos, K., Vail, T., Niedbala, R.S., Tanke, H.J. (1999) Detection of Cell and Tissue Surface Antigens Using Up-Converting Phosphors: A New Reporter Technology. *Analytical Biochemistry* **267**, 30-36.

Zong, C., Wu, J., Wang, C., Ju, H., Yan, F. (2012) Chemiluminescence imaging immunoassay of multiple tumor markers for cancer screening. *Anal Chem* **84**, 2410-2415.

Zou, L., Zhou, J., Li, H., Wu, J., Mo, Y., Chen, Q., Fang, L., Wu, D., Wu, J., Ke, C. (2012) Human adenovirus infection in children with acute respiratory tract disease in Guangzhou, China. *APMIS* **120**, 683-688.